NASA SP-3031

HANDBOOK OF THE PHYSICAL PROPERTIES OF THE PLANET JUPITER

NATIONAL AERONAUTICS AND SPACE ADMINISTRATION

NASA SP-3031

HANDBOOK OF THE PHYSICAL PROPERTIES OF THE PLANET JUPITER

by
C.M. Michaux
with contributions by
F.F. Fish, Jr., F.W. Murray,
R.E. Santina, and P.C. Steffey

Prepared under contract for NASA
by Douglas Aircraft Company, Inc.
Santa Monica, California

Scientific and Technical Information Division
OFFICE OF TECHNOLOGY UTILIZATION 1967
NATIONAL AERONAUTICS AND SPACE ADMINISTRATION
Washington, D.C.

For Sale by the Superintendent of Documents,
U.S. Government Printing Office, Washington, D.C. 20402
Price $0.60
Library of Congress Catalog Card Number 66–61838

Foreword

JUPITER IS THE LARGEST PLANET in the solar system and also the innermost of the nonterrestrial-type planets. Its large mass and low mean density indicate that the present chemical composition may be very similar to what it was when the planet was formed and that the relative chemical abundances are more solar-like than Earth-like. For these reasons, study of Jupiter from flyby, orbiter, or atmospheric entry spacecraft could reveal important information concerning the evolution of the solar system. However, because of its tremendous distance from the Earth, Jupiter is much more difficult to reach with a spacecraft than either Mars or Venus.

The cause of the wandering Great Red Spot, the production of the erratic decameter radio noise storms, the existence or nonexistence of a solid planetary surface, and the possible presence of internal heat sources are but a few of the important questions that have been raised which a close study of Jupiter could help answer. Ground-based observations of the planet have only whetted our appetite to learn more about the planet.

This handbook, current through December 1965, summarizes the present observational knowledge of Jupiter and briefly outlines the results of a great many theoretical studies of the planet. It was prepared in the Space Sciences Department of the Douglas Missile and Space Systems Division under Contract NASw-1013 with the National Aeronautics and Space Administration.

ORAN W. NICKS, *Director*
Lunar and Planetary Programs

Acknowledgments

IN PREPARING THIS HANDBOOK, valuable assistance has been provided by L. R. Koenig, J. H. Moore, S. T. Rollins, M. Weinstein, and G. Wells of the Douglas Aircraft Company, Inc.

Several portions of this material were reviewed by the late D. Brouwer of the Yale University Observatory, W. E. Brunk of the National Aeronautics and Space Administration, and G. Münch of the California Institute of Technology. Their comments and suggestions for improving the text are deeply appreciated.

Contents

1
Orbital Elements

THE ORBITS OF JUPITER AND EARTH

THE GIANT PLANET JUPITER moves slowly along an orbit approximately five times the distance of Earth from the Sun and completes one revolution in approximately 12 years. Its nearly circular orbit (eccentricity, $e=0.048$) is inclined to the ecliptic by slightly more than 1°. Figure 1–1 shows the respective positions of the orbits of Earth and Jupiter (ref. 1). Table 1–1 lists the important orbital constants derived from the orbital elements of both planets for 1960.

Dates for Jupiter's passage through its orbital positions of interest were September 28, 1963, at perihelion and July 20, 1954, at ascending node. These events recur on August 12, 1975, and May 31, 1966, respectively. Aphelion and descending node passages occur some 6 years from perihelion and ascending node passages.

ORBITAL PARAMETERS

The six orbital elements commonly used to describe the elliptical motion of a planet are the following:

(1) Semimajor axis, a

(2) Eccentricity, e

(3) Inclination of the orbit to the ecliptic, i

(4) Longitude of the ascending node, Ω, on the ecliptic measured from the vernal equinox

(5) Longitude of the perihelion, $\tilde{\omega}$, measured along the ecliptic from equinox to ascending node, then along the orbit from node to perihelion

(6) Mean longitude at epoch of the planet, L_0, which is the constant in the formula $L=L_0+nt$, for the mean longitude, L, at any time, t, after the epoch ($t=0$), where t is the time in ephemeris days since the epoch, and n is the mean daily motion. The mean anomaly is the difference, $L-\tilde{\omega}=L_0-\tilde{\omega}+nt$.

Planetary orbits are affected by the attractions of other planets and, thus, are not strictly elliptic. The actual or perturbed motion of a planet may be represented with the aid of osculating elements that correspond to the instantaneous position vector and velocity

vector at any epoch, therefore, the osculating elements change continuously. Expressed as functions of time, they contain both secular (that is progressively changing) and periodic terms. Mean elements obtained by ignoring the periodic terms cannot be used for the precise calculation of a planet's position but have the merit of exhibiting progressive changes in the orbit.

The mean distance, a, in an unperturbed orbit or in an osculating orbit is related to the mean motion, n, by Kepler's third law, $n^2a^3=k^2(1+m)$, where m is the ratio of the mass of the planet to the Sun, and k is the Gaussian constant of gravitation. If n and a are mean elements, the relation becomes $n^2a^3=k^2(1+m)(1+\delta)$, where δ is a small quantity that arises from the neglect of the periodic terms in the definition of the mean elements.

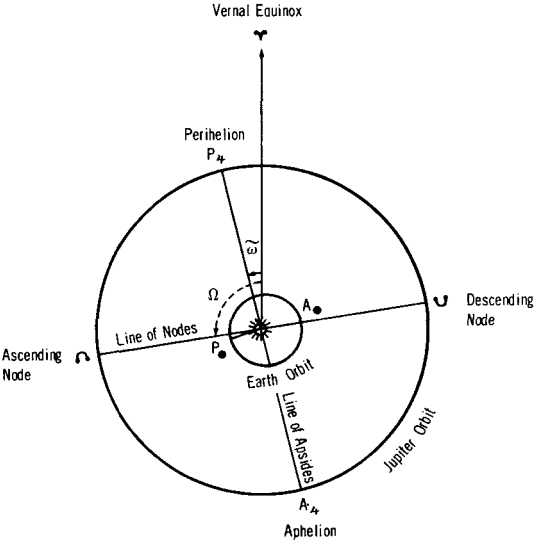

FIGURE 1-1.—Orbits of Jupiter and Earth

Mean elements[a]—Epoch: 1960, Jan. 1.5 ephemeris time	Earth	Jupiter
Mean solar distance, a, astronomical unit	1.000000	5.202803
Mean motion, n, deg/day	0.985609	0.083091
Eccentricity, e, deg	0.016726	0.048435
Inclination to ecliptic, i, deg	0.0	1.30536
Longitude of ascending node, Ω, deg	0.0	100.04444
Longitude of perihelion, $\tilde{\omega}$, deg	102.25253	13.67823
Mean longitude at epoch, L, deg	100.15815	259.83112

[a] From ref. 1.

TABLE 1-1.—*Derived Orbital Constants for Jupiter*

Orbital Time Intervals

Constant	Values		
	Earth sidereal years	Earth tropical years	Earth solar days
Jupiter sidereal year	11. 86177	11. 86223	4332. 587
Mean synodic period	1. 09205	1. 09210	398. 88

Distances From the Sun [a]

Constant	Values		
	Astronomical units	Kilometers	Miles
Mean solar distance	5. 202803	778.344×10^{6}	483.634×10^{6}
Perihelion distance	4. 950805	740. 635	460. 210
Aphelion distance	5. 454801	816. 032	507. 059

Distances From Earth [a]

Constant	Values		
	Astronomical units	Kilometers	Miles
Minimum distance	3. 9308	588.05×10^{6}	365.4×10^{6}
Maximum distance	6. 4363	962. 87	598. 3

Orbital Velocity

Constant	Values	
	Kilometers sec^{-1}	Miles sec^{-1}
Mean orbital velocity	13. 1	8. 1

[a] Using conversion factor, 1 astronomical unit $=1.495\times10^{8}$ kilometers.

JOVIAN ELEMENTS TABULATIONS

The osculating elements (elements of the tangent elliptic orbit) of Jupiter are given by *The American Ephemeris and Nautical Almanac* (ref. 2) for a succession of epochs of osculation separated by 40-day intervals. Table 1–2 lists the elements for the years 1965, 1966, and 1967 (ref. 2). The mean anomaly of the planet is given instead of the mean longitude.

These osculating elements are derived directly from the numerical theory of Eckert, Brouwer, and Clemence (ref. 3). The ephemerides of Jupiter's positions also are computed from the latter work which supplies the heliocentric equatorial rectangular coordinates of Jupiter.[1] The osculating elements and the heliocentric ephemerides do not contain the perturbations caused by the inner planets; the geocentric ephemerides, however, contain these perturbations, which were provided by Clemence (ref. 4).

Mean elements and their secular variation terms are seldom given for the outer planets because of the uncertainties remaining in the analytical theories of their motions and the difficulties in deriving these elements and terms from recent numerical theories. Table 1–3 presents the mean elements of Jupiter with the secular variations as given by *Connaissance des Temps* for 1960 (ref. 5) and established from the work of Gaillot (ref. 6), which improved Le Verrier's orbit (ref. 7).

In order to study Jupiter's perturbative effects on minor planets and comets, Clemence (ref. 8) has derived elements with their variational expressions which are intermediate, that is, between mean elements and osculating elements. They represent the average motion of Jupiter over a limited 200-year period and are based on Hill's theory for Jupiter, which used the fundamental epoch 1850, Jan 0.5 (ref. 9). Table 1–4 gives Clemence's values of these intermediate elements for every 10th year of the present century.

THE GREAT INEQUALITY

An outstanding long-period perturbation exists in the orbital motions of Jupiter and Saturn. It is produced by the near-commensurability of the periods of revolution which is almost in the ratio 2 to 5 (12 yr for Jupiter and 30 yr for Saturn). For centuries, the mean orbital velocities of the two giant planets had been found to be either continually increasing or decreasing along their neighboring orbits. As it is known in celestial mechanics, the Great

[1] At 40-day intervals (from 1653 to 2060) to 9 decimal places.

TABLE 1–2.—*Osculating Elements for Jupiter, 1965 to 1967*

[Mean elements are taken from *The American Ephemeris and Nautical Almanac* for 1965, 1966, and 1967 and are referred to the mean equinox and ecliptic of date]

Date	Julian date (243)	Inclination to the ecliptic, i, deg	Longitude of—		Mean distance from Sun, a, astronomical units	Mean motion, n, deg/sidereal day	Eccentricity of orbit, e	Mean anomaly $L-\tilde{\omega}$
			Ascending node, Ω, deg	Perihelion, $\tilde{\omega}$, deg				
1965								
Jan. 0	8760.5	1.30606	100.0981	13.4159	5.202 268	0.083 1040	0.048 2270	38.3054
Feb. 9	8800.5	1.30605	100.0990	13.4206	5.202 274	.083 1039	.048 2260	41.6267
Mar. 21	8840.5	1.30605	100.0999	13.4255	5.202 281	.083 1037	.048 2253	44.9478
Apr. 30	8880.5	1.30604	100.1009	13.4306	5.202 291	.083 1035	.048 2247	48.2686
June 9	8920.5	1.30604	100.1018	13.4360	5.202 303	.083 1032	.048 2243	51.5892
July 19	8960.5	1.30604	100.1027	13.4416	5.202 317	.083 1029	.048 2240	54.9094
Aug. 28	9000.5	1.30603	100.1036	13.4475	5.202 332	.083 1025	.048 2238	58.2294
Oct. 7	9040.5	1.30703	100.1045	13.4536	5.202 350	.083 1021	.048 2236	61.5491
Nov. 16	9080.5	1.30603	100.1054	13.4599	5.202 368	.083 1017	.048 2234	64.8686
Dec. 26	9120.5	1.30603	100.1063	13.4665	5.202 388	.083 1012	.048 2233	68.1878
1966								
Feb. 4	9160.5	1.30603	100.1072	13.4732	5.202 410	0.083 1007	0.048 2230	71.5068
Mar. 16	9200.5	1.30602	100.1081	13.4801	5.202 432	.083 1001	.048 2227	74.8256
Apr. 25	9240.5	1.30602	100.1090	13.4872	5.202 456	.083 0996	.048 2224	78.1442
June 4	9280.5	1.30602	100.1099	13.4944	5.202 480	.083 0990	.048 2219	81.4626

TABLE 1-2.—*Osculating Elements for Jupiter, 1965 to 1967*—Concluded

Date	Julian date (243)	Inclination to the ecliptic, i, deg	Longitude of—		Mean distance from Sun a, astronomical units	Mean motion n, deg/sidereal day	Eccentricity of orbit, e	Mean anomaly, $L-\tilde{\omega}$
			Ascending node, Ω, deg	Perihelion, $\tilde{\omega}$, deg				
1966—Continued								
July 14	9320.5	1.30602	100.1109	13.5018	5.202 505	0.083 0984	0.048 2213	84.7808
Aug. 23	9360.5	1.30602	100.1118	13.5093	5.202 531	.083 0978	.048 2206	88.0989
Oct. 2	9400.5	1.30601	100.1127	13.5168	5.202 557	.083 0971	.048 2197	91.4168
Nov. 11	9440.5	1.30601	100.1137	13.5244	5.202 584	.083 0965	.048 2187	94.7347
Dec. 21	9480.5	1.30601	100.1146	13.5320	5.202 611	.083 0958	.048 2175	98.0525
1967								
Jan. 30	9520.5	1.30601	100.1156	13.5397	5.202 639	0.083 0952	0.048 2162	101.3701
Mar. 11	9560.5	1.30601	100.1166	13.5475	5.202 666	.083 0945	.048 2147	104.6878
Apr. 20	9600.5	1.30601	100.1176	13.5550	5.202 694	.083 0939	.048 2131	108.0054
May 30	9640.5	1.30601	100.1186	13.5626	5.202 721	.083 0932	.048 2113	111.3231
July 9	9680.5	1.30601	100.1196	13.5701	5.202 749	.083 0925	.048 2094	114.6407
Aug. 18	9720.5	1.30601	100.1206	13.5776	5.202 777	.083 0919	.048 2073	117.9584
Sept. 27	9760.5	1.30600	100.1216	13.5850	5.202 804	.083 0912	.048 2051	121.2761
Nov. 6	9800.5	1.30600	100.1226	13.5922	5.202 831	.083 0906	.048 2028	124.5939
Dec. 16	9840.5	1.30600	100.1237	13.5994	5.202 857	.083 0899	.048 2004	127.9118

TABLE 1-3.—*Secular Variations of Mean Orbital Elements of Jupiter*

[Ref. 4]

Element	Value in 1900	Formula for secular variation
Mean distance from Sun, a	5.202561 astronomical units	
Mean daily motion, n	299″.1283 sec/Julian year	
Eccentricity of orbit, e	0.04833475	$+0.000164180\ T-0.0000004676\ T^2-0.0000000017\ T^3$
Inclination to the ecliptic, i	1°18′31″.45	$-20''.506\ T+0''.014\ T^2$
Ascending node longitude, Ω	99°26′36″.19	$+3637''.908\ T-1''.2680\ T^2-0.03064\ T^3$
Perihelion longitude, $\tilde{\omega}$	12°43′15″.34	$+5795''.862\ T+3''.80258\ T^2-0.01236\ T^3$
Mean longitude of Jupiter, L	238°2′57″.32	$+10930687''.148\ T+1''.20486\ T^2-0''.005936\ T^3$

(1) Fundamental epoch is 1900 January 0.5 ephemeris time 12^h E.T. or January 0.0 (0^h E.T.) old style (prior to 1925).
(2) Elements are referred to the mean equinox and ecliptic of date.
(3) Unit of time, T, is the Julian century of 36 525 mean solar days.

TABLE 1–4.—*"Intermediate" Elements of Jupiter for Every 10th Year From 1900.0 to 2000.0*

[After ref. 8]

Year	Mean distance from Sun, a, astronomical units	Mean centennial motion, η, deg	Eccentricity of orbit, e	Inclination to the ecliptic, i, deg	Ascending node longitude, Ω, deg	Perihelion longitude, $\tilde{\omega}$, deg	Mean longitude of Jupiter, L, deg
1900	5.2029 3056	3034.752631	0.0484 9844	1.30803	99.61066	13.79686	238.98710
1910	5.2029 4245	3034.741317	.0484 9194	1.30785	99.64700	13.83025	182.42020
1920	5.2029 5349	3034.731785	.0484 8479	1.30767	99.68441	13.86178	125.85231
1930	5.2029 6362	3034.723059	.0484 7712	1.30748	99.72279	13.89141	69.36660
1940	5.2029 7280	3034.715174	.0484 6902	1.30729	99.76202	13.91909	12.79696
1950	5.2029 8098	3034.708157	.0484 6063	1.30710	99.80204	13.94479	316.30968
1960	5.2029 8814	3034.702045	.0484 5204	1.30690	99.84270	13.96849	259.73864
1970	5.2029 9423	3034.696860	.0484 4338	1.30669	99.88394	13.99020	203.25012
1980	5.2029 9924	3034.692628	.0484 3477	1.30648	99.92561	14.00990	146.67805
1990	5.2030 0314	3034.689365	.0484 2633	1.30626	99.96763	14.02761	90.18868
2000	5.2030 0591	3034.687085	.0484 1816	1.30604	100.00986	14.04334	33.61596

(1) Epoch is the beginning of each year listed, January 0.5 universal time or January 0, Greenwich mean noon.
(2) Elements are referred to the ecliptic and mean equinox of 1950.0.
(3) $\eta = n \times 365.25 \times 100$.

Inequality (found to be of a period of approximately 900 yr) of their mean longitudes was first explained by Laplace in 1784, and it remains a classical example of a long-period perturbation. Brouwer and Clemence (ref. 10) stated that the deviations in longitude from elliptic motion may reach 0°.3 for Jupiter and 0°.8 for Saturn.

THEORIES OF THE MOTION OF JUPITER

Near the end of the last century, the analytical work of Le Verrier (ref. 7) and his tables of the motion of Jupiter provided the basis for all ephemerides. But as time passed, significant differences from observations became evident. Gaillot (ref. 6) eventually corrected Le Verrier's orbit; however, a need had been felt in the U.S. for a new analytical theory and simpler tables. Hill (ref. 9) developed a theory of Jupiter's motion which is still the classic work on the subject, despite imperfections in the theory. It is based on the general perturbations methods of Hansen and treats perturbations of the second order. In the case of the large mutual perturbations of Saturn and Jupiter, Hill's theory also provides a fairly good approximation to the third order for the perturbative forces. Hill's theory and tables of Jupiter (ref. 11) have been used consistently by the Nautical Almanac Office in both prediction and theoretical work.

In France, Gaillot refined Le Verrier's analytical theory by including higher than second-order perturbations, correcting for the inadequate (too small) mass accorded to Saturn, and using more observations (1750 to 1907). Gaillot in 1913 produced corrected tables which are still used today in computing the French national ephemerides (*Connaissance des Temps*).

The development of electronic computers 2 decades ago has made possible the rapid, numerical integration of orbits of outer planets. This method of computation is much more accurate than present analytical methods. In 1951, *Tables of Coordinates of the Five Outer Planets, 1653–2060,* was produced by Eckert, Brouwer, and Clemence (ref. 3), and since 1960, *The American Ephemeris and Nautical Almanac* has derived its ephemerides of the outer planets from these accurate tables. For Jupiter, the observations made from 1780 to 1940 were used for adjusting the numerical integration.

Meanwhile, the numerical theory itself was being improved by Clemence and others. Discrepancies between theory and observation in the longitude of Jupiter, pointed out by Krotkov and Dicke (ref. 12), were removed by Clemence in 1960 (ref. 13) by assigning a new mass for Saturn which was given by Hertz (ref. 14), and by incorporating two corrections to the motion of the perihelion (neglected effects of the inner planets and a revised value of Newcomb's precession).

TABLE 1–5.—*Jupiter-Earth Opposition Data, 1940–1980*

Opposition date		Distance			Heliocentric longitude, deg	Equatorial diam, sec of arc	Stellar magnitude
Year	Day	Astronomical units	Kilometers $\times 10^6$	Miles $\times 10^6$			
1940	Nov. 3	3.981	595.2	369.8	40.72	49.4	−2.4
1941	Dec. 8	4.090	611.5	379.9	76.40	48.1	−2.4
1943	Jan. 11	4.234	633.0	393.3	110.27	46.5	−2.2
1944	Feb. 11	4.365	652.6	405.5	142.09	45.1	−2.1
1945	Mar. 13	4.444	664.4	412.8	172.60	44.3	−2.0
1946	Apr. 13	4.451	665.4	413.5	202.54	44.2	−2.0
1947	May 14	4.385	655.6	407.4	232.71	44.9	−2.1
1948	June 15	4.261	637.0	395.8	264.07	46.2	−2.2
1949	July 20	4.115	615.2	382.3	297.24	47.8	−2.3
1950	Aug. 26	3.996	597.4	371.2	332.75	49.3	−2.4
1951	Oct. 3	3.949	590.4	366.9	8.10	49.9	−2.5
1952	Nov. 8	3.994	597.1	371.0	45.83	49.3	−2.4
1953	Dec. 13	4.112	614.7	382.0	81.338	47.9	−2.3
1955	Jan. 15	4.257	636.7	395.6	114.830	46.3	−2.2
1956	Feb. 16	4.381	655.0	407.0	146.440	44.9	−2.1
1957	Mar. 17	4.449	665.2	413.4	176.777	44.3	−2.0
1958	Apr. 17	4.335	648.1	402.7	206.666	44.3	−2.0
1959	May 18	4.368	653.1	405.8	236.992	45.1	−2.1
1960	June 20	4.239	633.8	393.8	268.590	46.3	−2.2
1961	July 25	4.095	612.2	380.4	302.075	48.0	−2.3
1962	Aug. 31	3.985	595.8	370.2	337.536	49.4	−2.4
1963	Oct. 8	3.952	590.9	367.2	14.250	49.9	−2.5
1964	Nov. 13	4.010	599.5	372.5	50.842	49.1	−2.4

1965	Dec. 18	4.113	618.0	384.0	86.042	47.6	−2.3
1967	Jan. 20	4.276	639.3	397.2	119.218	46.1	−2.2
1968	Feb. 20	4.393	656.7	408.1	150.623	44.8	−2.1
1969	Mar. 21	4.501	665.4	413.5	180.878	44.2	−2.0
1970	Apr. 21	4.436	663.2	412.1	210.810	44.3	−2.0
1971	May 23	4.352	650.6	404.3	241.288	45.2	−2.1
1972	June 24	4.220	630.9	392.0	273.122	46.6	−2.2
1973	July 30	4.079	609.8	378.9	306.868	48.2	−2.3
1974	Sept. 5	3.977	594.6	369.5	342.528	49.5	−2.4
1975	Oct. 13	3.956	591.4	367.5	19.288	49.9	−2.5
1976	Nov. 18	4.023	601.5	373.8	55.744	48.9	−2.4
1977	Dec. 23	4.151	620.6	385.6	90.679	47.4	−2.3
1979	Jan. 24	4.292	641.7	398.7	123.623	45.8	−2.2
1980	Feb. 24	4.402	658.2	409.0	154.868	44.7	−2.1

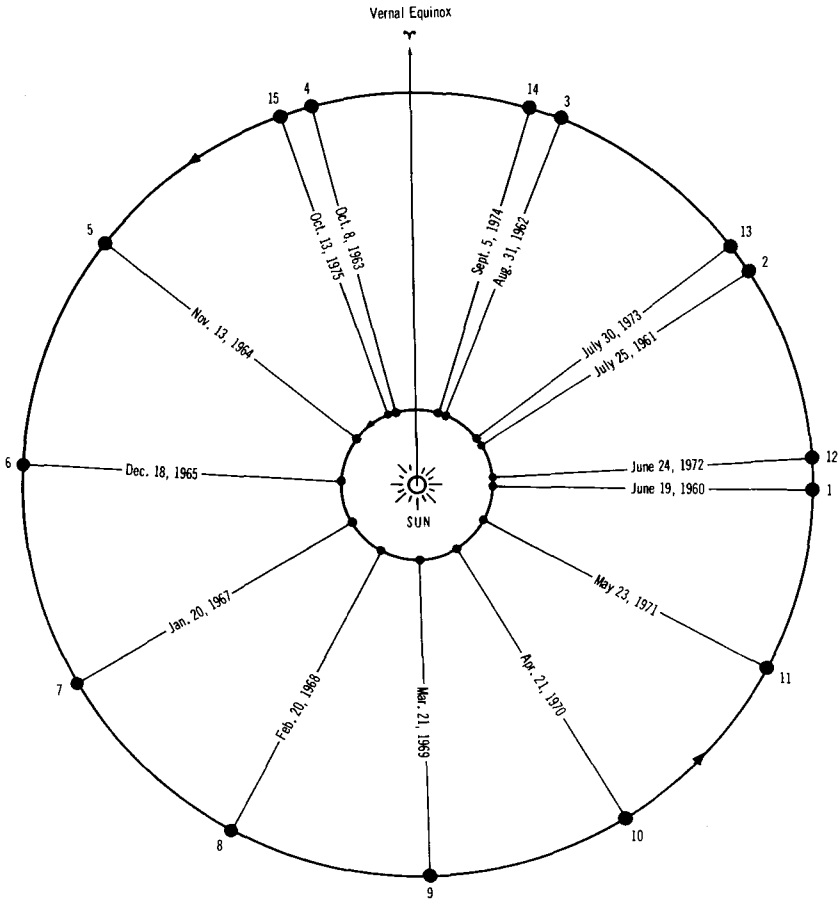

FIGURE 1-2.—Oppositions of Jupiter and Earth 1960 to 1975.

CONFIGURATIONS AND SEASONS

Oppositions and superior conjunctions of Jupiter with respect to Earth occur every 13 months. The mean synodic period of revolution (time from opposition to opposition) of the two planets is 399 days. The actual synodic period differs at most by 2 days from the mean period because of the nearly circular orbits of the two planets. Because of the large dimension of Jupiter's orbit, the distance at opposition between the two planets can vary by some 46.6 million miles. This distance ranges from 367 at perihelic oppositions to 413 million miles at aphelic oppositions. Table 1–5 presents the data for all oppositions of Jupiter-Earth from 1940 to 1980. It was constructed partly from data calculated by Heath (ref. 15), partly by interpolation-calculation from data found in *Planetary Coordinates* for the

years 1940 to 1980 (refs. 16 and 17), and supplemented with information from *The American Ephemeris and Nautical Almanac* volumes available to the year 1966. For exact times of oppositions, a correction for the effect of light-time should be incorporated.

Figure 1–2 illustrates schematically the series of successive Earth-Jupiter oppositions from 1960 to 1975. The 12-year cycle of oppositions around the Jovian orbit is immediately apparent, with 11 successive oppositions at 13-month intervals. The slight inclination of the equator of Jupiter to its orbit and the near circularity of the orbit should result in very weak seasonal effects. These effects have not been detected with certainty.

2
Mass

JUPITER'S MASS is only about one-thousandth that of the Sun but more than twice the combined masses of all the other planets. Compared to Earth, Jupiter is huge, with a mass some 318 times greater. Considering the remarkably low density, which is only a quarter that of Earth, its size is even more outstanding. (Only Saturn has a lower density.) Because of its mass, Jupiter causes significant gravitational perturbations on other members of the solar system, particularly on its neighboring planets, Mars and Saturn; on the closer swarm of minor planets or asteroids; and on occasional passing comets. These perturbations have been used in the determination of Jupiter's mass. Table 2–1, which lists reciprocal mass values obtained over a century, indicates that the mass of Jupiter is 1/1047.4 that of the Sun (refs. 10 and 18–34). This value is accurate within at least 10^{-4}. From discussions of the many available values derived since the classic effort of Newcomb (ref. 35), this value has been established as the weighted mean. *The American Ephemeris and Nautical Almanac* for 1965 used Newcomb's 1/1047.355 value for the mass of Jupiter, which includes the atmosphere and satellites.

Two general methods used for determining Jupiter's mass are: (1) the measurements of perturbations of the motions of planets, or minor planets, and (2) the scaling of the orbits of Jupiter's satellites. Earlier determinations of mass, based on the mean distances of Galilean satellites from Jupiter, were considered suspicious because of systematic errors inherent in the micrometric measurements. For the scaling of these satellite orbits, the heliometer is more reliable than the filar micrometer. De Sitter (refs. 32 and 36) used the best heliometer determinations for his weighted mean.

Undoubtedly the most reliable values of Jupiter's mass are those derived from its perturbative effect upon certain minor planets when their orbits are precisely known. The determination from perturbations of some of the innumerable minor planets (over 2,000 have been cataloged) deserves special attention. According to Newcomb (ref. 29) for accurate calculations the choice of a suitable minor planet should be governed by several conditions:

(1) Eccentricity—The minor planet's orbit should have large

TABLE 2–1.—*Mass Determinations of Jupiter*

Method	Author	Relative mass (reciprocal) (Sun=1)
Vesta	Encke (ref. 18)	1050.36
Satellite J–IV	Airy (ref. 19)	1046.77
Satellites J–I to J–IV	Bessel (ref. 20)	1047.871 ± 0.235
Satellites J–III and J–IV	Jacob (ref. 21)	1047.54
Egeria	Hansen (ref. 22)	1051.12
Faye's comet	Möller (ref. 23)	1047.788 ± 0.275
Themis	Kruger (ref. 24)	1047.538 ± 0 192
Satellites J–I to J–IV	Schur (ref. 25)	1047.232 ± 0 365
Winnecke's comet	Von Haerdtl (refs. 26 and 27).	1047.1752 ± 0.0136
Saturn	Hill (ref. 28)	1047.378 ± 0.121
Polyhymnia	Newcomb (ref. 29)	1047.34
Weighted mean	Newcomb (ref. 29)	1047.355 ± 0.065
Vesta	Leveau (ref. 30)	1045.63
Vesta	Leveau (ref. 31)	1046.04
Weighted mean	De Sitter (ref. 32)	1047.40 ± 0.03
Discussion	Makemson (ref. 33)	1047.4 ± 0.1
Weighted mean (rediscussion of Newcomb's material).	Brouwer and Clemence (ref. 10).	1047.39 ± 0.03
Discussion of all values	Clemence (ref. 34)	1047.41 ± 0.02

eccentricity so that the planet, at aphelion, approaches Jupiter and then Earth at perihelion; the perturbations in true longitude are maximized during perihelion passage.

(2) Inclination—The minor planet's orbit should be only slightly inclined to the orbit of Jupiter.

(3) Reliability—The minor planet's orbit should be well determined from observations over many revolutions so that the perturbations can be separated completely from the corrections to the orbital elements.

A rare circumstance which is most favorable to the determination of Jupiter's mass is the conjunction of Jupiter and the minor planet at aphelion followed by an opposition of Earth and the minor planet near perihelion. Such a determination was made with the minor planet Themis by Kruger (ref. 24) and with Polyhymnia by Newcomb (ref. 29).

Hill (ref. 37) suggested that an accurate determination of Jupiter's mass may be made from the study of the motions of minor planets with periods of revolution nearly half the period of Jupiter, and recommended in particular 12 asteroids which exhibit large long-

period inequalities in the mean longitude with periods ranging from 60 to 120 years. These 12 asteroids are now under observation and study at the U.S. Naval Observatory, Washington, D.C.

Griqua, a recently discovered asteroid, was proposed by Rabe (ref. 38) as highly suitable for determining Jupiter's mass since its motion undergoes enormous perturbations by Jupiter on its highly eccentric orbit which can bring it as close as 1.3 astronomical units to Earth.

Determinations of mass made by measuring the orbits of comets are unreliable because there are large systematic errors inherent in the physical constitution of comets. In addition to the uncertainties of their ephemerides, comets are unsuitable for Jupiter's mass determination because it is nearly impossible in such a diffuse, nonspherical body to locate its exact center of gravity. It is usually assumed in observations that a comet's center of gravity coincides with its center of light, but this is not necessarily true. The advantage in using comets for the determination of Jupiter's mass lies in the unusual magnitude of the perturbations. The masses of comets are extremely low (at best 10^{-4} that of Earth), and when they approach Jupiter, their orbits are disturbed markedly, sometimes changing from elliptic or parabolic to a hyperbolic orbit. Porter (ref. 39) lists more than 20 examples of such extreme perturbations, traced back by computers following Strömgren's pioneering work (ref. 40). Also, many so-called short-period comets (with periods of less than 10 yr), belonging to "Jupiter's family," were shown to have been most probably diverted from former long-period orbits through Jovian capture (see ref. 41).

3
Diameter and Shape

THE LARGE APPARENT DISK of Jupiter has been measured many times in the last century with both filar micrometer and heliometer. These measurements pertain to the visible planetary surface, that is, the top of a very dense cloud layer. The actual depth of this cloud layer is unknown, although theoretical estimates have been made. (See ch. 14.) From these estimates one can infer the possible diameter of the solid or liquid globe. The diameter of the visible globe of Jupiter is about 11 times that of Earth.

The shape of Jupiter's visible surface as revealed by any low-powered telescope is definitely oblate. Its apparent or optical oblateness is approximately 1/16 and is exceeded only by that of Saturn.

The shape of the actual solid (or liquid) surface is discussed in a subsequent subchapter. The dynamical oblateness, as determined from perturbations of the motion of close satellites, more than the optical oblateness gives a clue to the shape of this surface.

DIAMETER MEASUREMENTS

The measurements up to 1900 (still considered valid) were analyzed and summarized by See, who added his own results to them (ref. 42). The more reliable values of equatorial and polar angular diameters at 5.20 astronomical units are listed in table 3–1, which also shows the derived optical flattening values (refs. 43–55). Later, Rabe (ref. 48) analyzed some old and new filar and double-image micrometer measurements, including his own, and proposed corrected angular values of 38″.09 and 35″.76 for the equatorial and polar diameters at 5.2028 astronomical units (Jupiter's mean solar distance). However, since 1920, *The American Ephemeris and Nautical Almanac* has adopted the values obtained by Sampson (ref. 55) from the duration of eclipses of the Galilean satellites. These values are 37″.86 and 35″.33 at 5.2028 astronomical units if one takes 1 astronomical unit$=1.49504\times10^8$ kilometers.

In linear measure, Sampson's angular diameters correspond to about 71 387 and 66 618 kilometers for the equatorial and polar radii;

TABLE 3-1.—*Diameter Measurements and Optical Flattening*

Method	Author	Equatorial angular diam (at 5.20 A.U.), sec of arc	Polar angular diam (at 5.20 A.U.), sec of arc	Optical flattening (reciprocal)
Heliometer	Bessel (ref. 43)	37. 60	35. 21	15. 73
	Winnecke (ref. 43)	37. 43	35. 11	16. 10
	Schur (ref. 43)	37. 42	35. 10	16. 13
	Hartwig (ref. 44)	37. 447	35. 316	17. 57
Double-image micrometer.	Kaiser (ref. 45)	37. 54	35. 15	15. 65
	Kaiser (ref. 46)	37. 65	35. 41	16. 81
	Wirtz (ref. 47)	38. 254	35. 986	16. 87
	Rabe (ref. 48)	36. 20	34. 08	17. 07
Filar micrometer	Struve (ref. 49)	38. 33	35. 54	13. 74
	Secchi (ref. 50)	38. 35	35. 96	16. 05
	Schmidt (ref. 51)	38. 91	36. 42	15. 63
	Hough (ref. 43)	38. 96	36. 66	16. 94
	Barnard (ref. 52)	38. 522	36. 112	15. 98
	Pickering (ref. 43)	38. 03	35. 67	16. 11
	Dyson (ref. 53)	38. 339	35. 997	16. 37
	Lewis (ref. 53)	38. 219	36. 017	17. 36
	See (ref. 42)	38. 401	35. 921	15. 53
	Lohse (ref. 54)	38. 343	36. 031	16. 58
	Rabe (ref. 48)	38. 29	35. 97	16. 50
Average from discussion (filar and double-image).	Rabe (ref. 48)	38. 09	35. 76	16. 35
Timing satellites' eclipses.	Sampson (ref. 55)	37. 86	35. 33	14. 96

while Rabe's angular diameters correspond to radii of ~71 820 and ~67 247 kilometers.

SHAPE

The telescopic image of Jupiter yields an oblateness value of the disk called optical flattening. The orbital characteristics of certain appropriate satellites yields a flattening value of the gravitational equipotential surface which is called dynamical flattening.

The values of both optical and dynamical flattenings for Jupiter do not significantly differ, whereas for Mars, the optical flattening value is twice that of the dynamical. Sampson's diameters give an optical flattening value of only 1/15.0. Rabe found an optical flattening of 1/16.35 from critical averaging processes, and this value will be used here. Adams (ref. 56) and Cohn (ref. 57) from the motion of the

perijove of the fifth satellite of Jupiter, gave dynamical flattening values of 1/15.55 and 1/15.50. Later Brouwer and Clemence (ref. 10), from the precession of its ascending node found the value to be 1/15.34 which is used here.

Calculations have been performed here for the variation of radius with latitude, both for the visible, clouded globe (where the optical flattening value is to be used) and for the actual solid (or liquid) globe of Jupiter (where it is preferable to use the dynamical flattening value).

RADII OF THE VISIBLE GLOBE AND OF THE SOLID GLOBE

Because the oblateness of Jupiter is pronounced, the radius varies markedly with latitude. Retaining only terms to the first order in the oblateness formula, the radius of an oblate spheroid varies with planetocentric latitude according to:

$$R_\phi = R_{eq}(1 - \epsilon \sin^2 \phi)$$

where

R_{eq} equatorial radius

ϕ planetocentric, or zenocentric latitude (angle between a radius vector to the point and the equatorial plane)

ϵ flattening or oblateness

R_ϕ radius at latitude, ϕ

For the calculations, the value of the equatorial radius of the visible globe, R^v_{eq}, derived from Sampson's angular diameter of 37″.86 was selected as a basis, that is, R^v_{eq}=71 387 kilometers.

The value of the equatorial radius of the actual solid globe, R^s_{eq}, depends on the value assumed for the atmospheric depth, D. The latter depth is substracted from the Sampson value for the radius of the visible globe; thus, $R^s_{eq}=R^v_{eq}-D$. Five values of the atmospheric depth, D, were selected for the calculations: 100, 380, 500, 750, and 4250 kilometers. The calculations of the radius, R_ϕ, at any latitude on the surface of both the visible and the solid globes are performed through use of the following two values of the flattening, respectively:

$$\epsilon_{opt}=0.06117 \qquad \text{(Rabe)}$$

and

$$\epsilon_{dyn}=0.06518 \qquad \text{(Brouwer and Clemence)}$$

The results of the calculations are presented in table 3–2.

TABLE 3–2.—*Radius of Jupiter at Various Latitudes*

Zenocentric latitude, ϕ, deg	Radius at latitude, ϕ, of visible globe, R_ϕ^v (based on $\epsilon_{opt}=0.06117$)	Radius at latitude, ϕ, of solid globe R_ϕ^s, km (based on $\epsilon_{dyn}=0.06518$) atmospheric depth, D					
		0	100	380	500	750	4250
90	67 020	66 734	66 641	66 379	66 267	66 033	62 761
75	67 313	67 046	66 952	66 689	66 576	66 342	63 054
60	68 825	67 898	67 802	67 536	67 422	67 184	64 569
45	69 204	69 060	68 964	68 693	68 577	68 335	64 949
30	70 295	70 223	70 125	69 850	69 732	69 486	66 043
15	71 094	71 075	70 975	70 697	70 577	70 328	66 844
0	71 387	71 387	71 287	71 007	70 887	70 637	67 137

MEAN RADIUS AND ECCENTRICITY

The mean radius of an oblate spheroid is given by:

$$\overline{R}=\frac{2R_{eq}+R_{po}}{3}$$

$$=\left(1-\frac{\epsilon}{3}\right)R_{eq}$$

The mean radius of Jupiter's visible globe is 70 035 kilometers, while that of its solid globe overlaid by 500-kilometer high cloud cover is 69 347 kilometers.

For some investigations, it is desirable to know the eccentricity, e, of the meridional cross-section of the planet, that is,

$$e=\frac{\sqrt{R_{eq}^2-R_{po}}}{R_{eq}}$$

This quantity is related to the flattening,

$$\epsilon=\frac{R_{eq}-R_{po}}{R_{eq}}$$

by the relationship, $e=\sqrt{\epsilon(1-\epsilon)}$. In the case of Jupiter, e is equal to 0.23146, if ϵ_{opt} is used, and is equal to 0.24684 if ϵ_{dyn} is used.

DYNAMICAL FLATTENING

The dynamical flattening or dynamical oblateness is understood to be the oblateness of figure calculated from the motions of the pericenter and ascending node of a close satellite.[1] These motions depend on the parameters that arise in the expression for the gravitational potential of a rotating planet. The assumption that the surface of the planet is an equipotential surface results in a relation between the oblateness of figure and these parameters in the gravitational potential. If the effect of the atmosphere on the gravitational parameters may be neglected, it can be assumed that the dynamically determined oblateness is that of the solid or liquid boundary surface of the planet.

The dynamical flattening of Jupiter can be calculated empirically with fairly good accuracy from the perturbations that it exerts on the

[1] This definition was proposed by D. Brouwer in a private communication (Nov. 1965).

motion of its satellites. The orbit of a planetary satellite is subject to three principal perturbations: (1) the gravitational effect resulting from the oblateness or equatorial bulge of the primary, that is, the deviation from spherical symmetry of the primary's gravitational potential; (2) the gravitational attraction of the Sun; and (3) the gravitational attraction of other satellites of the same planet. The importance of oblateness is indicated by the ratio,

$$J\left(\frac{R_{eq}}{a}\right)^2$$

where

the gravitational potential coefficient, $J=\frac{3}{2}\cdot\frac{C-A}{M_p R_{eq}^2}$

and

R_{eq}	equatorial radius of the primary
a	semimajor axis of the satellite's orbit
M_p	mass of the primary
C and A	moments of inertia of the primary with respect to the polar axis (rotation axis) and to any axis in the equatorial plane

The coefficients J and K used in this chapter are defined by the classical expansion (in a series of spherical harmonics) of the external gravitational potential of a planet:

$$V(r,\phi)=-\frac{GM}{r}\left[1-\frac{2}{3}J\left(\frac{R_{eq}}{r}\right)^2 P_2(\sin\phi)+\frac{4}{15}K\left(\frac{R_{eq}}{r}\right)^4 P_4(\sin\phi)-\ldots\right]$$

where

r	radial distance from planet center
ϕ	planetocentric latitude
P_n $(\sin\phi)$	Legendre polynomials
M	planet's mass
G	constant of gravitation

Instead of J, K, the more general coefficients J_n are often used:

$$J_2=\frac{2}{3}J \qquad\qquad J_4=-\frac{4}{15}K$$

(Use of J_2 and J_4 is made later in ch. 7.)

The magnitude of solar perturbation is indicated by the ratio,

$(n_s/n_p)^2$, of the squares of the mean daily motions, n_s and n_p, of satellite and primary, respectively. The magnitude of another satellite's perturbation is on the order of m_s/M_p, where m_s is the mass of the perturbing satellite. (See ref. 10.)

The following application of these calculations is given for Jupiter's innermost satellite, designated J–V. The relative order of magnitude of the perturbations described above is approximately 10^5, 1, and 10^3; thus, the total perturbation is primarily caused by Jupiter's oblateness or nonsphericity. According to Brouwer, since the orbital eccentricity and inclination of J–V to Jupiter's equatorial plane are small, the motion (precession) of the node in the equatorial plane is given (if θ is the longitude of the node) by:

$$\frac{d\theta}{dt}=-n_s\left(J\frac{R_{eq}^2}{a^2}-\frac{3}{2}J^2\frac{R_{eq}^4}{a^4}+K\frac{R_{eq}^4}{a^4}\right) \tag{3-1}$$

where the gravitational coefficient, K, is related to the dynamical oblateness, ϵ, by

$$K=6\left[\left(J+\frac{\phi_1}{2}\right)(1+J)-\epsilon\right] \tag{3-2}$$

and

$$\phi=\frac{(1-\epsilon)}{GM_p}\omega^2R_{eq}^3$$

that is, $(1-\epsilon)$ times the ratio of the centrifugal force to the gravity force at the equator. Observation of the motion of J–V's node, $d\theta/dt$, leads to a relationship between J and K. Similar data for the orbits of the Galilean satellites after allowance is made for mutual perturbations (and in the case of J–V, correction for the solar perturbation) leads to a value of J alone, while the terms in K are negligible. The motion of J–V's node (eq. 3–1) can then yield a value of K, from which ϵ is obtained through equation (3–2).

Using the following values of the constants, Brouwer and Clemence calculated the dynamical oblateness, ϵ, of Jupiter as:

$\frac{d\theta}{dt}=-2^\circ.5041\pm0^\circ.0010$ per mean solar day (ref. 58)

$n_s=722^\circ.63173$ per mean solar day (ref. 58)

$J=0.02206\pm0.00022$ (ref. 59)

R_{eq} from $98''.489$ at 1 astronomical unit (ref. 55)

a from $250''.06$ at 1 astronomical unit (from Kepler's third law, modified to include the effects of disturbing forces)

The equation for the motion of the node (eq. 3–1) gives coefficient, $K=0.00253\pm0.00141$. With the following additional constants,

$\omega=2\pi/P=2\pi/9^{h}52^{m}$ (angular rate of rotation, ω, from period of rotation, P, taken as the mean of Systems I and II periods)
$M_p=1.989\times10^{33}$ g/1047.39 (ref. 10)
$G=6.668\times10^{-8}$ dyne cm^2 g^{-1} (constant of gravitation)

The equation (3–2) relating K, J, R_{eq}, and ϵ yields $\epsilon_{dyn}=0.06518$, that is, a dynamical oblateness or flattening of about one-fifteenth ($\epsilon=1/15.34$) for Jupiter.

4

Rotation: Rate and Axis

ROTATION RATE

JUPITER SPINS ON ITS AXIS in a general rotation period of nearly 10 hours which is the shortest rotation period of any of the nine major planets. Early telescopic observation by Cassini in about 1690 revealed not only this very rapid rate, but also that the cloud bands concealing the actual surface rotated at slightly different rates. The equatorial region, for example, was found to rotate some 5 minutes faster than most of the other regions, that is, in about 9 hours, 50.5 minutes. The question arose as to what was the actual rotation period of the surface (solid or liquid) beneath the thick clouds. Although the different rotation rates of the various bands seemed to have maintained some constancy throughout 250 years of observation, this question remained unanswered. It was only with the discovery in 1955 of strong radio-emission sources on Jupiter, apparently rotating with the planet at a constant rate, that modern observations could provide answers. The "radio-period" of rotation was found to be 9 hours 55.5 minutes.

The three general methods used for determining the rotation rate of Jupiter are: (1) the optical (or visual) method, long used for the cloud surface; (2) the spectroscopic (or Doppler shift) method for the upper atmosphere, which is seldom used; and (3) the radio-emission method, used extensively today. These methods and their results are reviewed according to importance.

OPTICAL PERIODS.—The optical method consists in the timing of successive transits of well-defined and long-lived markings (spots, ends of streaks, etc.) rotating across the central meridian of the Jovian disk. The observation is usually made visually, although photography can be used if the markings are large enough to be resolved. Visual measurements are easily made because of the large size of the Jovian disk, and many reliable results have been obtained from amateur astronomers.

What is measured, however, is the rotation period of a cloud feature which may be endowed with its own erratic motions within the cloud band in which it lies. Hopefully, these motions are relatively small

248-761 O-67—3

compared to the general drift observed. However, it is apparent that measurements are necessary of many selected markings at the same latitude (or in the same band, at least) to obtain a representative average period. Such a period, even when determined accurately, is only valid for the time of the determination, since the clouds and cloud bands are slowly changing. Variations in the rotation period were found to be usually very slight for the Jovian bands in their normal behavior, when there were no obvious disturbances.

The results of many years of observations by both amateurs and professionals, who systematically applied the method since about 1880, were compiled by Peek (ref. 60). Table 4–1, a summary of the more reliable determinations, lists the average rotation periods of the Jovian bands in various latitudes and names the different currents which may be distinguished, even within one band.

The results separate into two main rotation periods, the equatorial or faster one and the nonequatorial or slower one. For purposes of convenience for observers of Jovian cloud markings, two reference systems of longitudes based on the two basic rates of rotation found optically were devised toward the end of the last century. These two systems, inaugurated by Marth (ref. 61) in the construction of his last physical ephemeris for Jupiter, are still perpetuated by all national Almanac Offices because their use proved to be very practical in physical observations of Jupiter's visible surface. The reference systems are: System I, used for all markings and features found in the Equatorial Zone or on its boundaries, has an adopted rotation period $P_1 = 9^h50^m30^s.003$, and an adopted longitude of the central meridian $\tilde{\omega}_1 = 47°.31$ at the adopted epoch (common to both systems) $t_0 =$ Greenwich mean noon, July 14, 1897. System II, used for all markings and features outside the conventional limits of the "Great Equatorial Stream" (roughly 10° N and S in latitude), has an adopted rotation period $P_2 = 9^h55^m40^s.632$, and an adopted longitude of the central meridian $\omega_2 = 96°.58$ at the adopted common epoch stated. These rotational systems are listed in more detail in table 4–2 which provides comparison with the modern radio-longitudes reference system known as System III (refs. 61 and 63).

SPECTROSCOPIC METHOD.—The measurement of the Doppler shift of Fraunhofer lines of the solar spectrum reflected by a clouded planet of high albedo is possible in the case of Jupiter because of its rapid rotation. The results are in agreement with those of the other two methods, within the limits of its accuracy, of 4 to 5 minutes, in the period of nearly 10 hours. This method was used for both Jupiter and Saturn early in this century at the Lowell Observatory, especially by Slipher. It is seldom used today because of its low accuracy and experimental difficulties.

TABLE 4–1.—*Summary of Optical Rotation Periods*

[After ref. 60]

Situation and/or name of current	Approx latitude, deg	Change of longitude in 30 days		Rotation period			Number of apparitions
		λ_1, deg	λ_2, deg	hr	min	sec	
N Polar Current	+90 to +47		+1	9	55	42	19
NNN Temperate Belt (NNN Temperate Current).	+43		−15	9	55	20	9
NN Temperate Belt and Zone (NN Temperate Current A).	+40 to +36		+1	9	55	42	35
S edge of NN Temperate Belt (NN Temperate Current B).	+35		−78	9	53	55	6
N edge of N Temperate Belt and S Part of N Temperate Zone (N Temperate Current A).	+33 to +29		+18	9	56	5	24
Middle of N Temperate Belt (N Temperate Current B).	+27		−105	9	53	17	6
S edge of N Temperate Belt (N Temperate Current C).	+23	−62		9	49	7	[a]6
N Tropical Zone and N part of N Equatorial Belt (N Tropical Current).	+22 to +14		−9	9	55	29	52
Middle of N Equatorial Belt 1898–1900	(?)		−6	9	55	32	2
Middle of N Equatorial Belt 1927–1948	+13		−67	9	54	9	7
S edge of N Equatorial Belt and N part of Equatorial Zone (Great Equatorial Current: Northern Branch).	+10 to +3	−4		9	50	[b]24	47
Middle of Equatorial Zone (Great Equatorial Current: Central Branch).	+3 to −3	−4		9	50	[b]24	14

See footnotes at end of table.

TABLE 4-1.—*Summary of Optical Rotation Periods*—Concluded

[After ref. 60]

Situation and/or name of current	Approx latitude, deg	Change of longitude in 30 days		Rotation period			Number of apparitions
		λ_1, deg	λ_2, deg	hr	min	sec	
N edge of S Equatorial Belt and S part of Equatorial Zone (Great Equatorial Current: Southern Branch).	−3 to −10	A−3	------	9	50	[b]26	39
		B+38	------	9	51	21	11
S edge of S Equatorial Belt (normal).	−19	--------	−1	9	55	39	13
S edge of S Equatorial Belt (Northern Branch of Circulating Current).	−19	--------	+132	9	58	43	6
S Tropical Zone	−21 to −26	--------	−3	9	55	36	7
The Great Red Spot, 1872–1948.	−22	--------	−2	9	55	38	64
N edge of S Temperate Belt (Southern Branch of Circulating Current).	−27	--------	−116	9	53	2	5
S Temperate Belt (S Temperate Current).	−29	--------	−15	9	55	20	47
S edge of S Temperate Belt to SS Temperate Zone (SS Temperate Current).	−31 to −45	--------	−25	9	55	7	42
SSS Temperate Belt and S Polar Region.	−45 to −90	--------	−8	9	55	30	5

[a] Not included here are the values for 1880, 1891, and 1892.

[b] Although these three mean values are almost identical, in any given year the rates of drift of the different branches of the Great Equatorial Current may be quite independent of one another.

RADIO PERIOD AND LONGITUDE SYSTEM.—In the mid-1950's it was noticed that decameter radio bursts were emitted by Jupiter and could be roughly correlated with position on the planet (refs. 62 and 64). It, therefore, became possible to define a new rotation system, assuming that the radio signals were emitted from fixed locations. Statistical analysis, using histograms of probability-of-occurrence as a function of the longitude of the central meridian in

TABLE 4–2.—*Systems of Longitudes for Physical Observations of Jupiter*

Reference	Longitude reference system	Period of rotation, P	Angular rate of rotation, R, deg/day	Longitude at epoch for central meridian, ω_0, deg	Epoch to—	
					Julian date	Calendar date
Marth (ref. 61)------	System I (optical)-----	$9^h50^m30^s.003$	877. 90	47. 31	241 4120. 0	1897, July 14 0^h U.T.
Marth (ref. 61)------	System II (optical)----	$9^h55^m40^s.632$	870. 27	96. 58	241 4120. 0	1897, July 14 0^h U.T.
Morrison (ref. 63)----	System III (radio) (1957.0).	$9^h55^m29^s.37$	870. 544	108. 02	243 5839. 5	1957, Jan. 1 0^h U.T.

System II, of radio signals received at ~18 Mc/sec showed three sources at three different longitudes. The first analysis, made by Carr et al. (ref. 65) from all data available up to those obtained by Shain (ref. 66), resulted in a period of $9^h55^m28^s.8$. A provisional System III was defined as having this period and coinciding with System II in longitude of the central meridian at the epoch 1957, January 1, at 0^h universal time. Three years later Carr et al. (ref. 67), after plotting the 1959 and 1960 data and noticing a slight shift, revised the period to $9^h55^m29^s.35$. An independent analysis by Douglas (ref. 68) of all previous data yielded almost the same value ($9^h55^m29^s.37$).

In 1962, the International Astronomical Union (I.A.U.) (Commission 40) adopted this last period in the definition of an official system, known as System III (1957.0), which is otherwise identical with the provisional system. The period of System III is $11^s.26$ shorter than that of System II. This corresponds to a gradual displacement in longitude of the central meridian since the epoch 1957, January 1.0 of almost exactly 100° per year. A simple conversion formula is given by Smith et al. (ref. 69) who summarized the state of knowledge of radio rotational periods. If ΔT is the difference in seconds between periods T_1 and T_2, then the longitude displacement, $\Delta\lambda$, in degrees per year is given by: $\Delta\lambda = 876 \frac{T}{T_1 T_2}$. A comparison between the radio-longitude and optical systems used today is presented in table 4–2. Radio-longitude ephemerides from 1961 to 1967 in System III (1957.0) for use by all radio observers of Jupiter have been computed by Morrison (ref. 63) at the U.S. Naval Observatory.

CONSTANCY OF THE RADIO-PERIOD.—If it is assumed that the radio sources used are small (relative to the disk) and fixed (relative to each other) so that a period of rotation is deduced readily from their successive positions; then it is reasonable to assume a constant period.

This constancy was the case until 1961 when reduction of the records by Six (ref. 70) showed a suspicious drift in System III (1957.0), and reduction of the 1962 records by Douglas and Smith (ref. 71) established a persistent longitude drift of some 10° per year, or some $0^s.8$ difference in the period of rotation. Smith et al. (ref. 69) replotted the 1951 to 1963 data in System III (1957.0) and found that the drift had started in early 1960. He calculated the rate of the drift to be 10°.45 per year, or a change in period of $1^s.17$.

Because of its magnitude and compared to the irregularities in the Earth's rate of rotation (only msec.), this change was surprising. The generally accepted explanation is that a change in the core occurred and, if the magnetic field originates in the core, it is plausible

that the sources of decametric radiation on Jupiter are changed as well. Another recent interpretation suggests a coupling between the planet's magnetic field and the interplanetary medium (ref. 72). Also, it is possible that the change is virtual; that is, it is linked to the variations in the focusing properties of the Jovian ionosphere, magnetosphere, or even the interplanetary medium (Lebo, 1964, in an unpublished dissertation quoted by Smith et al. (ref. 69). However, Smith remarked that the change is not a sudden shift in position but rather a steady drift. In this connection, an interesting observation was made concerning the Great Red Spot. Its optical period changed also, lengthening by $1^{s}.01$ per year at approximately the same time or just before. It is possible that these two phenomena are related.

ROTATION AXIS

The position of Jupiter's equatorial plane is readily derived from continued observations of the parallel bands. *The American Ephemeris and Nautical Almanac* for 1965 used the adopted position of the axis as derived for 1750 by De Damoiseau (ref. 73). The coordinates (in right ascension, α, and declination, δ) of the North Pole of Jupiter at the beginning of any year, t, are written

$$\alpha_0 = 17^{h}\ 52^{m}\ 00^{s}.84 + {}^{s}.0247\ (t - 1910.0)$$

$$\delta_0 = +64°33'34''.6 - 0''.60\ (t - 1910.0)$$

The corresponding position of Jupiter's equatorial plane is given by the *Connaissance des Temps* for 1960 from the revision by Souillart (ref. 74) of De Damoiseau's early work. Taking as reference plane Jupiter's orbit of 1750, the inclination of its equator, I, and the longitude of its ascending node, θ, (counted from the mean equinox of date) are:

$$I = 3°4'5''.0 + 0''.0249\ (t - 1750.0)$$

$$\theta = 313°21'55''.0 + 50''.3357\ (t - 1750.0)$$

5
Mean Density

THE MEAN DENSITY OF AN OBLATE SPHEROID is approximately the same as that of a sphere having a radius equal to the mean radius of the spheroid if the oblateness is sufficiently small. Including only first-order terms in the oblateness, the mean density is

$$\bar{\rho}=(1+\epsilon)\, M/\frac{4}{3}\pi R_{eq}^3$$

where

M	mass
R_{eq}	equatorial radius
ϵ	oblateness

Employing the dynamical oblateness, $\epsilon=0.06518$ and the values $M=1.899\times10^{30}$ grams and $R_{eq}=71\ 387$ kilometers, the mean density of Jupiter is

$$\bar{\rho}=1.327\pm0.008\ \text{g cm}^{-3}$$

The principal uncertainty is in the equatorial radius. Such a low density is typical of all the Jovian planets, and is one of the principal physical characteristics distinguishing them from the terrestrial planets.

6
Surface Gravity

THE MARKED DEPARTURE OF THE GLOBE of Jupiter from sphericity and its rapid rate of axial rotation introduce necessary correction terms into the expression for the net surface gravitational acceleration. To the first order in the oblateness, the value of gravity at the equator is given by

$$g_{eq}=(GM/R_{eq}^2)[1+\epsilon-3\omega^2(R_{eq}^3/2GM)]$$

where

G	constant of universal gravitation$=6.670\times10^{-8}$ dyne cm g^{-2}
M	mass
R_{eq}	equatorial radius
ϵ	oblateness
ω	angular velocity of rotation
g_{eq}	gravitational acceleration at the equator

To the same degree of accuracy, the gravity at any latitude, ϕ, is

$$g_\phi=g_{eq}\left[1+\left(\frac{5\omega^2R_{eq}^3}{2gM-\epsilon}\right)\sin^2\phi\right]$$

The latitude used is the planetocentric or zenocentric (analogous to geocentric latitude), that is, the angle between a radius vector to the surface point in question and the equatorial plane. Uncertainty in the rate of axial rotation, which is accurately known for the cloud layer but is unknown for the solid surface, is the main difficulty encountered in computing the surface gravity of Jupiter. It can be assumed, for this computation that the rotation rate for the solid globe does not differ much from that of the cloud layer above. Considering that observed periods of the three principal latitude zone systems in the cloud layer differ by less than 1 percent, a mean of these periods can be adopted to represent the period of the globe. Following Brouwer and Clemence (ref. 10), a period of 9^h52^m is adopted, corresponding to angular velocity 1.769×10^{-4} rad sec^{-1}. Table 6–1 gives the resulting gravity of Jupiter in centimeter-gram-second (cgs) and terrestrial units (g) at 15° intervals of zenocentric latitude at the visible surface.

TABLE 6–1.—*Gravitational Acceleration at Jupiter's Visible Surface* [a]

Zenocentric latitude, ϕ (north or south), deg	Absolute value of gravity, g_ϕ, cm sec^{-2}	Relative value of gravity, terrestrial "g" units [b]
0	2312	2.36
15	2358	2.40
30	2404	2.45
45	2496	2.55
60	2589	2.64
75	2656	2.71
90	2681	2.74

[a] Based on the same values of the constants (R_{eq}, M, and ϵ) used previously for mean density and $P=9^h52^m$.

[b] 1 terrestrial "g" unit=980.6 cm sec^{-2}.

It should be noted that the centrifugal force term, $\omega^2 R_{eq}^3/GM$ (frequently denoted m), in the expression for g_ϕ exceeds the oblateness term at all latitudes for Jupiter. At the equator, contributions to the net gravity are 2485, 162, and −335 cm sec^{-2} from the spherical, first-order oblateness, and centrifugal force terms, respectively. These terms have not always been properly introduced in the literature; for example, Peek (ref. 60) quotes values of gravity at the equator and pole of Jupiter which differ by only 1 percent or one-tenth the difference found here.

The theory of Radau and Darwin (summarized by ref. 75) concerning a rotating planet in hydrostatic equilibrium shows that $m=2\epsilon$ for a high degree of central mass concentration, and $m=4\epsilon/5$ for constant internal density. Applying these extreme cases to Jupiter, $g_{eq}=2261$ and 2429 cm sec^{-2}. The close agreement between the former and actual values for Jupiter at the equator indicates a high concentration of mass toward the center of the planet; this distribution is supported by detailed mathematical models of the interior.

7
Internal Structure

INTRODUCTION

THERE IS NO OBSERVATIONAL EVIDENCE for the composition of the solid (and liquid) part of Jupiter. All suppositions relating to the composition of the planet depend on the following:

(1) The known planetary parameters.—These are the mass, the radius, and the second- and fourth-harmonic coefficients of the gravitational field (J_2 and J_4).

(2) An assumed equation of state of the planetary material.—This equation is based on experimental data at high pressure extrapolated to the much higher pressures existing in Jupiter; the extrapolation is guided by theoretical predictions of the behavior of matter at very high pressures.

(3) Reasonable cosmogonic arguments on the chemical composition of Jupiter.—Such a composition may be derived from the known abundances of elements in the solar system, especially from the Sun.

The method of calculation of the density distribution is briefly described in the following statements. An equation of state of the planetary material is assumed. The hydrostatic equilibrium equation is integrated inward from the known radius and a total mass calculated. If the calculated mass is less than the known mass, a dense core is introduced to give the known mass. This density distribution is then used to calculate J_2 and J_4 of the model, which are compared with the known coefficients. (This step was not always performed in the earlier calculations.) If disagreement of values occurs, adjustments to core size and density and the equation of state for the mantle material are made to reduce the discrepancy to an acceptable value. In this process, the total mass requirement must be maintained. Excellent reviews of the internal constitutions of the planets are given by Wildt (ref. 76) and DeMarcus (ref. 77).

EARLY MODELS

Until the first part of this century, it had been generally supposed that Jupiter was entirely gaseous. However, Jeffreys (ref. 78)

showed that for a planet in which the interior is in complete thermal communication with the surface (i.e., by convection), sufficient heat would be lost during the aging of the solar system to solidify the planet for any reasonable initial temperatures. By means of a theorem which gives an upper limit to the surface density of a planet in terms of its mean density and moment of inertia, Jeffreys (ref. 75) showed that the surface density of Jupiter must be less than 0.8 g cm^{-3}. Nonetheless, he did not accept this figure at face value and suggested instead that Jupiter consists of a rocky core, a mantle composed of solid water and carbon dioxide, and a very tenuous but deep atmosphere. Such an atmosphere was shown by Wildt (quoted by Jeffreys) and others to be in serious conflict with the equation of state of gases.

Wildt (ref. 79) concluded that a literal interpretation of the low surface density is unavoidable which implies that substantial amounts of solid hydrogen and helium are present at the surface. He proposed a model consisting of a core comprised of metals and silicates, a lower mantle consisting of a high-pressure solid phase of water, an upper mantle of solid hydrogen and helium, and a shallow atmosphere. The Wildt model and a subsequent modification were influenced by the ideas that prevailed at the time regarding hydrogen abundance in stellar material. Wildt thus assumed a hydrogen abundance for Jupiter which was small compared with present ideas. However, these two papers and a review paper by Wildt (ref. 80) enforced the idea that hydrogen must be a major constituent of Jupiter; moreover, suggestions by Wildt and Kothari (ref. 81) have led to general acceptance of the notion that the metallic phase of hydrogen plays an important role in the internal constitution of Jupiter.

Alfvén (refs. 82, 83, and 84) is one of the few who does not accept the general theories. According to his theory of the formation of the planets, Jupiter consists mainly of carbon, nitrogen, and oxygen gas. The difficulties of Alfvén's theory have been pointed out by Öpik (ref. 85), and his views will not be considered here.

PARALLEL DEVELOPMENTS

The increasingly accepted idea that hydrogen is a major constituent of Jupiter was strongly influenced by two parallel developments. The first involved the formulation of an equation of state of hydrogen at high pressures. Wigner and Huntington (ref. 86) first studied the existence of a metallic phase of hydrogen. Kronig et al. (ref. 87) presented an equation of state for hydrogen upon which several subsequent calculations of Jupiter's density distribution were based.

Following Stewart's (ref. 88) experimental determination of the equations of state of hydrogen and helium at 4.2° K and pressures of

up to 20 000 bars, DeMarcus (ref. 89) found that all previously proposed equations of state of hydrogen were inadequate and formulated an equation by extrapolating Stewart's data. DeMarcus also presented an equation of state of helium, the details of which are not critical in construction of Jupiter models since helium is thought to make up a relatively small part of Jupiter.

The second development, which had awaited a formulation of the equation of state of hydrogen, was the calculation of model planets of pure, cold, solid hydrogen. Following a suggestion by H. N. Russell that cold bodies must have a maximum radius regardless of their mass, Ramsey (ref. 90) and DeMarcus (ref. 91) independently calculated model hydrogen planets. Using the equation of state of Kronig et al. (ref. 87) and Abrikosov (ref. 92), they performed similar calculations using a slightly different equation of state.

The results reached by DeMarcus are shown in figure 7–1. The logarithm of the mass of the planet is plotted agianst the radius. The Jovian planets are also plotted on the diagram. The boundary of the shaded region represents the case for bodies of pure hydrogen. The points on the curve at large mass and small radius represent white dwarfs of pure hydrogen (which, however, are not now believed to exist). The area to the right of the curve is forbidden since for any body, a pure hydrogen body is the least dense for a given mass. The

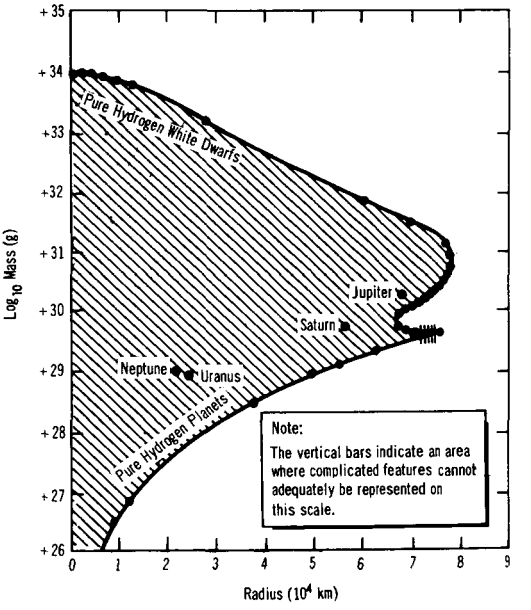

FIGURE 7–1.—Mass-radius diagram for spherical cold cosmic bodies of solid hydrogen. (After ref. 91.)

details of the curve in the vicinity of the cusp are uncertain (and indeed the cusp may not exist), because they critically depend on the somewhat uncertain pressure of the phase transition from molecular hydrogen to metallic hydrogen. It is clear from figure 7–1 that there is a maximum possible radius for cold hydrogen bodies and that Jupiter is near the maximum radius.

The density of Jupiter differs from that of a pure hydrogen planet by a factor of less than two. If it is assumed that all other substances are at least twice as dense as hydrogen at any pressure, then Jupiter consists of substantial amounts of hydrogen. With this qualitative demonstration of the importance of hydrogen in the interior of Jupiter and with the existence of an equation of state of hydrogen, construction of high hydrogen-content models of Jupiter was begun.

JOVIAN MODELS

Ramsey (ref. 90), Miles and Ramsey (ref. 93), and Fessenkov and Massevich (ref. 94) calculated models of Jupiter based on the equation of state of hydrogen formulated by Kronig et al. (ref. 87). However, as previously noted, DeMarcus (quoted in Kronig) showed that this equation of state was not consistent with Stewart's experimental data and formulated a new equation of state. He calculated models of Jupiter based on this equation of state and on the assumption of a mixture of solid hydrogen and helium with the percent of helium by weight increasing inward. A small core of pure helium was inserted to force the model to reach the correct mass. However, to fit the gravitational moments of Jupiter, DeMarcus had to assume that the density of molecular hydrogen at high pressures was 10 percent less than that given by his original equation of state. The details of his model are given in table 7–1.

Based on some reasonable assumptions, DeMarcus found that the amount of hydrogen in Jupiter is more than 78 percent by weight. This lower limit to the hydrogen abundance is insensitive to the abandonment of all his assumptions except the assumed temperature. Even this would not change the hydrogen abundance greatly if the internal temperatures are only a few thousand degrees centigrade. A striking result of his calculations was that the hydrogen abundance is quite stable with respect to large variations in the equation of state of molecular hydrogen. This explains why the DeMarcus results differ only slightly from those of Ramsey and Miles.

Peebles (ref. 95) extended the calculations of DeMarcus by using an electronic computer to examine the effect of varying the helium abundance over a wide range to investigate the effect of different assumptions of depth, temperature, and density of the atmosphere,

TABLE 7–1.—*Jovian Interior Model*

[After ref. 91]

Relative radius, r/R	Density, ρ, g-cm^{-3}	Mass, M $\times 10^{27}$, g	Pressure, $p \times 10^{12}$, dyne-cm^{-2}	W_{He} [a]
1.000	0.00016	1 902.0	0	0
0.998	.032	1 901.92	0.00033	0
.996	.103	1 901.34	.0027	0
.994	.138	1 900.31	.0068	0
.992	.162	1 899.04	.0121	0
.990	.181	1 897.60	.0181	0
.98942	.185	1 897.15	.0200	0
.98942	.197	1 897.15	.0200	0
.98	.246	1 888.49	.0568	0.018
.94	.367	1 840.11	.283	.038
.90	.479	1 778.72	.614	.058
.86	.593	1 707.76	1.06	.090
.82	.714	1 628.92	1.62	.11
.802	.777	1 591.13	1.93	.13
.802	1.08	1 591.13	1.93	.13
.800	1.09	1 585.16	1.98	.13
.75	1.31	1 431.29	3.37	.14
.7	1.56	1 270.27	5.07	.16
.65	1.83	1 105.11	7.12	.20
.6	2.12	940.33	9.52	.23
.55	2.40	780.05	12.3	.24
.5	2.66	630.96	15.3	.25
.45	2.90	496.32	18.5	.26
.40	3.14	379.85	21.9	.26
.35	3.37	281.40	25.5	.26
.3	3.58	203.05	29.2	.26
.25	3.81	142.88	33.1	.26
.2	4.08	100.37	36.7	.27
.15	4.40	72.19	43.2	.27
.1	19.09	33.98	63.5	1.0
.05	27.90	5.19	96.3	1.0
0.0	30.84	0	110	1.0

[a] The quantity W_{He} is a function of pressure defined by the equation

$$\frac{1}{\rho(p)} = \frac{W_{He}}{\rho_{He}(p)} + \frac{1 - W_{He}}{\rho_H(p)}$$

where

$\rho(p)$ = altered density of pressure p

ρ_{He} = estimated density of helium at pressure p

ρ_H = density of hydrogen at pressure p

and to determine whether a fit to J_2 and J_4 could be made using the original equation of state of DeMarcus rather than the lower hydrogen densities that he was forced to use to fit J_2 and J_4. Peebles used several equations of state which represent different atmospheric models. (See fig. 7–2.) He constructed two sets of models; one had high-density cores of unspecified composition, and the other had pure helium cores. By varying the size of the core and the hydrogen abundance, Peebles was able to obtain models which fit both J_2 and J_4 for all the equations of state in figure 7–2, except number 5. Some of the parameters of these models are given in table 7–2. All acceptable models have percentages by weight of hydrogen greater than 75 percent which is consistent with DeMarcus's conclusion that the weight percent of hydrogen in Jupiter must be greater than 78 percent. Figure 7–3 shows two resulting density-depth models for Jupiter, one corresponding to an adiabatic atmosphere and one to an isothermal atmosphere.

According to Peebles, satisfactory models of Jupiter can be obtained by assuming either a very deep or a very shallow atmosphere. He

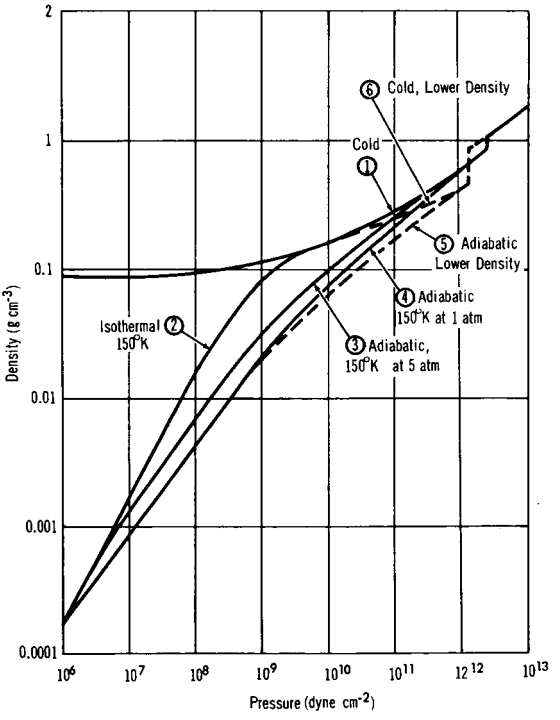

FIGURE 7–2.—The six equations of state of hydrogen (+ helium) assumed in Peebles' density models of Jupiter. (After ref. 95.)

TABLE 7-2.—*Models for Jupiter Fitted to the Observed Value of J*

[After ref. 95]

	Model*				
	1	2	3	4	6
Number ratio of helium to hydrogen above core.	0.025	0.032	0.050	0.083	0.053
Mass of high-density core, units of planetary mass.	.07	.05	.03	0	.03
Hydrogen abundance by mass, X, high-density core model.	.85	.83	.80	.75	.80
Hydrogen abundance by mass, X, pure helium core model.	.80	-------	-------	.75	-------
Gravitational moment, K	.0029	.0028	.0027	.0025	.0027

*The model numbers refer to the curves in fig. 7-2. Model 5 was omitted here because it fits a value of J some 10 percent smaller than the observed J.

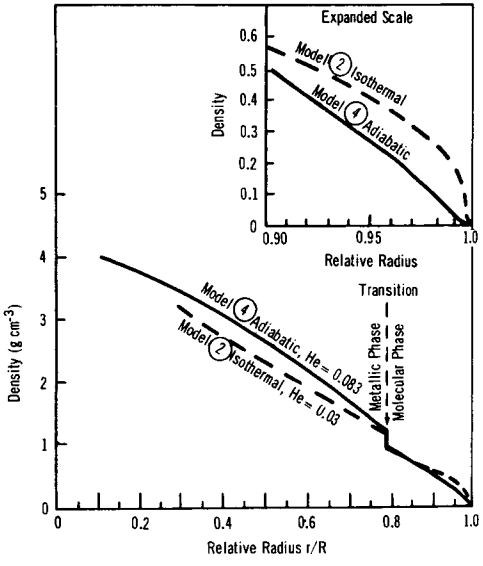

FIGURE 7-3.—Two density models of Jupiter. (Based upon drawing by ref. 95.)

TABLE 7-3.—*Model Planet for Jupiter*[a]

[After ref. 95]

Relative radius, r/R	Pressure, $p \times 10^{12}$, dyne-cm^{-2}	Density, ρ, g-cm^{-3}	Relative mass
1.0	3.0×10^{-6}	5.5×10^{-4}	1.0
0.995	3.7×10^{-4}	0.0164	0.99995
.99	2.8×10^{-3}	.055	.9996
.98	0.020	.147	.997
.96	.095	.28	.988
.94	.23	.40	.973
.92	.38	.47	.957
.9	.57	.55	.941
.85	1.29	.76	.878
.8	2.2	.96	.815
.75	3.5	1.39	.74
.7	5.2	1.63	.64
.65	7.2	1.84	.55
.6	9.5	2.1	.46
.55	11.9	2.3	.38
.5	15.0	2.5	.30
.4	20.5	2.9	.19
.3	26	3.3	.11
.2	34	3.7	.05

[a] Assuming an adiabatic atmosphere, 3 atmospheres pressure, and 150° K at the cloud layer, and hydrogen abundance X = 0.80 in the material above the core.

prefers a very deep atmosphere because (1) Saturn can be fitted only by models with deep atmospheres, and (2) the acceptable shallow atmosphere models have helium concentrated toward the center and this is not consistent with his preferred hypotheses regarding the origin of the planets. The details of a deep atmosphere model based on an equation of state lying about midway between numbers 3 and 4 (fig. 7-2) are given in table 7-3.

8

Electromagnetic and Particle Fields

THE MAGNETIC FIELD

THE STRENGTH AND ORIENTATION of the magnetic field of Jupiter have been estimated in various ways. The basic information is provided by the radio emission characteristics of the planet (ch. 10). If the decimetric radiation is caused by cyclotron emission, polar field strengths on the order of 10^5 gauss must exist if the center of the dipole field is assumed to be at the center of Jupiter (refs. 96 and 97.) However, if the decimetric radiation is caused by relativistic electrons in the Jovian magnetic field (synchrotron emission), polar fields on the order of only 100 gauss exist, and the fields in the emitting region at $\sim 3R_J$, (R_J, radius of Jupiter) are on the order of 1 to 10 gauss. To explain the characteristics of the decametric radiation from Jupiter, Warwick (ref. 98) has proposed a dipole magnetic field with a magnetic moment of $\sim 4 \times 10^{30}$ gauss cm^3, which would give field strengths at $3R_J$ of ~ 0.1 to 1 gauss. However, the center of the dipole is displaced from the center of the planet, as shown in figure 8–1. The dipole center is near the axis of rotation ($\sim 0.1R_J$ displacement) but is $\sim 0.7R_J$ south of the equatorial plane. The longitude of the dipole center is slightly displaced from $\lambda_{III}=200°$, where λ_{III} is a System III longitude. An off-center dipole field is required by Berge and Morris (ref. 99) to explain the time variations of decimeter emission, but their calculated dipole center was $0.5R_J$ north of the equatorial plane and is farther away from $\lambda_{III}=200°$ than Warwick's calculated dipole center.

Warwick's theory also determines the sense of the dipole field. The north pole of Jupiter is also the north magnetic pole; thus, Jupiter's magnetic moment is opposite in sense to that of Earth.

Some observations of the decimetric radiation have shown that the plane of polarization rocks as Jupiter rotates. This rocking suggests that the axis of the magnetic field of Jupiter is at an angle to the rotational axis (which is the same with Earth). There are various estimates of this angle, ϕ, ranging from 9° reported by Morris and Berge (ref. 100) to 24° reported by Bash et al. (ref. 101). Thus, the observations are consistent with a tilted dipole having a displaced

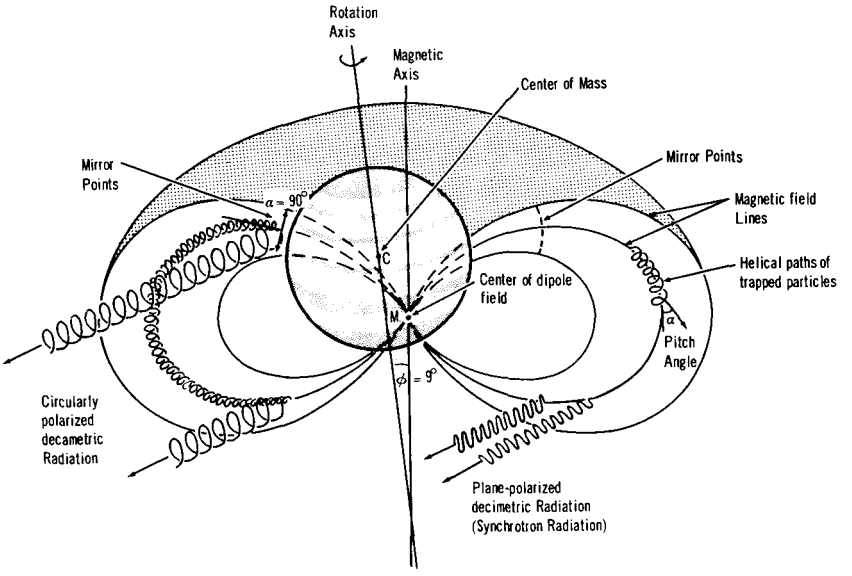

FIGURE 8-1.—The off-center radiation belts of Jupiter. (Based upon drawing by ref. 98.)

center, but more observations are required to locate the center and define the angle of tilt.

Since it is probable that the solar wind extends as far as Jupiter according to Axford et al. (ref. 102) the sunside of the Jovian magnetosphere is confined somewhat like that of Earth. If M_J (M_J, magnetic moment of Jupiter) is assumed to be 5×10^4 M_E (M_E, magnetic moment of Earth) and the formulas of Mead and Beard (ref. 103) are used, the distance from the center of Jupiter to the boundary will be $\sim 40R_J$. Carr et al. (ref. 104) have estimated the boundary to be on the order of $50R_J$. As in the case of Earth, the extent of the magnetic field on the nightside of the planet is unknown.

THE TRAPPED RADIATION BELTS

Since decimetric emission is thought to be synchrotron radiation, the properties of the relativistic electrons trapped in the Jovian Van Allen belt can be inferred. Little can be said about the low energy electrons except that their intensity is so low that there is no appreciable cyclotron emission. This assumes a harder energy spectrum than that found in Earth's magnetically trapped radiation.

The synchrotron model does not impose strict requirements on the intensity of the electrons for a given power output of decimetric radiation, but it does place requirements on the product of the magnetic field strength in the emitting region and the number of radiating

electrons. Based on data by Chang and Davis (ref. 97) the flux of electrons (assuming an E^{-1} differential spectrum for the energy distribution) for various field strengths are:

At 0.1 gauss, $\phi_e \simeq 5 \times 10^8$ electrons cm^{-2} sec^{-1} between $\sim$10 and 100 MeV.

At 1.0 gauss, $\phi_e \simeq 5 \times 10^7$ electrons cm^{-2} sec^{-1} between $\sim$2.5 and 25 MeV,

and

At 10 gauss, $\phi_e \simeq 5 \times 10^6$ electrons cm^{-2} sec^{-1} between $\sim$1 and 10 MeV.

Depending upon which combination is correct, the corresponding flux presumably extends only to 3 R_J. From $3R_J$ to $\sim 50R_J$ (the boundary of the Jovian magnetosphere), the flux of electrons is too low to emit decimetric radiation which can be detected from Earth.

From the observation of Radhakrishnan and Roberts (ref. 105) that the emission is strongly polarized, it has been inferred that there are many electrons trapped in flat helices, that is, large pitch angles (fig. 8–1). Further, since the emission is more strongly polarized in the outer regions of the source, the proportion of electrons with large pitch angles increases with distance from the planet out to $3R_J$.

The source of the electrons which are trapped in the Jovian magnetosphere is presumably the same source that supplies the Earth's trapped radiation (the solar wind). How electrons are injected into a magnetosphere and accelerated to relativistic energies remain unsolved problems in the field of space physics.

9
Temperature

IN THE ABSENCE OF AN INTERNAL HEAT SOURCE, the temperature of a planet is determined by its use of solar energy. The theoretical mean temperature of the planet may be found from Stefan's law by equating the energy absorbed by the planet to that radiated from it, with the reasonable assumption of equilibrium conditions. In applying this equality, it is generally assumed that the planet acts as a blackbody relative to its thermal radiation characteristics, and in the case of a rapidly rotating body such as Jupiter, it is generally assumed that a constant radiative temperature over the entire surface is maintained so that energy is radiated over an area four times larger than that in which it is effectively received.

Thus:

$$T_{eq}^4 = S_J \frac{(1-A)}{4\sigma}$$

where

S_J the mean solar constant of Jupiter
σ the Stefan-Boltzmann constant
A the planetary albedo

The solar constant at Jupiter's mean distance from the Sun ($a=5.20$ astronomical units) is approximately 0.073 ± 0.001 cal cm^{-2} min^{-1}, which is about 1/27 the observed value for Earth. Also, Jupiter definitely has a high planetary albedo (not yet well established), of about 0.50. These two factors indicate that little solar energy actually is absorbed by the planet, and that its equilibrium temperature should be quite low. Using Kuiper's proposed albedo value of 0.51 for Jupiter, the mean planetary temperature calculated is $T_{eq}=102°$ K. Taylor (ref. 106), using his recent bolometric albedo of 0.45 for Jupiter, obtained $T_{eq}=105 \pm 3°$ K.

RADIOMETRY

In 1926, Menzel, Coblentz, and Lampland, the pioneers of planetary radiometry, measured the emission from Jupiter in the 9- to 13-

micron Earth atmospheric window and derived an equivalent blackbody temperature of $T_{rad}=130°$ K for the planetary disk (ref. 107). Murray and Wildey (ref. 108) have recently derived a temperature of 128° K from emissions in the same window region. These values and measurements taken at longer wavelengths are listed in table 9–1 (refs. 109–123). Fom these data, it may be seen that there is a clear upward trend for the equivalent blackbody disk temperature at wavelengths longer than about 3 centimeters. The general agreement of the temperatures derived from microwave measurements between 1 and 3 centimeters and infrared measurements supports the general conclusion that radiation in both of these ranges is of thermal origin and that these emissions provide a measure of the temperature of the planet. There is some uncertainty, however, about the exact level in the atmosphere to which the measurements refer.

Ammonia, the main radiating constituent[1] of the Jovian upper atmosphere, absorbs very strongly in the 8- to 14-micron region (with a strong band ~10.5 microns) which is used in making the infrared measurements. According to Kuiper (ref. 124), the blackbody radiation temperature of 130° K for Jupiter obtained by infrared radiometry arises from, or corresponds to, an effective level in the atmosphere that is well above the cloud layer. His conclusion is based on the observation that 1 cm-atm of ammonia is nearly opaque in the 8- to14-micron region, and since this is only a small fraction of the total ammonia present (700 cm-atm), more than 1 cm-atm of ammonia should lie above the cloudtops. By making measurements outside the 8- to 14-micron region, away from the strong absorption of ammonia, emissions from a lower level should be detected. This was verified by Thornton and Welch (ref. 114), who measured the Jovian emission at 8.5 millimeters and found an equivalent blackbody temperature of 144° K. They also showed by a comparison calculation based on Kuiper's atmospheric model that at 8.5 millimeters the expected temperature was approximately 150° K. Temperatures derived from measurements in the 3-centimeter region approximate this value, and, therefore, it is concluded that these measurements are of energy that originates at the cloudtops. After a lengthy analysis of the available data Öpik (ref. 85) concluded that the most probable cloudtop temperature is $T_c=156°$ K.

Comparison With Theoretical Temperature.—The difference between the radiometric and the equilibrium temperatures was ascribed by Öpik, following earlier theorizing by Kuiper, to radiation of the internal heat produced from the original gravitational

[1] Methane is much less important in this region.

TABLE 9–1.—*Temperature Measurements*

Wavelength	Method	Temperature, °K	Author
	Thermal		
0.83 μ	H_2 quadrupole lines.	170	Zabriskie (ref. 109)
0.83 μ	H_2 quadrupole lines.	120	Spinrad (ref. 110)
1.1 μ	CH_4 rotation vibration band.	200±25	Owen (ref. 111)
9 to 13 μ	Thermocouple and water cell.	130±10	Menzel et al. (ref. 107)
8 to 13 μ	Thermocouple and monochromator.	131.5	Sinton and Strong (ref. 112)
9 to 14 μ	Ge bolometer	128±2.3	Murray and Wildey (ref. 108)
8.8 μ	Thermocouple and monochromator.	139	Sinton (ref. 113)
8.35 mm	Microwave radiometer.	144±23	Thornton and Welch (ref. 114)
3.03 cm		171±20	Giordmaine et al. (ref. 115)
3.15 cm		140±56	Mayer et al. (ref. 116)
3.15 cm		145±26	
3.17 cm		173±20	Giordmaine et al. (ref. 115)
3.3 cm		193±16	Bibinova et al. (ref. 117)
3.36 cm		189±20	Giordmaine et al. (ref. 115)
3.75 cm		200	Drake and Ewen (ref. 118)
	Nonthermal		
10.2 cm	Microwave radiometer.	640±85	Sloanaker (ref. 119)
21 cm		2500±450	McClain (ref. 120)
22 cm		3000±1700	Drake and Hvatum (ref. 121)
31 cm		5500±1500	Roberts and Stanley (ref. 122)
32 cm		7500±2500	McClain (ref. 120)
68 cm		70 000±30 000	Drake and Hvatum (ref. 121)
70 cm		26 700±1300	Hardebeck (ref. 123)

contraction. Öpik, by using the values $T_{rad}=130°$ K and $T_{eq}=102°$ K, calculated that Jupiter radiated 1.6 ± 0.4 times the solar input. Taylor (ref. 106), using $T_{rad}=130°$ K and $T_{eq}=105°$ K, finds only 1.2 times the solar input, or 5×10^{24} erg/sec. Dissatisfied with various other explanations he had analyzed (radioactivity of the interior, tidal dissipation, meteor bombardment, magnetic field decay), he came to the same conclusions as Kuiper and Öpik. An alternative interpretation, based on solar radiation alone, was proposed by Trafton (ref. 125) in terms of an atmospheric greenhouse effect created by pressure-induced transitions in the abundant molecular hydrogen. The models he calculated, however, taking into account the thermal opacities of not only hydrogen but also of helium and ammonia, seem to fit the observations if allowance is made for a small internal heat source greater than $\frac{1}{10}$ the incident solar flux (ref. 126). Still, opacity from other absorbers could alter this picture. The simplest interpretation would be to assume Jupiter merely reradiates the absorbed solar radiation as a graybody of emissivity $\epsilon=0.27$ at a temperature $T_g=145°$ K comparable to that of the cloudtop, although this is undoubtedly an oversimplification of the problem (ref. 106).

Temperature Distribution.—Radiometric (8 to 14 μ) temperature maps over the Jovian disk were presented recently by Wildey et al. based on observations with the 200-inch Mount Palomar telescope (refs. 127 to 129). Their composite map, pictured in figure 9–1, shows very slight temperature variations: only a 5-degree decrease from disk center, at an average of 129° K, to the limbs. The isotherms are roughly concentric, but all the maps show a definite structure and orientation somewhat related to the Jovian bands. The results are preliminary. The equatorial belts seem to be 0.5° K warmer than adjoining tropical zones, and the Great Red Spot was found to be cooler by 1.5 to 2.0° K than its surroundings. The most prominent common feature of the maps was the general limb darkening, indicative of an increase of temperature with depth. This information, coupled with the high rotational temperature (170° K) derived from hydrogen absorption at $\sim$0.8 micron for deeper atmospheric levels, implies the existence of an efficient greenhouse mechanism such as that proposed by Trafton.

Hot Shadow Effect.—Murray et al. (ref. 130) while scanning the Jovian disk radiometrically in the 8- to 14-micron region found repeatedly a notable enhancement of the emission in the disk portions shadowed by the two large satellites Europa (J–II) and Ganymede (J–III). The temperatures derived for the umbra were as high as 190° and 185° K, respectively. Although Wildey (ref. 128) later detected no such enhancement with Io (J–I) or even Europa's shadow, he maintained that the "hot shadow" effects discovered

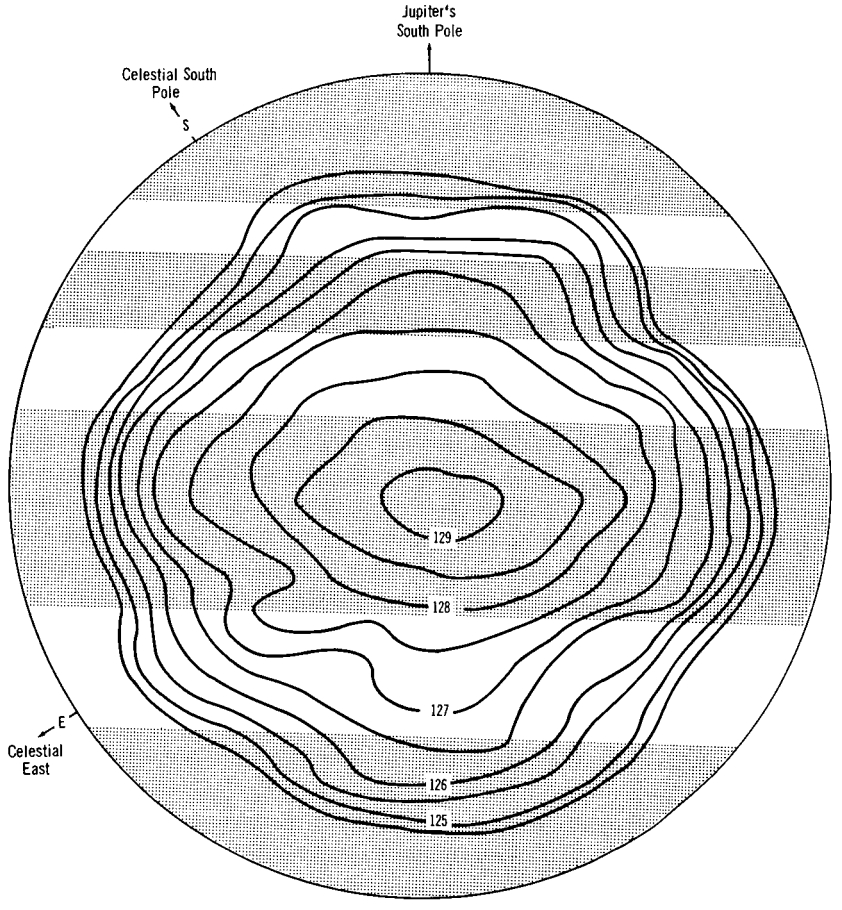

FIGURE 9–1.—Composite map of 8 to 14 micron brightness temperature distribution (°K) over the Jovian disk. (After ref. 129.)

previously were real, but perhaps variable with time. The only explanation offered was a change with depth of the concentration of the infrared radiating species by readjustment of the photoequilibrium under cessation of insolation.

MICROWAVE RADIOMETRY

Table 9–1 lists equivalent blackbody disk temperatures of Jupiter that have been measured at various wavelengths in the microwave region. A clear trend for the radiative temperature to rise with increased wavelength starting at about 3 centimeters is evident from

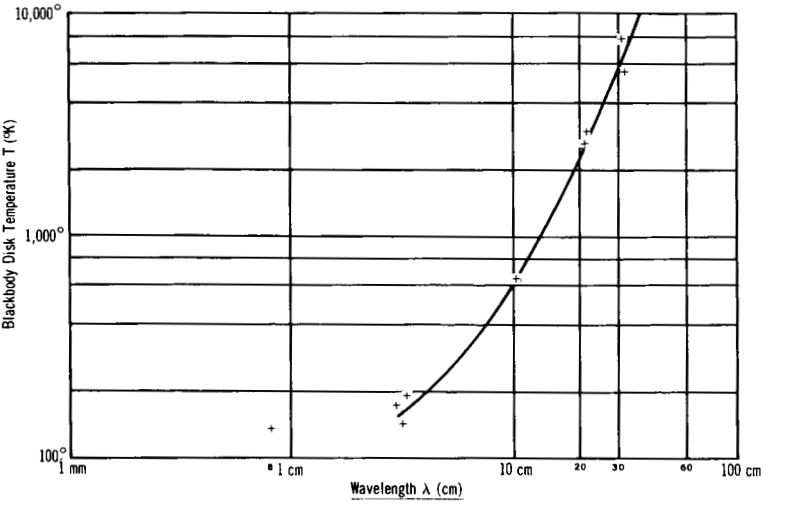

FIGURE 9–2.—Microwave brightness temperature curve.

the plot of figure 9–2.[2] Between 1 and 3 centimeters, the equivalent blackbody disk temperature is sufficiently close (approximately 150° K) to that obtained from measurements of the infrared emissions from the planet; therefore, it is generally believed that emissions in both ranges are of thermal origin. At about 3.3 centimeters the equivalent blackbody disk temperature has been found to be 190° K (ref. 117). The emissions at wavelengths longer than 3 centimeters are believed to have increasingly important contributions from nonthermal sources. Nonthermal sources contribute the larger portion of the energy measured at 10 centimeters and dominate rapidly at longer wavelengths. The strong, somewhat irregular (decimetric) emission apparently originates in the Jovian radiation belts. A discussion of the characteristics of these emissions is contained in chapter 10.

[2] If the curve of flux-density versus wavelength were plotted, it would show a slowly decreasing trend departing from that expected for blackbody emission at a fixed temperature.

10

Radio-Frequency Radiation

INTRODUCTION

THERE ARE AT LEAST THREE TYPES of radio-frequency emission from Jupiter. At about 3 centimeters the thermal emission is caused by the thermal motion of the molecules in the Jovian atmosphere. Between ~3 and ~70 centimeters, the decimetric emission is thought to be the result of electrons spiralling in the Jovian magnetic field and is called cyclotron emission if the radiating electrons are nonrelativistic, and synchrotron emission if they are relativistic. Between the wavelengths of ~70 centimeters and ~7 meters, the emission (metric) is not well known because of observational complications (galactic background) and technical requirements (highly sensitive receivers), however, some successful observations at about 1 meter have been made (ref. 131). From ~7 to 62.5 meters, the decametric emission is also nonthermal, but its origin is as yet not fully understood. At longer wavelengths, ionospheric attenuation (or opacity) of Earth blocks out any incoming emission from Jupiter. Such radiation (hectometric) is thought to exist.

The complete picture of Jupiter's radio spectrum is schematically and tentatively given in figure 10–1, which was suggested by Carr et al. (ref. 104) and shows the relationship between the three known main emissions (decametric, decimetric, and thermal). The dashed portions of the curve are conjectural because of the unavailability of observations. A suspected correlation of Jovian activity (either decametric or decimetric) with solar activity has not yet been clearly established.

DECAMETRIC RADIATION OF SPORADIC EMISSION

Intense bursts of decametric radio emission from Jupiter discovered in 1954 by Burke and Franklin (ref. 132) at 22.2 Mc sec^{-1} caused great surprise to planetary astronomers. Subsequent investigations have shown the occurrence of emission in the frequency range of 4.8

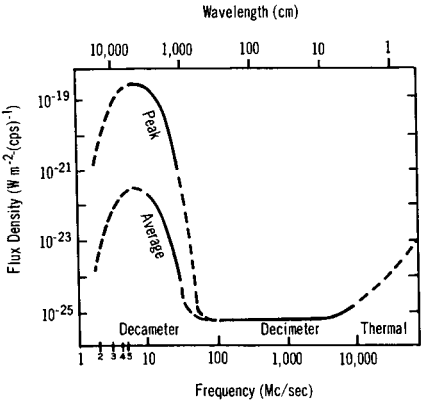

FIGURE 10–1.—Jupiter's complete radio spectrum. (As suggested by ref. 104.)

Mc sec^{-1} to 43 Mc sec^{-1} (refs. 133 and 134). The bursts are most commonly detected at frequencies of about 18 Mc sec^{-1}. Although emission below 4.8 Mc sec^{-1} probably does occur, absorption by the Earth's ionosphere prevents detection at the surface (ref. 133). The upper frequency limit seems to be a property of the radiation itself (ref. 70).

The most outstanding property of the decametric radiation is that it is not received continuously, but sporadically in a series of short bursts from milliseconds to tens of seconds in duration according to Gardner and Shain (ref. 135) and Douglas and Smith (refs. 136 and 137) that form an intense storm lasting a few minutes to several hours (ref. 138). Another characteristic is the considerable intensity of the bursts—with flux densities of about 10^{-20} W m^{-2} (cps)$^{-1}$—exceeding that of any other source except the disturbed Sun. The intensity distribution of the radiation seems to increase monotonically with decreasing frequency down to 10 Mc sec^{-1} (refs. 104 and 139). This is contradictory to previously published reports by Gardner and Shain, and Kraus. The peak intensity is $\sim 10^{-18}$ to 10^{-19} W m^{-2} (cps)$^{-1}$ at 10 Mc sec^{-1} and decreases to $\sim 10^{-21}$ W m^{-2} (cps)$^{-1}$ at 27.6 Mc sec^{-1} (ref. 104). Mean intensities averaged over quiescent and active times are several orders of magnitude lower. During active periods the 18 Mc sec^{-1} bursts are received about one-third of the time.

Shain (ref. 64) found that by plotting the times of burst activity at 18.3 Mc sec^{-1} against the central meridian longitude in System II (see ch. 4), the existence of localized zones of activity, or radio sources could be demonstrated, which rotated with Jupiter at a slightly faster rate, however, than that adopted in System II. Subsequent investigations by Gallet and Bowles (ref. 140), Carr et al. (ref. 67), and Burke (ref. 141) have confirmed the above conclusions. The period

was found by Douglas (ref. 139) to be $9^h55^m29^s.37$ as the average over 9 years (from 1950 to 1960), a value to be adopted in 1962 as basis of System III radio longitudes.

Longitude profiles showing the probability of emission as a function of the central meridian longitude and frequency have been constructed by many workers. At the higher frequencies, these profiles usually exhibit prominent peaks at $\lambda_{III}=200°$ and 280° and a secondary peak between 90° and 160° (refs. 67 and 98). The peaks seem to be narrower at higher frequencies according to Franklin and Burke (ref. 142), Gardner and Shain (ref. 135), Carr et al. (ref. 67), and Ellis (ref. 133), although this may be a function of the sensitivities of the receivers (ref. 143). At 10 Mc sec^{-1}, individual sources are difficult to notice according to Carr et al. (ref. 66), and at 4.8 Mc sec^{-1}, the probability of emission is independent of longitude (ref. 133). It was shown by Ellis, however, that the intensity of the 4.8 Mc sec^{-1} events does show a longitude dependence, with maxima between $\lambda_{III}=130°$ and 200° and near 360°. Carr et al. (ref. 67) also showed that the longitude of the principal source was usually less at higher frequencies.

In many cases of noise storms from Jupiter, the frequency of the radiation seems to drift up or down the spectrum. Warwick (ref. 98) has found several characteristic features of the frequency-time profile that are repeatedly apparent; near 225° longitude, the storm seems to drift to lower frequencies, but near 120° it drifts in the opposite sense. These observations also imply that the radiation from Jupiter is beamed in a very narrow cone, and it has also been established that the radiation originates in an area smaller than one-third of the planet's disk (ref. 144).

The first observations of the polarization of the burst radiation from Jupiter were made at 19.6 Mc sec^{-1} by Gardner and Shain (ref. 135) and at 22.2 Mc sec^{-1} by Burke and Franklin (ref. 132). Both showed that the bursts had a strong component of circular or elliptical polarization which was right-handed (as seen along the direction of propagation). Subsequent investigations at 22.2 Mc sec^{-1} by Smith and Carr (ref. 145) and Carr et al. (ref. 67), at 10 Mc sec^{-1} by Dowden (ref. 146), at several frequencies ranging from 15.2 to 24.2 Mc sec^{-1} by Sherrill and Castles (ref. 147), and from 16 to 26 Mc sec^{-1} by Barrow (ref. 148) have shown that the majority of the radiation is polarized, that left-hand polarization has a stronger component at low (<20 Mc sec^{-1}) frequencies, and that the ratio of right- to left-handed polarization may be a function of the longitude of emission.

As first pointed out by Bigg (ref. 149) and confirmed by Dulk (ref. 150), the angular position of Io, one of the satellites of Jupiter, has an influence on the probability of radio emission. It was shown

that Io increases the probability of emission when its position and the Jupiter longitude are simultaneously favorable. Lebo et al. (ref. 151) found similar correlations with probability of emission and the positions of the first three Galilean satellites (Io, Europa, and Ganymede).

ORIGIN OF THE DECAMETRIC RADIATION

Many hypotheses have been proposed in an attempt to explain the characteristics of the decametric radiation from Jupiter. Some mechanisms used to explain the characteristics of the radio-frequency radiation are

(1) Lightning-like discharges in the Jovian atmosphere (ref. 62)

(2) Plasma oscillations in the Jovian ionosphere caused by a turbulent atmosphere (ref. 152); or shock waves caused by volcanos (refs. 135 and 153)

(3) Focusing of distant radio sources by the Jovian ionosphere (ref. 154)

(4) Chemical explosions in the Jovian atmosphere (ref. 155)

(5) Cerenkov radiation emitted by electrons precipitating into the Jovian ionosphere (ref. 98)

(6) Maser-like amplification of radiation from mildly relativistic electrons (ref. 156)

(7) Cyclotron emission by bunches of electrons at anomalies in the magnetic field of Jupiter (ref. 157)

(8) Amplified whistlers (low-frequency waves) in the Jovian magnetosphere (ref. 158)

(9) Coherent cyclotron emission (ref. 70)

At present, no theory is generally accepted.

DECIMETRIC RADIATION

Nonthermal decimetric radiation was discovered in 1958 at a wavelength of 10 centimeters (ref. 119). The spectral distribution of the nonthermal centimeter emission is approximately flat between $\sim$5 and 70 centimeters, although the intensity may increase slightly with increasing wavelength. The intensity level is 0.5 to 1×10^{-25} W m^{-2} (cps)$^{-1}$ from 10 to 70 centimeters (ref. 159).

Various investigations have shown that, except for a short time late in 1959 and early in 1960, the intensity of the radiation near 10, 20, 30, and 70 centimeters appears to be constant over long periods of time (refs. 100, 119, 121 to 123).

Radhakrishnan and Roberts (ref. 105) discovered that 31-centimeter radiation from Jupiter has a component of linear polarization

amounting to 0.3 of the total emission with the electric vector approximately parallel to the equator of Jupiter. Subsequent studies by Morris and Bartlett (ref. 160), Rose et al. (ref. 161), and Bash et al. (ref. 101) at 10 centimeters; by Morris and Berge (ref. 100) and Gary (ref. 162) at 20 centimeters; and by Morris and Berge (ref. 100) at 30 centimeters have all shown that a component of the radiation is linearly polarized. It has been shown by Bash et al. (ref. 101) that the fraction of polarized radiation decreases gradually with decreasing wavelength and that the source is more strongly polarized in its outer regions (ref. 105).

As suggested by the investigations of McClain (ref. 163) and Sloanaker and Boland (ref. 164), a modulation of the total radiation intensity occurs with two maxima appearing per revolution of Jupiter. The maxima were 10 percent greater than the minima and occurred when the tilt of the plane of polarization relative to Jupiter's equator was greatest. Subsequent studies at 10 centimeters by Bash et al. (ref. 101) and at 20 centimeters by Miller and Gary (ref. 165), Rose et al. (ref. 161), and Gary (ref. 162) have verified the change of intensity with rotation. It was shown that the direction of the electric vector of the radiation rocks through an angle, ϕ, with the period of rotation of the planet. Various estimates of ϕ have been obtained, and the implications of these estimates are discussed in chapter 8.

The dimensions of the emitting region were first obtained by Radhakrishnan and Roberts (ref. 105) at 31 centimeters and confirmed by Morris and Berge (ref. 100) at 22 and 31 centimeters. It was found that the emitting region extends approximately three planetary diameters in the equatorial plane of Jupiter, while the polar extent is about one planetary diameter. Subsequent investigations by Kerr (ref. 166) at 70 centimeters indicated similar results, and it seems that the emitting region has the same dimensions for all wavelengths in the region of 5 to 70 centimeters.

ORIGIN OF THE DECIMETRIC RADIATION

Since the discovery that the decimetric radiation from Jupiter has a strong linearly polarized component and a source dimension several times the size of the visible disk, the suggestion that the radiation is due to electrons trapped in the magnetic field of Jupiter, forming a Van Allen belt similar to that about Earth, has been generally accepted.

Cyclotron radiation (caused by nonrelativistic electrons) has been discussed in detail by Field (refs. 96, 167, and 168). Since cyclotron radiation would require a very large Jovian magnetic field, a very steep particle spectrum, and a polar extent larger than that observed, this type of radiation has been dismissed in favor of synchrotron

emission. Drake and Hvatum (ref. 121), Roberts and Stanley (ref. 122), and especially Chang and Davis (ref. 97) have considered synchrotron emission and concluded that the predicted polarization, source dimensions, and time scales due to energy losses by the electrons are consistent with the observations. Reasonable values for the strength of the required Jovian magnetic field are obtained.

11
Optical Properties

THE LARGE DIAMETER AND HIGH ALBEDO of Jupiter make this planet a conspicuous astronomical object. It is an exterior planet and cannot be seen at phase angles larger than 12°. Only a small portion of the nightside of the planet can ever be observed from Earth. Jupiter appears distinctly flattened and marked by alternate light and dark bands which are generally parallel to the equator and are usually interpreted as summits of clouds. Their colors are caused by the varying chemical composition and height of particulate matter. However, Sharonov (ref. 169) has suggested that the coloration is caused by light scattering effects in colorless gases and aerosols. These explanations are similar to those proposed as the cause of the yellowish color of Venus. At one time, the colors were believed to result from radiation from a hot planetary surface. The bands are termed zones or belts, depending upon their general color (yellow or gray, respectively). According to Peek (ref. 60), the coloration is subdued but with eye adaptation, traces of brown, red, and blue may be seen. Both the color and the structure of the bands change with time. Light and dark spots and rifts are common in the bands and suggest vigorous motions in the clouds.

LUMINOSITY OR BRIGHTNESS

The traditional system of stellar magnitude has been employed as a measure of the luminosity of planets. In practice, relative magnitudes are determined, and the difference between the magnitude of the planet and some accepted standard of reference is reported. The scale defined in such a way that the relative magnitude is equal to $2.5 \log L_s/L_p$, where L_s is the luminosity of the standard and L_p is the luminosity of the planet. Thus, one unit of magnitude corresponds to a difference in brightness of a factor of approximately 2.5, and the smaller the magnitude, the brighter the body. Discrete frequencies or selected regions of the spectrum may be used to describe magnitudes. The magnitude system was devised primarily for stellar astronomy. Because of the time dependence of the position of the planets with

respect to Earth and the Sun, the observed magnitudes of planets are commonly reduced to a standard distance and a zero phase angle for purpose of comparison. The reduction of observed brightness to a standard distance, generally, where the product of the distances of the planet from Earth and from the Sun equals $1(\text{A.U.})^2$, results in magnitude values that are not related to the visual appearance of the planet. For example, the reduced magnitude of Jupiter is about -9 and indicates a very bright body; this value may be compared with the values of -28.81 for the Sun, -4.29 for Venus, and about $+0.21$ for the Moon.

Since Jupiter cannot be seen from Earth at all phase angles, there is relatively little data on its brightness variation with solar phase angle. Müller (ref. 170) indicated a phase coefficient of 0.005 mag/deg, which is a small value. The data discussed by Becker (ref. 171) and Harris (ref. 172) contain evidence that the mean-opposition magnitudes vary with an amplitude of 0.34 magnitude in a period of 11.6 ± 0.4 years, close to Jupiter's 12-year period of revolution (see table 11–1 (refs. 170, 172 to 175)). Rubaschev (ref. 176), however, suggested linking the variation in Jupiter's magnitude to the solar activity cycle (mean sunspot period: 11.04 years). Becker also suspected that Jovian magnitude variations may be correlated with changes of its surface features.

ALBEDO

The brightness of the planet Jupiter is a result of its large size and moderately high albedo. Several conventions are used to describe albedo. The geometric albedo, p, is the ratio of the average luminance of the planet at full phase to the luminance of a perfectly diffusing, flat surface at the same distance from the Sun and normal to the incident radiation, and can be computed if the relative magnitude of the planet and its diameter are known. The albedo may be computed for Jupiter to an accuracy of approximately 5 percent. The Bond, or spherical, albedo, A, is the ratio of the total luminous flux reflected by the planet in all directions to the total flux incident upon the planet in a beam of parallel light. The Bond albedo, A, is equal to the geometric albedo, p, times the phase integral, q, and is very helpful in discussing planetary characteristics.

The phase integral should be based on observations of the variation of the brightness of the planet with phase angle. Since the necessary measurements cannot be taken for Jupiter, the phase integral is derived from assumptions concerning the radiative properties of the planet's atmosphere. Harris (ref. 172) mentions three alternatives: (1) adopt the value of q that has been found for Venus because the

TABLE 11–1.—*Reduced Visual Magnitudes of Jupiter*

[Portions of data listed by Becker and reduced by ref. 172]

Method	Observer	Years observed, opposition	Reduced visual magnitude, V
Visual	Zöllner (ref. 173)	1862	−9.22
		1863	−9.22
		1864	−9.34
	Müller (ref. 170)	1878	−9.03
		1879–1880	−9.14
		1880–1881	−9.19
		1881–1882	−9.28
		1883	−9.24
		1883–1884	−9.28
		1885	−9.25
		1886	−9.18
		1887	−9.11
		1889	−9.09
		1890	−9.07
Photovisual	King (refs. 174 and 175)	1915	−9.39
		1916	−9.18
		1918	−9.16
		1920	−9.24
		1921	−9.41
		1922	−9.30
Photoelectric	Harris (ref. 172)	1951	−9.46
		1952	−9.48
		1954	−9.39
Mean value			−9.25

two planets are completely cloud covered and evidently have massive atmospheres; thus, their reflectivities should be similar, (2) assume that the cloud surface acts as a perfectly diffuse reflector (that is, it obeys Lambert's law), or (3) assume an optically thick atmosphere and infer the phase integral from data on limb darkening. Harris (ref. 172) has adopted a value of q that considers these alternatives. The q value is listed in table 11–2 with p for various spectral regions and visual Bond albedo, A. In the ultraviolet, one rocket measurement placed Jupiter's albedo near λ2700 Å at 0.26 (ref. 177). This was confirmed in 1963 by obtaining one spectral scan in the ultraviolet (λ1700 to 4000 Å) from a similar rocket flight (ref. 178).

Either the geometric or Bond albedo may refer to a restricted

TABLE 11–2.—*Monochromatic Albedos*

[After ref. 172]

Geometrical albedos

p (U)	p (B)	p (V)	p (R)	p (I)
0. 270	0. 370	0. 445	0. 466	0. 347

Phase integral (q (V)): 1.65
Spherical albedo (A (V)): 0.73

spectral region. The radiometric albedo (or integral spherical albedo), A^*, refers to the entire spectral region of solar radiation, thus, $1-A^*$ is that portion of the incident solar energy that is absorbed by the planet and available to heat the planet and its atmosphere, to drive the atmosphere, and to enter into the photochemical reactions. The radiometric albedo of Jupiter was only recently estimated by Taylor (ref. 106) at 0.45.

COLOR INDICES AND COLORIMETRY

The difference in the magnitudes of a body in two spectral regions is the color index of the body. The index was first devised to describe the approximate spectral distribution of light from stars that were too faint to provide a detailed spectrogram. Several different conventions have been used to specify the color index. The most common difference occurs between the blue and the visual magnitudes (the B—V color index). The U, B, V, R, and I systems used in planetary work are defined by arbitrary combinations of light filters and sensors, so that U, B, V, R, and I indicate predominant sensitivity in the ultraviolet, blue, visible, red, and infrared regions of the spectrum respectively (ref. 172).

Color index nomenclature has been adapted to planetary astronomy to provide a rough indication of the planet's color and a measure of its selective reflectivity. If a planet has the same color index as the source of its illumination (the Sun), the planet is a gray (nonselective) reflector; if, however, there is a difference in color indices, selective reflectivity is indicated. Table 11–3 contains some values of the color indices of Jupiter and the Sun and of the magnitude differences between Jupiter and the Sun in different spectral regions. It is apparent that Jupiter selectively absorbs shortwave solar radiation and has higher reflectivity in the longer wavelengths. Similar optical characteristics of the satellites are given in chapter 18.

TABLE 11–3.—*Mean Color Indices and Color Differences*

[After ref. 172]

Body	Mean colors			
	U−B	B−V	V−R	R−I
Jupiter	+0.48	+0.83	+0.50	−0.03
Sun	.14	.63	.45	.29
Color differences, Jupiter-Sun				
U	B	V	R	I
+0.54	+0.20	0.00	−0.05	+0.27

Some of the results of an extensive photometric study by Plaetschke (ref. 179) of Jupiter in various spectral regions are shown in figure 11–1. Both intense limb darkening and the variation in color as a function of latitude are apparent.

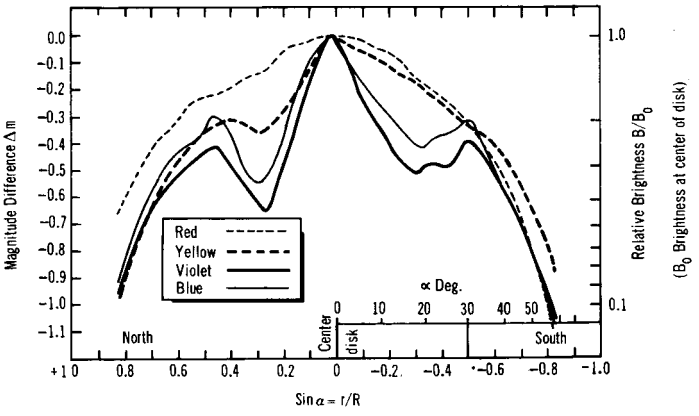

FIGURE 11–1.—Change in brightness along central meridian of Jupiter. (After ref. 179.)

α Zenocentric angular distance from center of disk (along central meridian)
r Linear distance from center of disk (along central meridian)
R (Linear) polar radius of the disk

Effective wavelengths:

Violet	Blue	Yellow	Red
3610 Å	3840 Å	5280 Å	6700 Å

POLARIZATION

Scattering in a purely molecular atmosphere will cause the light to become strongly polarized, but scattering in clouds generally will decrease polarization. Polarization effects in clouds will be a function of the chemical composition and form (state, shape, and size) of the cloud particles. The atmosphere above clouds will increase polarization. Lyot (as discussed by ref. 180) found that the polarization of Jupiter was strongest at the gray-colored polar regions and steadily decreased near the equatorial region. The polarization at the poles was independent of both phase angle and wavelength. Polarization in the tropical regions was not strongly wavelength dependent, but variation with phase angle was noted. Adjacent features distinguishable by their color did not show differences in polarization. The refutation by Dollfus (ref. 180) of the atmosphere model of Jupiter that envisions an optically thick, opaque cloud layer covered by a thick, transparent atmosphere is based upon the polarization increasing rapidly with phase angle, making it strongly wavelength dependent (λ^{-4}). Dollfus interprets the evidence to indicate that a thin fog with particles of about 1 micron in diameter extends over most of the planet but disappears over the polar regions. Barabashov and Semejkin (ref. 181) have interpreted photometric data to indicate that Rayleigh scattering is not valid in the atmosphere of Jupiter and that the atmosphere is filled with clouds of solid particulate matter. This is the more common interpretation.

12
Cloud Markings

THE SURFACES OF BOTH Venus and Jupiter are obscured by perpetual cloud covers. Very little detail is visible across the planetary disk of Venus. In contrast, the visible surface or cloudtop of Jupiter exhibits a band-like structure that is in a continual state of unrest manifested by changes in shape, detail, motion, and coloration. Jupiter has long been a popular object for planetary astronomers, and a variety of motions and forms have been well documented. There is no better summary of the planetary surface as seen from Earth than the description given by Peek (ref. 60). He observed the planet over a long period of time and his description of the belts, zones, and special features is summarized here.

APPEARANCE OF THE VISIBLE SURFACE

NOMENCLATURE

The visible surface of Jupiter can be divided into alternating dark and light bands termed belts and zones, respectively, as shown in figure 12–1. South is at the top of the disk as seen through an inverting telescope from the Northern Hemisphere of Earth. Besides the dusky polar regions, there are four belts and five zones across the middle which are permanent features, but are subject to variations of width and intensity: the North and South Equatorial and Temperate Belts, the Equatorial Zone, and the North and South Tropical and Temperate Zones. The belts are, at times, further divided into two or even three components; such a division is a common aspect for the South Equatorial Belt. Further north and south one or two more temperate belts and zones may occur, possibly geminated or simply merging with the polar regions, which also vary in extent.

Another characteristic, and apparently permanent, Jovian feature is one very large oval region or ring indenting the southern component of the South Equatorial Belt—the famous Great Red Spot, unique to the Southern Hemisphere.

Both hemispheres have irregularly distributed smaller features within the banded pattern consisting of an assortment of markings

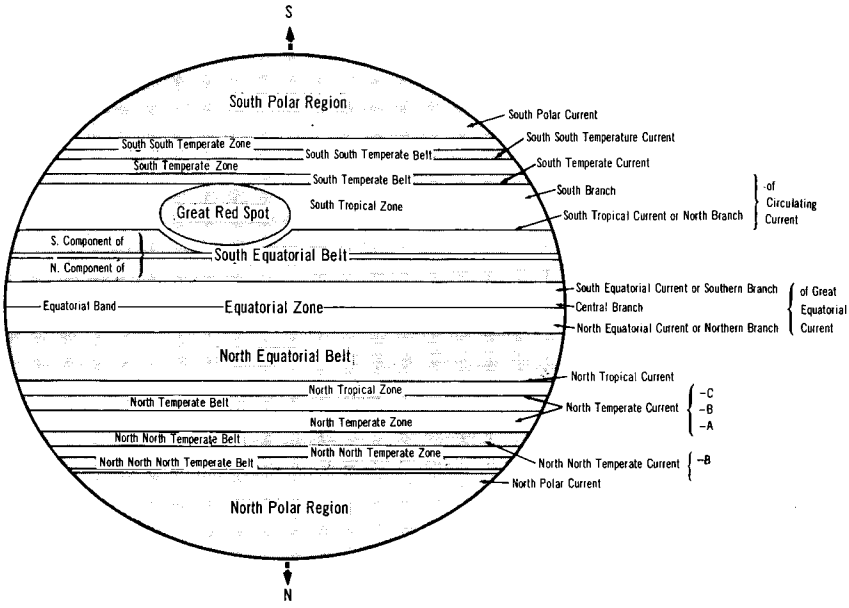

FIGURE 12–1.—Nomenclature of Jovian belts and zones and associated visible surface currents. (Adopted by the British Astronomical Association.)

in the form of streaks, wisps, arches, and loops, as well as patches, lumps, or spots of either darker or lighter material, the association of which often produces mottlings and chains. Persistent observation of the relative motions of conspicuous markings or spots have revealed a number of more or less permanent "surface currents" or "drifts" within, or alongside, the bands, and the names and positions of these are included in figure 12–1.

It is important to remember that the face of Jupiter is ever changing, within the described pattern of bands and belts and the Great Red Spot as shown in figure 12–2.

COLORS

The belts are usually gray but can exhibit great variability in tones of subdued reds and blues. The zones generally appear pale yellow or creamy white; the polar regions are gray and the Great Red Spot is red, when prominent.

LATITUDES OF THE BELTS

Table 12–1 summarizes filar micrometric measurements of the latitudes of the belts over 40 years (ref. 60). It may be seen that, in general, the positions vary. The South Temperate Belt is relatively constant, although it reached a very high southern latitude in 1947.

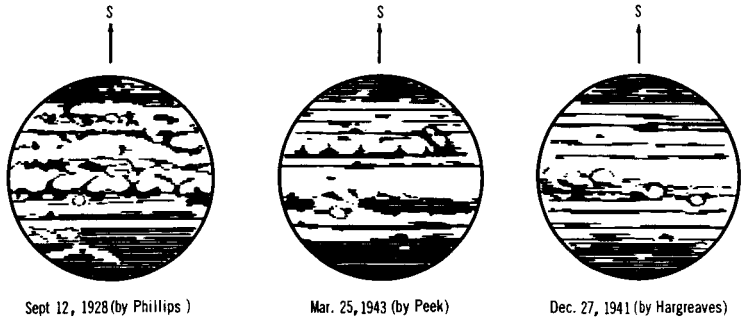

FIGURE 12-2.—Examples of the constant changes in the belts and zones. (Drawings taken from ref. 60.)

Widths of the North Equatorial and South Equatorial Belts are derivable from the latitudes given for their boundaries. Periodicities coincident with Jupiter's optical period of revolution are very uncertain.

CHEMICAL NATURE

Of all the proposed possible atmospheric constituents that can be expected in Jovian atmospheres subject to vapor-pressure restrictions of the cloudtop temperatures, ammonia (crystals) is considered the most reasonable and unchallenged choice (ref. 124). Ammonia fits the modern physical-chemical picture of the visible cloudtops of Jupiter as obtained and confirmed by spectral evidence. At this level, sublimation-condensation of ammonia must occur. Kuiper suggests that the clouds are ammonia cirrus clouds above which ammonia vapor is undersaturated, but on or below which the pressure has reached saturation value.

Of the other cloud-forming candidates, mention must first be made of the relatively abundant methane. To condense methane however, appreciably lower temperatures would be required for the observed clouds. (The freezing point of methane under 1 atm pressure is 90° K.) It has been suggested that the cloudtops of the grayish polar regions are constituted of condensed methane. Water or ice clouds are probably also formed at very deep levels where prevailing high pressures compensate for the low saturation vapor pressure of water. Öpik (ref. 85) describes the process as a snowing out of the water in the deeper, unobservable atmospheric layers. Other possible constituents, such as carbon dioxide (CO_2), ethane (C_6H_6), and ethylene (C_2H_4), have appropriate vapor pressures, but have not been detected in Jovian spectra.

TABLE 12–1.—*Latitudes of the Belts (Micrometrical Measurements of the Latitudes of the Belts from 1908 to 1947)*

[After ref. 60]

Apparition	N Polar Region S edge lat, deg	N N Temperate Belt lat, deg	N Temperate Belt lat, deg	N Equatorial Belt lat, deg		S Equatorial Belt lat, deg		S Temperate Belt lat, deg	SS Temperate Belt lat, deg	S Polar Region N edge lat, deg
				N edge	S edge	N edge	S edge			
1908–1909	+50. 2	+36. 4	----------	+20. 4	+8. 8	−7. 3	−19. 6	−29. 8	−41. 6	
1909–1910	49. 4	[a] 42. 4	+24. 5	14. 0	8. 2	9. 0	19. 1	29. 1	41. 7	
1911	----------	----------	29. 3	[b] +11. 9	--------	7. 5	16. 4	29. 2	44. 5	−57. 4
1912	----------	----------	28. 7	[b] +8. 3	--------	8. 5	17. 2	30. 1	----------	
1913	----------	38. 2	----------	20. 2	7. 9	8. 7	19. 2	30. 4	----------	
1914	48. 5	37. 3	30. 4	19. 3	8. 7	8. 9	19. 5	29. 5	39. 0	
1915	----------	38. 8	26. 4	18. 0	7. 5	8. 3	19. 8	29. 3	43. 5	
1916–1917	48. 5	36. 9	25. 8	17. 1	7. 8	7. 2	19. 3	27. 5	38. 7	
1917–1918	42. 5	38. 3	25. 7	13. 3	6. 3	6. 9	18. 3	26. 7	37. 0	
1918–1919	----------	37. 4	28. 0	18. 8	7. 0	6. 5	17. 7	27. 8	41. 1	
1919–1920	----------	39. 5	29. 3	18. 7	8. 0	4. 4	18. 1	27. 7	42. 0	
1920–1921	45. 7	33. 1	27. 6	12. 7	6. 1	7. 2	19. 2	28. 5	40. 0	
1922	----------	----------	31. 2	22. 0	7. 5	6. 3	19. 2	27. 0	39. 8	
1923	----------	----------	28. 8	19. 2	6. 2	6. 6	18. 9	29. 4	----------	
1924	----------	----------	30. 6	16. 3	4. 9	6. 1	18. 9	28. 7	44. 2	
1925	----------	----------	28. 5	13. 4	6. 1	7. 4	18. 3	29. 5	44. 1	
1926	----------	----------	25. 1	13. 9	6. 1	(9. 5)	--------	28. 7	40. 7	
1927–1928	----------	34. 7	25. 0	17. 5	6. 2	(8. 8)	--------	29. 1	----------	
1928–1929	----------	37. 0	25. 4	19. 8	8. 6	8. 7	17. 2	28. 5	----------	
1929–1930	----------	38. 4	25. 2	16. 6	7. 3	5. 9	17. 6	28. 5	41. 3	
1930–1931 [c]	----------	----------	26. 4	14. 7	6. 5	6. 3	16. 9	29. 3	----------	
							21. 4			

1931–1932			29. 4	21. 0	6. 3	8. 2	19. 7	29. 7	
1932–1933			27. 5	19. 0	6. 6	7. 5	20. 1	29. 9	39. 8
1934 [c d]	+40. 0		30. 1	14. 0	6. 1	7. 4	19. 1 22. 6	28. 6	[e] 41. 9
1935 [c]		[f] 33. 1		18. 6	6. 4	6. 6	17. 4 21. 6	28. 7	43. 3
1936		35. 3	32. 2	19. 6	7: 5	5. 9 (8. 9)	19. 7	28. 9	
1937		[f] 33. 8	27. 9	18. 3	4. 5	(9. 3)		30. 1	45. 4
1938			27. 5	15. 9	7. 4	5. 6	18. 9	29. 6	
1939–1940		38. 9	26. 7	15. 4	8. 7	8. 2	16. 8	27. 2	
1940–1941			24. 8	14. 0	7. 4	6. 4		28. 2	
1941–1942		+36. 5	26. 8	20. 1	7. 1	5. 6	21. 4	29. 3	
1942–1943			27. 0	20. 2	8. 0	7. 4		28. 5	
1943–1944			26. 4	13. 4	7. 4	6. 1	19. 3	28. 6	[e] −44. 9
1944–1945			29. 5	19. 6	9. 0	5. 5	20. 3	29. 2	
1946			29. 6	19. 9	8. 7	7. 7		29. 2	
1947			+30. 3	+19. 5	+6. 8	−7. 2	−21. 8	−30. 5	

[a] Phillips recorded this as a measurement of the NN Temperate Belt; but the high latitude suggests that this belt was missing and that the settings refer more properly to the NNN Temperate Belt.

[b] The micrometer web was placed on the middle of the N Equatorial Belt. This belt was narrow and faint in 1912.

[c] In these years the latitude of the south edge of the S Equatorial Belt was markedly lower in longitudes preceding the preceding end of the South Tropical Disturbance than following it. The 2 figures relate to these different longitudes.

[d] The object measured was described as NNN Temperate Belt.

[e] The belt measured was described as the SSS Temperate Belt. It will be noted that in 1934 its latitude was lower than that of the SS Temperate Belt in 1935. What is implied is that there was another belt visible between this and the S Temperate Belt and Phillips suggested in the former instance that its designation might have been SS Temperate Belt.

[f] The latitude is so low that this may perhaps be considered as a north component of the N Temperate Belt.

All latitudes are zenographical.

Figures enclosed in parentheses indicate that the center of the north component, not the north edge, of the S Equatorial Belt was measured.

Settings on the Equatorial Band, made in 1938 and 1939–1940, reduced to latitudes of $+0^{\circ}.1$ and $-0^{\circ}.6$, respectively.

COLOR THEORIES

According to Wildt (ref. 182) and cited by Kuiper (ref. 124), the Jovian cloud colors result from various solutions of metallic sodium in liquid or solid ammonia, and the temperature determines the color. Below 161° K, gray is present; above 161° K, brown appears; and above 195° K, the (liquid) solutions assume a blue shade. Kuiper remarks that the temperatures required by the chemistry agree with computed cloud temperatures. Although the origin of the sodium atoms remains to be explained, it is possible that it is cosmically supplied from comets' tails, etc. Calcium, also cosmically abundant, would coexist and account especially for the complete range of hues from yellow and delicate gold to red and bronze which, perhaps, fits the theory regarding the color variations of the Great Red Spot. Since carbon (methane, CH_4) and hydrogen are proven constituents of the Jovian atmosphere, organic polymers have also been proposed. An example is cuprene $(C_2H_2)_n$, a red polymer of acetylene formed by ultraviolet irradiation of methane (ref. 183).

A more modern but partial interpretation of Jovian colors in terms of free radicals stabilized in "ices" at low temperatures has been advanced by Rice (refs. 184 to 186), who has supported it with chemical experiments. The possible transitory radicals amine (NH_2), imine (NH), hydrazine (NH_2NH), methyl (CH_3), and methylene (CH_2) could be formed during the absorption of ultraviolet sunlight by the ammonia (NH_3) and methane (CH_4) of Jupiter's atmosphere and could be frozen for periods of time in this extremely cold environment. The colors exhibited by the free radicals, however, are mostly yellows and blues.

Papazian (ref. 187) suggested charged-particle bombardment at the tips of the Jovian radiation belts, at three different latitudes (north and south), to explain the observed colored bands of Jupiter, but this explanation may be artificial according to Field (ref. 168). In support of theories postulating color changes dependent on temperature or solar activity, correlations have been claimed by both Williams (ref. 188) for temperature and Peek (ref. 60) for solar activity.

CLOUDTOP MORPHOLOGY

The clouds of Jupiter were at first assumed to be flat-topped, but the evident turbulent cloud motions observable with any low-powered telescope suggest that various forms of cloudtops must be present. Hess (ref. 189) investigated the possible variations in heights and temperatures of the Jovian ammonia cloud surface. He studied the ammonia and methane absorptions in the visible spectrum bands centered at 6441 Å and at 6190 Å, respectively. The absorptions

were found to decrease slightly toward the limbs (at 60° from the center of the disk), and Hess concluded that the cloud surface rises toward the limbs. The unequal solar heating that sublimes the ammonia crystals faster at the equator was also held responsible for maintaining a small difference in temperature (approximately 6° C) between 60° latitude and the equator and, likewise, a small difference in cloud heights (possibly 10 km). However, Hess's cloud layer was assumed to be flat-topped.

A different hypothesis was advanced by Squires (ref. 190) on the basis of observations by Hess. Assuming a temperature much in excess of 170° K (Hess assumed 150° K) for the main cloud-deck level, Squires proposed the existence of large cumuliform equatorial clouds with tops reaching perhaps 20 to 30 kilometers above the main cloud deck. The temperature between the Jovian cumuli towers could reach 230° K if the ammonia vapor pressure there is well below the saturation value and if the towers are extensive enough to provide efficient shielding. Squires' theory was recently favored by spectroscopic temperature determinations which used a methane band at 1.1 microns, and gave the value of 200° K (ref. 111). This high value was thought to be caused by increased penetration into the atmosphere at this wavelength band.

DESCRIPTION OF JOVIAN BELTS AND ZONES

EQUATORIAL ZONE

This large zone straddles the equator, but seldom symmetrically, and covers about ⅛ of the planet surface. Its latitudinal width, averaging 14°, has varied greatly from 17.6° (in 1914) to 11.0° (in 1924) over a 40-year period of observation (1908–1947). The boundaries oscillate some 2° north or south of their mean (nearly symmetric) latitudes at +7.2° N and −7.1° S. A thin, dusky line known as the Equatorial Band sometimes indistinctly divides the zone within 1° of the true equator. It is usually fragmentary but can be prominent (1937–1940) and even wider and darker, and at times geminate. Gray wisps from the North and South Equatorial Belts may curve and merge into fragments of this band.

The Equatorial Zone's intensity can change from brightest on the planet (white in 1924) to a deep sombre tone (in 1920), usually with tawny or leaden hues. Many structural details and delicate mottlings can be resolved in the frequent light spots and dusky patches. The Equatorial Zone is separated into three branches by features created by rotation. These are the Northern, the Central, and the Southern Branches of the Great Equatorial Current. Their mean periods are similar (about $9^h50^m25^s$).

NORTH HEMISPHERE

NORTH EQUATORIAL BELT.—The great width and darkness of this belt make it the most conspicuous on Jupiter. Only rivalled by the South Equatorial Belt which may become darker, it usually differs from it by appearing as one broad belt, although partial division does occur (1906–1908). Its width is highly variable, from 1° to 15°, with the south edge anywhere from latitudes 4.5° to 9.0° N, and the north edge from 13.3° to 22.0° N, as seen in table 12–1. Faint and narrow (~1°) in 1904 to 1906, it suddenly became the broadest (~15°) and darkest belt on Jupiter in 1906.

Since 1900, the North Equatorial Belt has been the most consistently active region of Jupiter with dark projections forming frequently and rapidly from its southern edge and moving with the North Equatorial Current. The less active northern edge merges into the North Tropical Current, which draws out small dark spots into long streaks. Large round white spots seem more enduring. Rotation periods are quite variable for these spots. The North Equatorial Current is some 30 minutes faster. At opposite edges of the North Equatorial Belt, dark projections form with shapes varying from tiny humps or short spikes to large elongated masses or streaks. The humps and spikes often develop into gray wisps, dispersing into the Equatorial Zone, but more often curving around into loops or arches. A fascinating series of gray arches may be seen. The elongated masses or streaks, which can be quite conspicuous, may also appear rectangular or chain-like.

The central portion is sometimes very active, breaking out with white spots or rift-like streaks of different brilliances and structures (straight or curved, with bright nuclei) changing form very rapidly. Rotation periods are intermediate to those of the two currents mentioned. Colors reported for the different regions show great variability (and also inconsistencies).

NORTH TROPICAL ZONE.—This zone is usually conspicuous but also highly variable in breadth, complementary to that of the North Equatorial Belt. Dark spots and streaks are characteristic along the edges, but occasional white spots are general in the northern half of the zone. Brightness varies considerably with time and longitude; however, sometimes it is the brightest zone of Jupiter.

NORTH TEMPERATE BELT AND ZONE.—This belt and zone vary in width and intensity. The zone may be the brightest zone or practically disappear. Large white spots appear at times, with slow drift rates. The belt can be very broad (~9°) and even geminate, but usually it is narrow. Spots at its edges appear with widely different rotation periods, very long at the north and very short at the south

(sometimes the shortest on Jupiter). The rotation periods reveal two currents, North Temperate Currents A and C. There is also an intermediate North Temperate Current B, which seems to carry the aftermath of outbreaks of the rapidly moving southern spots (ref. 60). Dull colors, mostly grays and blue-grays, are usually associated with the North Temperate Belt.

NORTH NORTH TEMPERATE BELT AND ZONE.—This zone is frequently lost in the general north polar shading and seldom displays conspicuous features, such as occasional white spots.

The belt is often broken up into faint and dark fragments and (in places) may appear double, although not very distinctly. A fairly steady current (NN Temperate Current A) was derived from the dark spots.

NORTH NORTH NORTH TEMPERATE BELT AND ZONE.—This belt and zone are only intermittent additions to the Jovian striped pattern. The zone, when visible, may not fully circle the planet. Usually featureless, it may show only one or two bright spots. The belt, limiting the zone, varies in latitude, which makes it difficult to identify, especially when fragmented. It may also be geminate.

NORTH POLAR REGION.—A large variable dusky area, this polar cloudcap region extends to about 48° N latitude. No periodicity was found in its variation. The duskiness varies, too (very dark in 1924). Although its periphery may divide itself into thin belts (up to 60° N lat), the North Polar Region does not seem to be finely striated, as was thought in the 1890's. The contrast or grayishness of the North Polar Region does not differ much from that of its southern counterpart (South Polar Region) (ref. 191). Though usually featureless, there are occasional appearances of duskier patches or streaks and also rare white spots. A North Polar Current apparently exists with a steady drift rate of $9^h55^m42^s$ (ref. 60).

SOUTH HEMISPHERE

SOUTH EQUATORIAL BELT.—The South Equatorial Belt generally consists of two distinct components separated by a wide, bright space similar to a zone. The south component is indented deeply by the Great Red Spot. The total width of the South Equatorial Belt is greater than that of the North Equatorial Belt, and varies less. It is also far less active, although at times it is the most conspicuous belt on the planet (1892–1908, 1912, 1925). Peek (ref. 60) summarized its behavior for more than 40 years as "long periods of quiescence, punctuated by outbursts of intense activity such as have never been rivalled by the North Equatorial Belt," and following periods when the south component had disappeared or faded out. He described these remarkable "revivals" of the South Equa-

torial Belt which took place in 1919–1920, 1928–1929, 1942–1943, and 1949. At such times, the south component provided spots endowed with the longest rotation periods ever recorded, some of which are associated with the North Circulating Current. Dark projections and light rifts also may be present, but none of the dark elongated patches or large white spots so characteristic of the north edge of the North Equatorial Belt. This again shows the lack of symmetry between hemispheres. The space between components is usually calm and featureless. The north component shows occasional projections and wisps, and most of its spots move with one of the branches of the South Equatorial Current. Color estimates of the South Equatorial Belt vary widely. Sometimes gray or gray-blue, it is more often pink, with differing tints for each component.

SOUTH TROPICAL ZONE.—The South Tropical Zone is the most remarkable region of the whole planet. To quote Peek: "That one zone, comprising only about 10° of latitude, should be the site of the Great Red Spot, the South Tropical Disturbance, the Circulating Current, the Oscillating Spot of 1940–1941 and 1941–1942, and the Dark South Tropical Streaks of 1941–1942 and 1946, is little short of bewildering." These phenomena are discussed separately later.

If the disturbed portion of this zone is often heavily shaded, the undisturbed portion is always conspicuous by its brightness and usually its whiteness. In both portions many spots and markings appear, but they seem unrelated to any special phenomenon, as shown by their rotation periods. There is no special south tropical current in these tropical latitudes.

SOUTH TEMPERATE BELT AND ZONE.—The South Temperate Belt is narrow but permanent and it has attracted much interest. At times it is the darkest belt on Jupiter, and its intensity around the planet can vary to extremes. It may also be geminate in places. Frequent spots (dark and light) or sections of the belt are controlled by the steady South Temperate Current. Its series of objects may have years of longevity. A little to the north a delicate gray line with dusky spots may appear which defines the South Circulating Current. The color of the belt is predominantly gray.

The South Temperate Zone is frequently wide and sometimes divided over long stretches by a thin gray line which may form bends. The bends are probably formed by the action of the South South Temperate Current. The zone brightness is quite variable, and dusky strips associated with white spots may develop (one was named the South Temperate Disturbance). The color of the zone is usually creamy yellow or white. The South Temperate Current controls objects of the belt and the zone, but the steadier South South Temperate Current may dominate the whole temperate region for years.

SOUTH SOUTH TEMPERATE BELT AND ZONE.—Although the rotation periods of its spots and markings are comparatively constant, the South South Temperate Belt assumes various aspects. The color is faint and gray with occasional brown tinges. Considerable disturbances took place in this belt from 1927 to 1929. The South South Temperate Zone, which is also poorly known, seems to suffer frequent interruptions when encircling the planet. The South South Temperate Current, flowing steadily over a wide range of latitudes, is prominent and well determined.

SOUTH SOUTH SOUTH TEMPERATE BELT AND ZONE.—A rather ephemeral feature, the South South South Temperate Belt may be classified as a south component of the South South Temperate Belt, but usually is immersed in the South Polar Region shading. It seems, however, that a dependence upon the South South Temperate Current exists, as was evident in 1934. The South South South Temperate Zone is seldom described, and little is known about it.

SOUTH POLAR REGION.—The boundary of the gray south polar shading is much higher in latitude than for its northern counterpart, the North Polar Region, but this boundary varies greatly, often reaching the South South Temperate Belt. Featureless most of the time, the South Polar Region does have a tendency to form dusky belts within its domain (1929–1930, 1941–1942, etc.). The most northern one may be the South South South Temperate Belt or perhaps the South South Temperate Belt. Otherwise there is no striated pattern, as claimed by early observers.

SPECIAL FEATURES AND DISTURBANCES

THE GREAT RED SPOT

Discovered in 1665 by Cassini and called the "eye of Jupiter," the famous Great Red Spot of Jupiter seemed to have been little noticed despite its tremendous size until the years 1878 to 1882 when it had gained a striking redness in coloration. Shaped as an enormous oval of some 40 000 kilometers in length and 13 000 kilometers wide, it has repeatedly faded into invisibility and then reappeared with great contrast. Its length may vary somewhat, and the oval may become pointed at the ends of its long axis which lies parallel to the equator (the common direction of all Jovian bands). Situated mostly in the South Tropical Zone, the northern portion of the large oval cuts a large bay called the Red Spot Hollow into the South Equatorial Belt. This hollow is always noticeable and permits location of the Red Spot when the Spot is invisible or very faint. There is usually a

space between the two features. The usual aspect of the Red Spot (assumed in this century) is that of an oval ring with a very faint center; however, it may also assume uniform contrast or shading over its entirety. The long axis of the oval has on rare, short occasions been seen slightly inclined to the equator. When this axis was shortest, during 1936, and occupied 27° of longitude, the Red Spot appeared at its darkest since 1881. Its greatest extent, when the pointed ends are present, spans up to 40° in longitude. The variations in longitudinal positions of the Red Spot are notable. A study by Peek (ref. 60), who utilized reliable records that dated as far back as 1831, established its wanderings to be over 3529°, using System II, or nearly 10 complete rotations. This total, however, could be reduced to 1080°, or exactly 3 rotations, if another reference system were chosen. Figure 12–3, from the same study, depicts the erratic wanderings of the Great Red Spot in longitude over the 124 years between 1831 and 1955. The motion had an important reversal around 1880.

A curious connection apparently existed between the Red Spot and the feature known as the South Tropical Disturbance (discussed in a subsequent paragraph) which was another remarkable but not a permanent feature of the South Tropical Zone between 1901 and 1940. The shorter period of rotation of the South Tropical Disturbance enabled it to catch up with the Red Spot and even bypass it in a very unusual way which is discussed in the next paragraph. Theories about the Great Red Spot are reviewed in chapter 13.

SOUTH TROPICAL DISTURBANCE (1901–1940)

In February 1901, a few degrees of latitude of the South Tropical Zone became heavily shaded in its middle and developed brilliant white spots at both ends. The dusky portion became known as the South Tropical Disturbance because of its extraordinary behavior. At first it was situated some 90° ahead of the Red Spot, but with a rotation period some 21^s shorter, it was able to catch up with the Red Spot in June 1902. In the process, its preceding end had traveled some 270° in longitude to reach the following end of the Red Spot. Then, very unexpectedly and within a few days instead of the expected 6 weeks, a facsimile of the preceding end of the disturbance formed at the other end of the Red Spot Hollow and continued to progress at the same rate as before. This rapid leap across the Red Spot, which extended the disturbance over some 90° in longitude, was terminated by September 1902. The duration of the "conjunction" had been 3 months. About nine such conjunctions occurred in the career of the South Tropical Disturbance, which ended in 1940 when its lengthening rotation period reached that of the Red Spot.

Table 12–2, compiled by Peek (ref. 60), gives the history of the

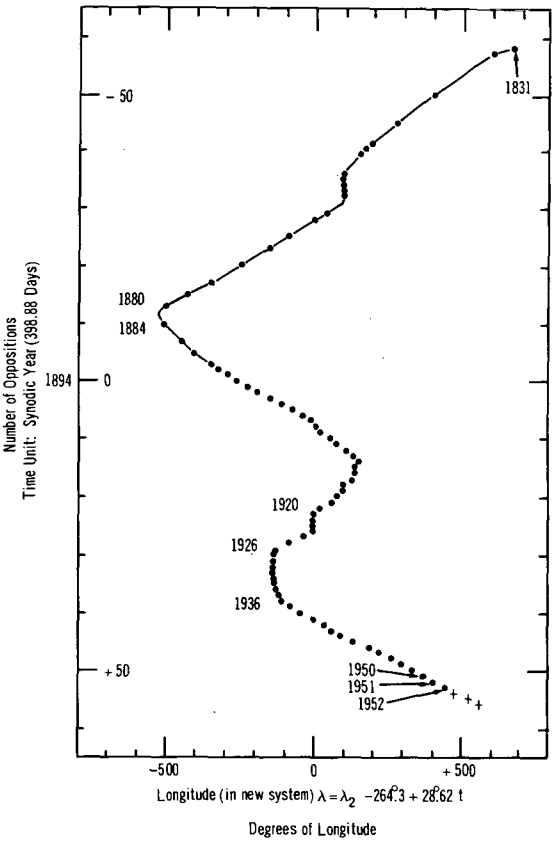

FIGURE 12-3.—The wanderings of the Great Red Spot in longitude, 1831 to 1955. (After ref. 60.)

interaction. The ninth conjunction lasted for 10 years, while the eighth was shorter than expected and was abortive. The length of the disturbance generally increased, too (a record 230° in 1935), always marked off by the two terminal bright spots. In the closing years, the long and once uniform dusky shading became mottled, and grew progressively fainter and disappeared in 1940, while the white spots gradually lost their brilliance.

DARK SOUTH TROPICAL STREAKS.—In 1941, a dark object just preceding the Red Spot developed into a streak some 30° long then drew away from the Red Spot, keeping a constant length for several months. It resembled the South Tropical Disturbance of 1903, but was much shorter and moved more rapidly. (See sketches by Hargreaves (ref. 192).) In 1946, a very similar streak recurred of about 40° length, and vanished in 1947. There seems to be a close connection between such streaks an the Red Spot Hollow.

TABLE 12–2.—*Interaction of the Great Red Spot and the South Tropical Disturbance*

[After ref. 60]

Apparition	Rotation period of Red Spot	Rotation period of disturbance		Conjunction	Length of disturbance
		Preceding end	Following end		
1901	9h55m41s	9h55m20s	9h55m20s		A few degrees
1902	39	16	16	1st	Max about 90°; Min 35°
1903	41	Center 9h55m21s			
1904–1905	40	9h55m21s	9h55m23s	2d	Max 80°; later 30°
1905–1906	41	19	23	3d	65°
1906–1907	42	22	22		57°–45°
1907–1908	41	17	22	4th	90°–100°
1908–1909	42	20	26		57°–70°
1909–1910	38	21	20	5th	108°
1911	38	20	30		115°
1912	39	27	26		65°
1913	35	28	24	6th	Max at least 140°
1914	36	28			109°
1915	37	31	28		92°
1916–1917	36	28	28	7th	119°
1917–1918	34	25	31		167°
1918–1919	37	30	30		Max 190°+
1919–1920	35	33	29		136°
1920–1921	38	30	33		134°
1922	39	31	32	8th (partial)	151°
1923	37		32		160°±

1924	32	34	41		145°
1925	33	34	39		150°
1926	36				Invisible
1927–1928	38				Invisible
1928–1929	38	15	41		220°
1929–1930	38	32	36		214°
1930–1931	39	33	37		202°
1931–1932	38	35	37		213°
1932–1933	39	37	37		227°
1934	39	38	39	9th	224°
1935	39	38	40		230°
1936	41				Invisible
1937	42				Invisible
1938	42	33			Uncertain
1939–1940	44	38	34	Beginning of 10th?	207°

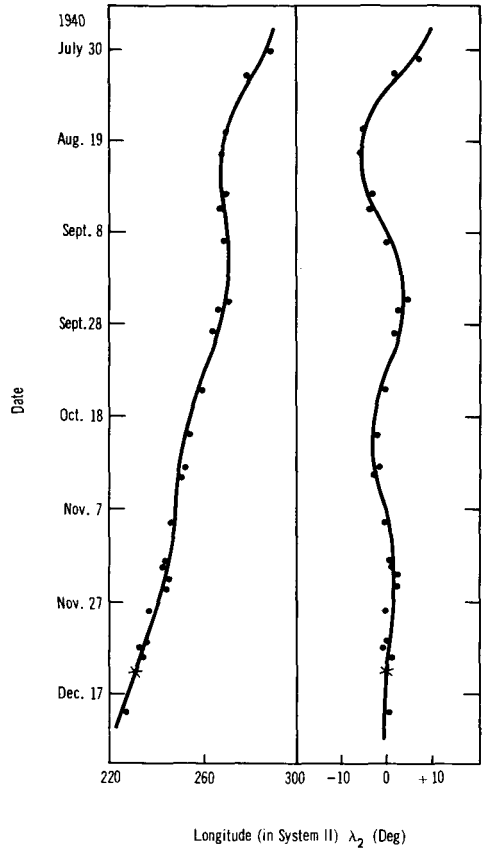

FIGURE 12–4.—Motion in longitude of the oscillating spot of 1940–1941. (After ref. 60.)

OSCILLATING SPOTS.—In 1940, a dark spot appeared in the South Tropical Zone at a constant latitude, but showed remarkable oscillations in longitude which Peek fitted very well with a damped harmonic curve (fig. 12–4). In 1941, a second object almost similar in size, location, darkness, and motion appeared but ended with very definite oscillations in latitude as it progressed northward across the South Tropical Zone. Peek theorized that the spots originated as solid fragments detached from the Jovian crust and rose with the damped vertical motion of a floating body in the atmosphere of a rotating planet.

CIRCULATING CURRENT.—In 1920, a pair of dark spots appeared in the South Tropical Zone and moved along the south component of the South Tropical Zone toward the preceding end of the South Tropical Disturbance. Upon reaching the concave edge of the

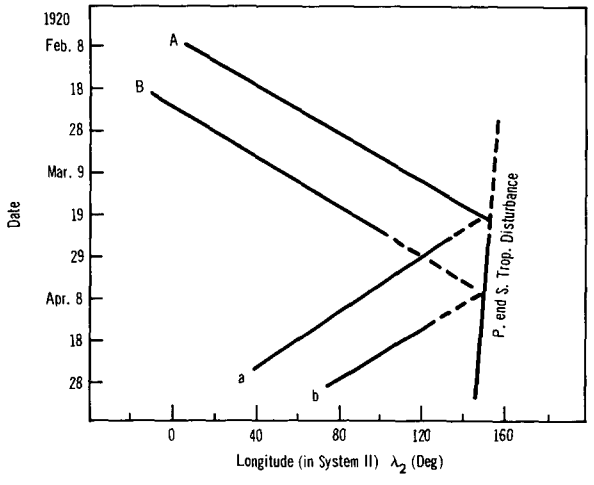

FIGURE 12–5.—The motion in longitude of the circulating spots of 1920. (After ref. 60.)

latter, the spots were swept back in the opposite direction and continued at the same rate along the north edge of the South Temperate Belt (fig. 12–5). The current responsible for the sweeping, reflecting effect was named the Circulating Current. Similar events recurred at other apparitions until 1934 but with less definiteness.

13

Atmospheric Composition

SPECTROSCOPY PROVIDES the only reliable means of detecting gaseous constituents in the atmospheres of distant planets. The spectra of Jovian planets differ radically from those of terrestrial planets; they exhibit, especially in their red portion, absorption bands of such intensities that they can easily be seen visually. In the early 1930's these bands were proved to be caused by moderate amounts of ammonia and methane. The presence of such gases strongly suggested the presence of molecular hydrogen, which was already suspected but was undetectable at the time. By the late 1950's hydrogen was detected on Jupiter, and its abundance was estimated to be enormous, far exceeding that of ammonia or methane. Only these three constituents have been ascertained in the upper atmosphere of Jupiter; however, others are being sought.

Kuiper (ref. 124) has theorized that since Jovian atmospheres are chemically reducing, while terrestrial atmospheres are oxidizing, the former are direct descendants of the protoplanets, while the latter are definitely secondary in origin. The protoplanets, in this theory, were condensations of the original solar nebula and contained, like the Sun, a great predominance of hydrogen together with substantial amounts of helium.

AMMONIA AND METHANE

Exploratory work on the structure of the strong bands of Jovian spectra was carried out for many years by Slipher (refs. 193 to 195) at Lowell Observatory, first in the red and then in the infrared. The interpretation in terms of ammonia and methane was provided by Wildt (ref. 196) in Göttingen, who succeeded in identifying many of the lines and bands. Confirmation followed almost immediately when Dunham (ref. 197), using the new Coudé spectrograph of the Mount Wilson 100-inch telescope, obtained the first high-dispersion spectra of Jupiter.

Later, the abundances of ammonia and methane were estimated by Kuiper (ref. 124) from comparison with laboratory spectra of pure gases in pipes. Under the assumption that the observed atmosphere of Jupiter is a clear (Rayleigh) layer overlying a reflecting cloudtop,

he found the values of 7 m-atm[1] of ammonia and 150 m-atm of methane. These values are considered approximate, since Kuiper's assumption is still unconfirmed. In fact, the upper atmosphere of Jupiter may not be as clear as assumed, in which case particle scattering may complicate the normal formation of the absorption lines. Another effect also may be present, such as reemission (sky luminescence). For these reasons Herzberg (ref. 198), considering these two effects, ventured to say only that Jupiter's observed atmosphere appears to have about 10 m-atm of ammonia and about 500 m-atm of methane.

Modern high-dispersion spectrography has resolved the fine structure of Jupiter's prominent orange, red, and near-infrared bands. Kiess et al. (ref. 199) presented tabulations of the wavelengths and estimated intensities of the lines making up the bands of ammonia at 6450 and 7900 Å and of methane at 6190, 7250, 8420, and 8620 Å. Further work was done by Spinrad and Trafton (ref. 200) in the visible and by Owen (ref. 201) in the infrared (from 9700 to 11200 Å).

The stability of the ammonia and methane concentrations observed in the Jovian atmosphere was examined first by Wildt (ref. 202) and much later by Cadle (ref. 203) from the standpoint of photochemistry. Wildt took into account the importance of ultraviolet photodecomposition of methane and ammonia, which produces free radicals CH_3 (methyl), NH_2 (amino), and others, as well as that of secondary chemical reactions such as hydrogenation, recombination, and polymerization. Thus, he could explain the great stability of methane, as the end product of all reactions involving carbon in the Jovian atmosphere, but could offer no scheme of reactions regenerating the irreversibly photolyzed ammonia.

Cadle, using modern information, suggested that a slow photolysis of $H_2 \rightarrow 2H$ from continuous absorption of vacuum ultraviolet can occur down to great depth in the atmosphere, maintaining the ammonia and methane concentrations through a chain of possible accessory compounds formed from the radicals NH_2 and CH_3 which descend by convection or diffusion from the upper photolytic zone.

HYDROGEN

The low mean density and the considerable mass of Jupiter, the presence of ammonia and methane in its atmosphere, and the predominance of hydrogen in the Sun suggested to astronomers at least 30 years ago the probability that molecular hydrogen was abundant

[1] The amount of gas in a single vertical column through the atmosphere of the planet is equivelent to 7 meters of ammonia at atmospheric pressure (1 atm STP).

on Jupiter (ref. 204). Its detection by spectrograph was not a simple matter and came about only a few years ago. The hydrogen molecule (H_2), like the nitrogen molecule (N_2), has no dipole moment and, therefore, displays no ordinary spectrum. Herzberg (ref. 205) noted earlier that molecular hydrogen had a quadrupole moment with possible energy transitions producing a "quadrupole rotation-vibration spectrum," but that the lines would be detectable only if sufficiently large amounts were present, which could be precisely the case with the major planets. He even predicted the wavelengths and the approximate strengths of the various lines making up the bands expected in the visible and infrared. The quadrupole lines are exceedingly narrow or sharp (being practically unaffected by pressure broadening), and, therefore, are detectable only under the very highest resolutions.

Kiess et al. (ref. 199), accomplished the identification of four weak lines lying in the near-infrared spectrum (8046 to 8497 Å) of Jupiter which are known as the $Q(1)$, $S(0)$, $S(1)$, and $S(2)$ lines of the (3–0) quadrupole band, or transition of H_2. A rough estimate of the H_2 abundance can be derived from comparison of the strengths of the lines against theoretical values (oscillator strengths, also called f-values). Zabriskie (ref. 109), using f-values calculated by James and Coolidge (ref. 206), obtained an abundance of $\sim$5 km-atm of hydrogen above the cloudtop of Jupiter. Using more recent f-values by Kolos and Roothaan (ref. 207) and new spectra, Spinrad and Trafton (ref. 200) found an abundance of about 27 ± 9 km-atm. The underlying assumptions for both estimates are: (1) the cloudtop is an even spherical reflecting surface, (2) the quadrupole lines are unsaturated, and (3) the temperature along the atmospheric column is constant. The second assumption may be unfounded, in which case the estimates are lower limits. Foltz and Rank (ref. 208) suggested a tenfold increase to 270 km-atm. An equilibrium rotational temperature of about 170° K was used in the two abundance estimates. This temperature is derived from the ratio of two quadrupole line-strengths, the ratio of their f-values, and the use of the Boltzmann temperature relation. It is possible that the temperature is as high as 230° K, if the clouds form towers instead of a smooth surface (ref. 190).

A recent review by Field (ref. 209) concerned with hydrogen abundance on Jupiter shows that 30 to 80 km-atm of hydrogen is an acceptable value, but 30 km-atm is more probable if one considers the absence of strong Rayleigh scattering in the near ultraviolet. Interestingly, such a value ($\sim$30 km-atm) agrees with the values obtained by Trafton (ref. 126) above the top of the convection zone of his model atmospheres of Jupiter.

The abundance ratio H/C in the Jovian upper atmosphere may be

computed from the H_2/CH_4 ratio. Taking the accepted values of 27 km-atm of H_2 and 0.15 km-atm of CH_4, the ratios are $H_2/CH_4=180$, and $H/C=360$. Comparing this last value with the corresponding one for the Sun, $H/C=2000$, it is apparent Jupiter's atmosphere has lost a great amount of hydrogen since the protoplanet stage, provided the carbon abundances have not changed greatly.

OTHER CONSTITUENTS

The presence in the observable Jovian atmosphere of gaseous elements and compounds, other than hydrogen, methane, and ammonia, is strongly suspected, but their discovery is still beyond reach of our ground-based spectroscopic techniques. Either our atmosphere handicaps the observations (too-narrow windows and too many telluric lines) or the dispersion of spectrographs is not yet high enough. However, for a number of reasons (cosmological, planetological, physicochemical, or photochemical), it is reasonable to expect that there are more constituents than the three already detected.

ELEMENTS.—The inert gases are known to be abundant in the solar atmosphere, with helium second only to hydrogen. Thus, they can be expected in the Jovian atmosphere on cosmological grounds. Planet formation dynamics led Kuiper (ref. 124) to estimate that Jupiter had retained 2.5 to 5 percent of its original gaseous envelope because of its considerable planetary mass. Moreover, two observed characteristics of Jupiter, its low mean density (1.6) and its stratospheric mean molecular weight (3 to 4), strongly suggest a helium abundance of the same order of magnitude as that of hydrogen. Spinrad and Trafton (ref. 200) and later Trafton (ref. 126) found physicochemical indications of roughly equal proportions of helium and hydrogen. Öpik (ref. 85), after a long planetological and cosmological discussion of Jupiter favored great predominance of helium.

Nitrogen (N_2) in the free state is also suspected to be present, but no upper limit of its abundance has been established in the ultra violet. Öpik found, from calculations of the statistical equilibrium condition between ammonia and hydrogen, that almost all of the nitrogen must be bound in ammonia. Similar reasoning also showed most of any carbon to be bound in methane (CH_4).

The isotope most likely to occur is deuterium, probably in the form of deuterium hydride, HD. Kuiper indicated that the ratio of deuterium to hydrogen might be considerably larger than the terrestrial value (1/6400), as a result of the lesser escape of deuterium hydride than hydrogen in the early history of Jupiter. Owen (ref. 201), a student of Kuiper, presented a ratio of deuterium to hydrogen $<1/1300$ and gave a spectroscopic upper limit for deuterium hydride.

COMPOUNDS.—Speculation is permissible concerning the occurrence of a number of gaseous compounds of physical and chemical properties of the known Jovian environment. Restrictions of vapor pressure, possibilities of secondary reactions, and photochemical equilibria conditions are paramount among the guidelines in selecting gases capable of stability. Kuiper (ref. 124) suggested, from his general list of planetary atmospheric gases, that on Jupiter the following be considered: water, hydrogen sulfide, NH compounds, phosphine PH_3, cyanogen C_2N_2, simple hydrocarbons and derivatives. The likelihood of finding water, which certainly must trap most of any occurring oxygen (O or O_2) in the presence of Jovian hydrogen, should not be overlooked. But, as Öpik (ref. 85) noted, water should occur as condensations in the deeper unobservable layers of the atmosphere, since any water vapor rising toward the cold cloudtop would be snowed out rapidly. Carbon dioxide, much more volatile than water or ammonia, is thought by Öpik to be scarce, because if not it would rise and form ice clouds obscuring the ammonia clouds, an effect which has not been observed. Chemical reactions in the deeper warmer layers must reduce any carbon dioxide, or even carbon monoxide, completely to methane.

Wildt (ref. 202) advised a search for traces for methylamine (CH_3NH_2) as a stable recombination product of the radicals CH_3 and NH_2 (formed under UV photolysis of methane and ammonia in the upper atmosphere), but rejected hydrazine (NH_2NH_2) as too photolabile and of too low vapor pressure. Also, he eliminated a priori all hydrocarbons other than methane, reasoning that active hydrogenation would break down all carbon-to-carbon bonds to the most stable methane and that rapid photodecomposition might take place. Years later, however, more information led Cadle (ref. 203) to favor the transitory formation of hydrazine as a part of a series of photochemical reactions, and to consider as quite possible the appearance of traces of simple hydrocarbons such as ethylene (C_2H_2) and particularly, ethane (C_2H_6).

Owen (refs. 111 and 201) set out to determine upper limits of abundances of a selected list of possible compounds by examining their nondetectibility on some infrared spectra [2] in the region 9000 to 11200 Å. His latest results are presented in table 13–1 which lists hydrogen cyanide (HCN), proposed by Sagan (ref. 210); methyl deuteride (CH_3D), proposed by Bardwell and Herzberg (ref. 211); the unusual silane (SiH_4), suggested by Eucken (ref. 212); and the controversial acetylene (C_2H_2), advocated by Sagan and Miller (ref. 155). Refinements to the upper limits given are expected by the

[2] Obtained in 1955 by Kuiper at McDonald Observatory, Arizona.

TABLE 13-1.—*Possible Gases in the Jovian Visible Atmosphere*

[After ref. 201]

Possible gases	Band used, Å	Upper limit abundance, m-atm
Acetylene (C_2H_2)	10 372	<3
Ethylene (C_2H_4)	8 715	<2
Ethane (C_2H_6)	9 060	<4
Methylamine (CH_3NH_2)	10 325	<3
Hydrogen cyanide (HCN)	10 385	<2
Silane (SiH_4)	9 738	<20
Methyl deuteride (CH_3D)	9 936	<20
Deuterium hydride (HD)	7 377 and 7 464	<500

authors from Jovian spectra taken with higher resolutions, in longer infrared wavelengths, and comparisons with low-temperature laboratory spectra.

COMPOSITION OF THE UPPER ATMOSPHERE

MEAN MOLECULAR WEIGHT.—An estimate of the mean molecular weight of the Jovian upper atmosphere has been provided by a rare photoelectric observation made by Baum and Code (ref. 213) with the 60-inch Mount Wilson telescope. They observed the occultation extinction of the 5.5-magnitude star σ-Arietis by Jupiter. The differential refraction of this star's light when passing through the Jovian stratosphere was recorded as a photometric extinction curve (intensity versus time), and the extinction rate (slope of the curve) was used for deriving the scale height. Since the scale height h is directly proportional to the absolute temperature T and inversely proportional to the mean molecular weight $\bar{\mu}$, it is possible to estimate the latter ($\bar{\mu} \sim T/h$) if the former is given, making the assumption of an isothermal stratosphere. Thus, Baum and Code obtained a value of $\bar{\mu}=3.3$ by taking Kuiper's value of $T=86°$ K (ref. 124). (The mean scale height derived was $h \cong 8.3$ kilometers.) The immediate interpretation of such a result was the direct observational confirmation of the predominance of the lightest gases, hydrogen and helium, in Jupiter's atmosphere.

In addition to the uncertainties in the data and several assumptions made, it should be noted that $\bar{\mu}$ is critically proportional to T. In fact, a value of $\bar{\mu}=4.3 \pm 0.5$ was recommended by Öpik (ref. 85) from his calculated radiative equilibrium temperature of $T=112 \pm 2°$

K for the occultation layer. This temperature value was calculated from an elaborate polychromatic radiation equilibrium analysis involving ammonia and methane as the two chief radiators in the Jovian atmosphere. The higher result for $\bar{\mu}$ favors a greater percentage of helium and heavier gases than hydrogen.

TOTAL PRESSURE.—Spectroscopic observation of pressure-sensitive absorption lines of gases detected in a planet's atmosphere can be used with advantage to make estimates of the total atmospheric pressure at a certain level. By analyzing line widths of the methane band at 6190 Å and assuming a Lorentzian shape for the lines, Spinrad and Trafton (ref. 200) used the pressure-broadening effect to determine an upper limit of 2.8 atmospheres for the total pressure at the base of the methane column observed, which is presumably also the level of the cloudtop.

Speculations on the optical properties of Jupiter's disk, coupled with Baum and Code's star occultation results, may also lead to an estimate of density or pressure of the Jupiter atmosphere (ref. 213). Öpik, using calculations by Van de Hulst of the optical depth at cloudtop level from scattering theory and his own evaluation of the optical depth at occultation level, was able to estimate the total pressure at cloudtop to be about 13 atmospheres. (See ref. 85.) This is about four times the spectroscopic upper limit given, but it should be noted that Öpik used various uncertain assumptions.

PROPOSED COMPOSITIONS.—From the observed spectroscopic abundances of ammonia, methane, and hydrogen and the two constraints of mean molecular weight and total pressure, it becomes possible to deduce the abundances of the remaining gases which are assumed to be mostly the inert gases helium, neon, and argon. Spinrad and Trafton (ref. 200) using their results for hydrogen abundance (27 km-atm) and total pressure ($P=2.8$ atm) as well as the value of $\bar{\mu}=3.4$, proposed a "working" atmospheric composition presented in table 13–2. The major gas is molecular hydrogen, about 60 percent of the total, followed by helium, at about 36 percent. Qualitatively, this composition is similar to that of the Sun and stars.

Öpik (ref. 85) proposed a radically different composition with regard to the ratio of hydrogen to helium in an attempt to combine Zabriskie's (ref. 109) value of hydrogen abundance (5 km-atm) with his own values of the two constraints ($P=13$ atm, and $\bar{\mu}=4.3$). Öpik's atmosphere is 97 percent helium with hydrogen reduced to a bare 2 percent to meet the high value of $\bar{\mu}$. Neon, methane, argon, and ammonia come next in order, as in Spinrad and Trafton's composition. Table 13–3 gives Öpik's probable percentages of the total, which has a resulting molecular weight of $\bar{\mu}=4.02$, practically that of pure helium. This surprising composition is attributed to an

TABLE 13–2.—*Probable Atmospheric Composition*

[After ref. 200]

Gases in the visible Jovian atmosphere	Molecular weight, $\bar{\mu}$	Abundance, percent	Abundance, km-atm
Hydrogen (H_2)	2	60	27
Helium (He)	4	36	16
Neon (Ne)	20	3	.7
Methane (CH_4)	16	1	.2
Ammonia (NH_3)			

TABLE 13–3.—*Probable Atmospheric Composition*

[After ref. 85]

Gases	Molecular abundance, percent
Helium (He)	97.2
Hydrogen (H_2)	2.3
Neon (Ne)	.39
Methane (CH_4)	.063
Argon (Ar)	.042
Ammonia (NH_3)	.0029

early snowing-out of hydrogen from the primordial nebular ring to form the bulk mass, or interior, of Jupiter with the subsequent accretion of a helium atmosphere. It should be noted that Öpik's comprehensive study of Jupiter was aimed primarily toward understanding the origin and evolution of a giant planet.

14
Atmospheric Structure

PRESENT DATA SUGGEST that Jupiter has a hot interior and a deep atmosphere according to Peebles (refs. 95 and 214), which is not the classical view of Jupiter as a cold planet with a relatively shallow atmosphere. Evidence supporting these data are: (1) revised solar abundance of elements heavier than helium given by Aller (ref. 215) indicating the possibility of greater radioactivity inside Jupiter which releases greater heat than previously supposed; (2) recent calculations on the interior by DeMarcus (ref. 89) pointing to a hot interior; (3) modern theories on the evolution of the major planets as protoplanets by contraction of the original solar nebula, with little gravitational separation of volatiles (H, He, Ar, CH_4, NH_3 . . .).

The present lower atmospheric models of Jupiter, provided with a hot base (Gallet-Peebles' models), will be reviewed after presentation of the valid earlier work on the upper atmosphere (Kuiper's models). The separation between lower and upper atmospheres here is the visible cloudtop or visible surface, which has been observed consistently.

UPPER ATMOSPHERE

KUIPER'S MODELS

The first consistent structural models of Jupiter's upper atmosphere were proposed by Kuiper (ref. 124) and based on the available radiometric (temperature) and spectral (chemical composition) data. Kuiper's two models, a and b, are hydrogen- and helium-rich atmospheres containing smaller amounts of ammonia and methane.[1] The model structures consist of an isothermal stratosphere at 86° K overlying a troposphere in adiabatic equilibrium. Below the tropopause separating them, the temperature is assumed to increase with depth

[1] The compositions adopted for Model a were by weight: 63.5 percent hydrogen, 34.9 percent helium, 0.26 percent ammonia, 0.11 percent methane with the remainder of neon (0.60 percent), water (0.34 percent), and argon (0.15 percent); compositions for Model b were 59.5 percent helium, 37.7 percent hydrogen, and practically the same percent of ammonia and methane as adopted for Model a.

at a constant lapse rate of $dT/dh=2.6°$ C/km for Model a and 4.0° C/km for Model b. Within the troposphere, at a level determined by pressure and temperature, the ammonia vapor condenses into ammonia crystals, forming opaque white clouds. (At that level, there is equilibrium between vapor and solid phases of ammonia.) From the spectrally observed amount of ammonia (7 m-atm at STP), which is contained above the cloud layer, Kuiper determines the temperature at the cloudtop; he finds $T_c=165°$ K for Model a and 168° K for Model b. Thus, Kuiper notes, the sizeable difference in composition between a and b has little effect on the cloudtop temperature. This results from the steep gradient of the ammonia partial pressure (and to a lesser extent, the temperature gradient). These models are illustrated in figure 14–1. According to Kuiper, the total pressure, which also increases steeply with depth, is, at the cloudtop: $P_c=24$ atmospheres for Model a and 2.0 atmospheres for Model b. He calculated P_c from the spectrally observed amount of methane (150 m-atm at STP) and the adopted $(H_2+He)/CH_4$ abundance ratios.[2] At both these pressures, with the low temperatures given as 160° K, Kuiper concludes that the ammonia clouds formed are of the cirrus type made of ammonia crystals. (Methane condenses at much lower temperatures.)

ÖPIK'S MODEL

Öpik (ref. 85) discussed the values obtained in Kuiper's models. Beginning with the same spectrally observed amount of ammonia (7 m-atm at STP or 0.53 g cm^{-2} of ammonia above the cloudtop) and assuming a scale height of about 10 kilometers, Öpik calculated the number density of ammonia, at the cloudtop, as 1.9×10^{16} ammonia molecules cm^{-3}. (A condition of complete atmospheric mechanical mixing was also assumed.) Then, from tables of ammonia vapor pressure, he obtained the saturation temperature of $T_c=156°$ K for the cloudtop. Adopting a predominantly helium atmosphere (97.2 percent helium, 2.3 percent hydrogen, with 0.0029 percent ammonia and 0.063 percent methane), Öpik obtained a probable total pressure at the cloudtop of $P_c=11$ atmospheres. His model strongly supports Kuiper's conclusion of the existence of an ammonia-cirrus cloud layer.

GROSS AND RASOOL'S MODEL

Gross and Rasool (ref. 216) have proposed two extreme models for Jupiter's upper atmosphere (above the clouds) based on the two values of the hydrogen to helium mixing ratio: H/He=20/1 by Urey (ref. 183) for Model I and H/He=0.03/1 by Öpik (ref. 85) for Model

[2] A cosmic abundance ratio of (H, He)/C was assumed for Model a.

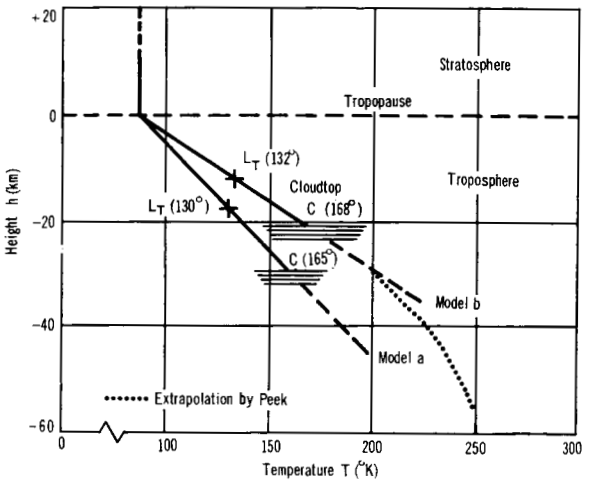

FIGURE 14–1.—Jovian upper atmospheric models. (After refs. 60 and 124.)

II. The respective mean molecular weights for the models are 2.2 and 3.95 and the pressure at cloudtop level for both is 3 atmospheres (ref. 200). The vertical temperature distribution above the clouds was calculated on the basis of radiative equilibrium and a gray atmosphere (absorption independent of wavelength) from the simplified radiative transfer equation:

$$T_z^4 = T_e^4(\tfrac{1}{2} + \tfrac{3}{4}\tau_z)$$

where

T_z temperature at any level z
T_e effective blackbody temperature of the planet
τ_z average infrared optical thickness above level z

If the total optical thickness measured from the cloudtop level, $z=0$ is τ_o, then at any level, z, the optical thickness (opacity) is given by $\tau_z = \tau_o\, e^{-z/H}$, where H is the scale height. The gases radiating in the infrared are ammonia and methane. The amounts assumed were those given by Kuiper (ref. 124): 7 m-atm of ammonia and 150 m-atm of methane. Gas absorption was computed for an effective 150° K blackbody energy curve. The total optical thickness found was $\tau_o = 0.66$. The results for the vertical temperature distribution of the two models are shown in figure 14–2.

TRAFTON'S MODELS

Trafton (ref. 126) constructed several nongray radiative models of Jupiter's atmosphere taking into account the thermal opacities of hydrogen, helium, and ammonia (using his own computations of

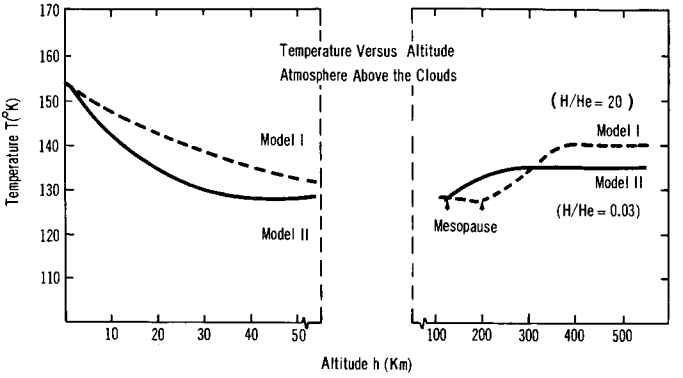

FIGURE 14-2.—Jovian upper atmospheric models. (After ref. 216.)

absorption coefficients of hydrogen and hydrogen plus helium mixtures in the infrared and microwave spectral regions). Using existing observations as a guide, and the fact that methane is also present, Trafton's models of Jupiter confirm the backwarming effect indicated by the radiometric measurements of Murray et al. (ref. 130). They predict the existence of a shallow convection zone in the Jovian upper atmosphere at about the cloudtop level, but extending to greater depths if there is a small planetary internal heat source which the models also seem to suggest. The amounts of hydrogen required by the models to cause convection (about 30 km-atm) seem compatible with the observed amounts above the cloudtop. Thus, the cloudtop and the top of the convection zone appear correlated in Jupiter's atmosphere, as they are for Earth.

LOWER ATMOSPHERE

GALLET-PEEBLES' MODELS

The deeper atmosphere structure below the visible cloudtops was studied by Gallet (ref. 217) and supplemented by Peebles' calculations for the interior (refs. 95 and 214). The atmospheres contemplated by both investigators are deep and hot at the base and somewhat reminiscent of semi-stellar atmospheres. Gallet's model, unfortunately, has not yet been submitted for publication. Only a brief description, which follows, was given by Peebles (ref. 95). Figure 14–3 presents Gallet's atmospheric model overlying one of Peebles (ref. 214) interior models.

The chemical constituents of Gallet's model are those assumed in earlier models (such as Kuiper's Model a): hydrogen, helium, neon, water, ammonia, and methane. Ammonia and water form a succession of clouded and clear layers, depending upon the prevalent atmospheric pressure and temperature which control vapor saturation.

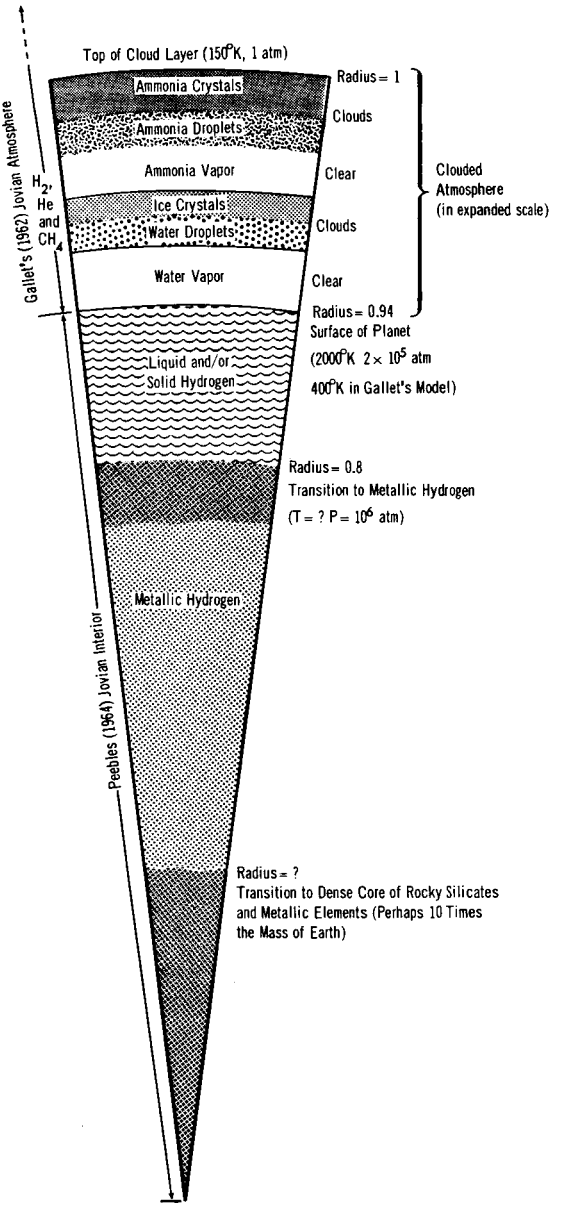

FIGURE 14-3.—Jovian cloud layers proposed by Gallet (ref. 217) overlying Jovian interior by Peebles (ref. 214).

Descending from the visible cloudtop, the layers are as follows: ammonia crystal clouds, ammonia droplet clouds, unsaturated ammonia-vapor clear region, water (ice) crystal clouds, water droplet

clouds, unsaturated water-vapor clear region, and the surface of the planet.

The depth of each layer mentioned and the temperature variation in Gallet's model are as uncertain as the mixing ratios (abundances) assumed for the constituents, especially for ammonia. With an accepted cloudtop temperature of 150° K and a pressure of 1 atmosphere, Gallet predicts a bottom temperature of about 400° K (near the surface) if the mixing ratio of ammonia (in the higher cold layers) is decidedly greater than that of nitrogen in the Sun, and even much higher temperatures if the ammonia is much less abundant.

Peebles' calculations, based on his models of the interior, indicate interface surface temperatures of about 2000° K and a pressure of 200 000 atmospheres at the bottom of a deep atmosphere, starting also from the same cloudtop boundary conditions (150° K and 1 atm). His calculations (models) are based upon evidence depending primarily on the distribution of mass in the subsurface layers (solid or liquid) of the planet. This distribution is revealed by the gravitational coefficients, J and K or J_2 and J_4. (See ch. 3.) Peebles' interior models, which best fit the values of J and K as well as other known planetary constants (radius, mass, and rotation rate), are those models starting with a very deep adiabatic atmosphere, with very large abundance of hydrogen and some helium, resembling the solar abundance. His "Model 4" is probably the most consistent with Jupiter data; it has a cloudtop of 150° K and 1 atmosphere and a bottom at about 2000° K and 200 000 atmospheres with abundances of hydrogen and helium ($\sim$76 percent hydrogen and $\sim$22 percent helium, by mass). The density versus pressure curve of this model is illustrated in figure 7–2.

If the relative number of radioactive isotopes in Jupiter's interior is assumed to be at least as large as that of the Sun, the radioactive heat flux generated is found to be sufficient to drive convection in the lower atmosphere of Jupiter. From it, determination of a dry adiabatic lapse rate, assumed valid over the temperature range 150° to 2000° K, results in a very great atmospheric depth consistent with that calculated for Model 4. The latter amounted to 6 percent of the planetary radius, about 4250 kilometers. Peebles' conclusion was corroborated by this very rough estimate of the heat flow expected from the decay of radioactive isotopes (K^{40}, U, Th).

15
Atmospheric Circulation

THE STUDY OF THE CIRCULATION of the atmosphere of Jupiter is complicated by the fact that no solid surface can be seen and, consequently, there is as yet no well-established, fixed zenographic coordinate system. Features of the atmospheric circulation must be referred to one of the three accepted systems of longitude (see ch. 4), at least two of which are, in turn, dependent on visible manifestations of the circulation. The quasi-constant radio period of rotation and derived longitude ephemerides of System III, claimed by many to be linked to the actual solid-liquid body of Jupiter, is the best base of reference for circulation studies.

This visible surface of Jupiter displays an alternation of light bands (zones) and dark bands (belts) parallel to an ill-defined equator. Superimposed on these semipermanent belts and zones are a number of transitory spots and other features, indicative of a vigorous circulation in the thick atmosphere below the visible cloud surface.

GENERAL CIRCULATION THEORIES

VOLCANO THEORY

One of the earlier attempts at a theoretical explanation of the atmospheric circulation of Jupiter is that of Schoenberg (ref. 218). Concerned with the constancy in latitude of the visible bands, he assumed a solid surface (at least below 40° latitude) with volcanic rifts or fissures along the parallels of latitude at the North and South Equatorial belts. He ignored solar heating altogether and assumed that the sole source of energy to drive the atmospheric circulation was internal heat released by volcanic eruptions. In Schoenberg's view, rings of heated gas would rise at 8° N and 8° S, move toward the equator, descend, and move poleward. In the latter stages, contraction of the rings would cause an increase in westerly wind through conservation of angular momentum. The dynamics of this circulation system resemble those of the model proposed by Hadley (ref. 219) to explain the terrestrial trade winds. The Hadley model is based on sound principles, but it has long been recognized as in-

adequate to describe the planetary circulation. Aside from Schoenberg's fanciful introduction of volcanic activity and his failure to consider that it is the difference between solar heating at two latitudes rather than the absolute magnitude of the heating that is important, his scheme would lead to westerly winds increasing away from the equator, which is contrary to observation. Schoenberg assumed vertical turbulent friction to overcome this difficulty. However, to achieve the desired result large-scale horizontal turbulent mixing is required, negating the assumption of conservation of absolute angular momentum basic to the theory.

VORTICITY THEORY

Hess (ref. 220) reconsidered the problem, starting with the assumption that large-scale horizontal mixing is important and building on a theoretical study by Rossby (ref. 221). Rossby assumed an atmosphere that could be considered as a thin, rotating spherical shell and proposed that the horizontal mixing would result in a velocity distribution so that poleward of some critical latitude (whose value is dependent on the shearing instability) the absolute vorticity would remain constant, while equatorward of the critical latitude, the latitudinal transport of absolute vorticity would be constant. Hess found this theory in agreement with observations of Jupiter if the critical latitude were 15°. However, he discovered that poleward of 15° the atmosphere of Jupiter appears to be in solid rotation; yet a latitudinal temperature gradient must exist, and the consequent mixing must act to destroy the state of solid rotation. Hess explained this phenomenon by noting that spectrographic evidence shows that the visible cloud surface rises toward the pole, while the thermal wind relation shows that the west wind increases with height. Hence, along a horizontal surface, the period of rotation increases toward the pole, but the visible surface happens to have the proper slope so that the observed period is constant.

CONSERVATION OF ANGULAR MOMENTUM

The studies of Schoenberg and, to a lesser extent, Hess, were made before the role of conservation of absolute angular momentum in a planetary general circulation had been clarified (ref. 222). It is now clear that on Earth, at any rate, large-scale eddies of preferred shape and orientation act to transport angular momentum against the gradient, permitting jet streams to be maintained despite frictional dissipation. A comprehensive theory of the general circulation of Jupiter's atmosphere must take these findings into account.

Schoenberg and Hess did not have the advantage of the System III

rotation period by which winds at the visible surface can be related to a presumed solid surface. Owen and Staley (ref. 223) have shown that in System III at the equator the wind at the visible surface is westerly at 105 m sec^{-1}. At 20° latitude it is easterly at 4 m sec^{-1}, and poleward of 20° the easterlies diminish. These findings have important consequences for conservation of angular momentum, because the mechanism that generates westerly angular momentum at the equator is unknown. Perhaps some systematic tilt in trough and ridge lines results in equatorward transport of angular momentum.

WINDS IN THE HIGHER ATMOSPHERE

Owen and Staley claim to have detected a long-term oscillation in the atmosphere of Jupiter. Their claim rests on observations by Spinrad and Trafton (ref. 200) of the Doppler shift of ammonia spectral lines originating in Jupiter's atmosphere above the visible surface as compared with that of Fraunhofer lines. The latter, representing light that has passed through the atmosphere above the visible surface twice, should have a double Doppler shift as compared to the former. Observations, however, showed varying shifts, indicating varying relative speeds between the visible surface and the upper atmosphere. Owen and Staley showed that the high-level winds relative to System III were -6700 m sec^{-1} in 1934, -3900 m sec^{-1} in 1961, and $+100$ m sec^{-1} in 1962, as compared with a relatively constant $+100$ m sec^{-1} for the low-level winds. These results show that stratospheric winds can vary over at least an order of magnitude, and even reverse their direction while tropospheric winds remain unaffected.

A DYNAMIC THEORY

A dynamic approach to planetary general circulations was devised by Mintz (ref. 224), whose theory is based on the premise that a planet with little equatorial tilt receives more solar heat at its equator than at its poles, so a circulation must arise that is capable of transporting the requisite amount of heat from the region of surplus to the region of deficit. He has shown that the general circulation of the atmosphere of a rotating planet falls into one of two regimes, depending on the speed of rotation and the equator-to-pole temperature gradient.

The symmetric regime, in which the winds are mainly parallel to the equator, cannot transport as much heat poleward as the wave regime, which is characterized by large-scale eddies. For a fast-rotating planet such as Jupiter, the symmetric regime is possible only if the differential heating between pole and equator is small. Although the absolute magnitude of solar heating on Jupiter is small, there is

no reason to expect its derivative along the meridian to be small; in fact, the extreme oblateness of Jupiter might contribute to a large value of differential heating. However, infrared temperature measurements of Jupiter do not show much evidence of latitudinal dependence on insolation, at least at the cloud level sensed (refs. 128 and 129). This can be seen in figure 9–1. The high brightness temperatures suggest an internal source of heat, which might, to some extent, counteract the latitudinal variation of solar heating.

On the other hand, the wave regime might predominate in the lower atmosphere of Jupiter despite the banded appearance from Earth in which case heat could be transported from the equator to the poles efficiently, resulting in uniform distribution of temperature.

CYCLONES AND ANTICYCLONES

Although the bands of Jupiter give a superficial impression of symmetry, they also show a fine structure that is indicative of strong thermal convection according to Focas and Banos (ref. 225) and of wave-like disturbances. Hess and Panofsky (ref. 226) report that the boundaries between adjacent belts and zones show distinct and persistent wave patterns that sometimes are shaped like the peak of an unstable wave. Also, there are many dark and bright spots, rifts, wisps, and other features. Shapiro (refs. 227 and 228) showed that the spots are found mostly in the latitude range 13° to 17° N and 8° to 17° S with a rapid decrease in frequency poleward of 22°. The approximately equal number of spots in the morning and afternoon hemispheres imply that they are not of convective or radiative origin, while the even distribution with longitude suggests a lack of topographic features to influence the spots. The spots are influenced by the Great Red Spot, and are deflected around it. Also, they are numerous in the latitude of the Great Red Spot. It has been suggested that the barrier effect of the Great Red Spot in some way promotes the development of the spots, although, even at its latitude, their frequency is independent of longitude.

Shapiro identifies the dark spots with cyclones and the light spots with anticyclones. In the former, there should be descending motion at high levels, carrying the ammonia clouds deeper into the atmosphere, while in the latter, there should be ascending motion at high levels, bringing the ammonia clouds into prominence. Some confirmation for this view is given by Hess and Panofsky. According to these authors, motions of the spots near the boundaries of the belts and zones indicate that the dark belts have cyclonic shear, and the bright zones have anticyclonic shear. Furthermore, some spots follow anticyclonic paths with respect to the bright tropical zone in the southern hemisphere. Satellite photographs of terrestrial clouds

show the opposite effect (bright cyclones and dark anticyclones). This is because the anticyclones are relatively cloudfree and permit the Earth's surface to be visible. If there were a solid cloud layer up to the tropopause, it would appear from another planet to be dark over cyclones where the tropopause is low and bright over anticyclones where the tropopause is high.

CLIMATIC ZONES

On Earth, the disturbances tend to occur just poleward of the jetstream. The boundary of the equatorial acceleration may be considered to be the Jovian counterpart of the jetstream. There is some evidence of a belt at 6° to 7° S on Jupiter corresponding to the subtropical anticyclones at 30° on Earth and also of a secondary jetstream at 25° to 30° N on Jupiter corresponding to one at 55° N on Earth. Shapiro suggests that the conventional climatic zones of Earth be shifted equatorward on Jupiter, as shown in table 15–1.

TABLE 15–1.—*Climatic Zones*
[After ref. 228]

Zone	Zenographic latitude, deg	Terrestrial latitude, deg
Equatorial	0–6	0–10
Tropical and subtropical	7–12	10–30
Temperate	13–25	30–60
Subpolar and polar	26–90	60–90

The names of the zones should not be construed to have any climatic meaning for Jupiter in the normal sense of the word but merely serve to designate regions that have circulation similar to that of the corresponding climatic zone on Earth. The equatorward displacement is partly explicable by the greater Coriolis force on Jupiter ($f=3.52\times10^{-4}$ sin ϕ for Jupiter as compared to $f=1.46\times10^{-4}$ sin ϕ for Earth, where ϕ is the latitude) which results in the presence of cyclonic disturbances at lower latitudes.

Mintz (ref. 229) suggested that because of the low latitude of the Jovian spots and because the spots seem to occur high in the atmosphere rather than low, they should not be compared with the terrestrial extratropical disturbances but with the subtropical cyclones described by Palmer (ref. 230). Furthermore, Palmer (ref. 231) demonstrated a degree of solar influence on subtropical cyclones, and Mintz showed evidence of the same type of influence on the spots of Jupiter. It should be noted, however, that in neither case was the evidence of solar influence conclusive.

GREAT RED SPOT THEORIES

The theories that have been proposed concerning the Great Red Spot fall generally into two classes: (1) that it is somehow connected with a feature of the underlying solid surface, and (2) that it is some sort of floating body. Both of these theories have interesting consequences for the atmospheric circulation.

Theories in the first category were favored early because of the constancy in latitude of the Great Red Spot. The Eötvös-Lambert force acting on a floating body would drive it toward the equator in order to minimize its potential energy (ref. 232). On the other hand, association with any solid surface is difficult, for since 1831 the Great Red Spot has varied in longitude by more than 3500° in System II_1 and by more than 400° in a special system devised to minimize its variation (ref. 60). Sagan has shown that an explanation of the second category is possible provided the floating body consists of some substance that can change phase with relatively small vertical motions and such that each phase has certain density properties. This explanation could solve the problem of the Eötvös-Lambert force and could account for the erratic changes in angular momentum which are sometimes observed. It is not known, however, what substances could have the appropriate properties for this model. The exacting conditions required for this model to be possible have led Sagan to reject it in favor of the Taylor column model.

Hide (ref. 233) proposed that the Great Red Spot is a Taylor column, that is, a feature of the circulation derived from the Proudman-Taylor effect. Proudman (ref. 234) showed theoretically and Taylor (ref. 235) confirmed experimentally that a rotating, homogeneous, incompressible fluid will tend to move two-dimensionally in planes perpendicular to the axis of rotation. Their work was expanded by Grace (ref. 236). Hide noted that since the Rossby number (defined as $R_o = U/L\Omega$, where U is a characteristic relative flowspeed, L is a horizontal length characteristic of the flow, and Ω is the angular speed of rotation) is very small on Jupiter ($R_o \simeq 10^{-3}$), the Proudman-Taylor effect should hold, at least, approximately. Then, if some topographical feature even of very small height exists on the solid surface of the planet, it will be surmounted by a column of stagnant air of the same horizontal dimensions, extending throughout the depth of the atmosphere, while the remaining air will flow around the column as if the column were solid.

Hide showed that the Great Red Spot could be a Taylor column if the atmosphere were no deeper than 2800 kilometers and, if its depth were only 1000 kilometers, the topographical feature causing the Taylor column could be as low as 1 kilometer. He explains the

drift in longitude by assuming that Jupiter consists of a fluid core with a thin, solid mantle and a deep, massive atmosphere. Exchanges of momentum between the atmosphere and the mantle could cause the rotation rate of the latter to vary from time to time. The rotation rate of the Great Red Spot would be the same as that of the mantle. As further evidence, Hide notes that the South Equatorial Belt has a pronounced indentation where it passes north of the Great Red Spot, and transitory spots are swept around as in laminar flow. There is no corresponding indentation south of the spot, and the abundance of transitory spots in this latitude suggests turbulent flow. This is in accordance with experimental results of laboratory investigations of Taylor columns. The color of the Great Red Spot would indicate that gas is not freely exchanged between it and its surroundings and that clouds do not easily develop in it. These characteristics are in agreement with the Proudman-Taylor theory. However, it has not yet been shown conclusively that the Great Red Spot is a feature of the atmospheric circulation rather than an actual body.

248-761 O-67—8

16

Atmospheric Depth and Surface

ATMOSPHERIC DEPTH AND PRESSURE

THEORETICAL MODELS of the lower and upper Jovian atmosphere furnish the only means of estimating its depth. The visible cloudtop is taken as the dividing line between the two atmospheres. The pressures calculated for the cloudtop are on the order of several atmospheres, and the pressure in the upper atmosphere at approximately 50 kilometers above the cloudtop may be on the order of 1 atmosphere or less; the atmosphere probably extends very high since its gases were proved to be very light (ref. 60).

The depth of the lower atmosphere from the cloudtop down to the surface of Jupiter is unknown and is difficult to determine theoretically. Nonetheless, this depth and the pressures below the cloudtops have been estimated in several models. The results of some calculations are summarized in table 16–1 (ref. 237). It can be seen that the estimates vary widely: depths range from 100 to 6000 kilometers. The pressures are on the order of several thousand atmospheres (200 000 atm at 4200 km) at the bottom and depend on the temperature there. The model of Peebles (ref. 95) with a very hot base (2000° K) has a depth of 4200 kilometers. Previous models, as given by Wildt (ref. 76), suggest a depth of approximately 500 to 750 kilometers.

SURFACE

Information on the nature of the Jovian surface proper can be but tentatively inferred from the meager (and mostly unproved) knowledge gained through study of the planet's interior and atmosphere. The fact that the material of Jupiter's outer layers is light and is largely constituted of a mixture of hydrogen and helium is generally accepted. That the atmosphere is very thick (on the order of 1000 km) is nearly certain, and it follows that the pressures at the bottom must attain thousands of atmospheres from its accumulated weight and the intense Jovian gravity. Thus, a high probability exists for a gradual transition between gaseous, liquid, and solid phases with an ill-defined oceanic interface at the bottom of the atmosphere.

TABLE 16–1.—*Depth of the Jovian Atmosphere*

Composition or mean molecular weight, $\bar{\mu}$	Cloudtop temperature, ° K	Temperature gradient	Other characteristics	Depth, units of h	Depth, km.	Reference
Hydrogen (H_2)	150	Isothermal	Perfectly compressible	20	[a]500	Wildt (ref. 79)
	150–1000	Adiabatic	Variation of C_p/C_v with temperature		[b]500	Wildt (ref. 76)
	150	Isothermal	Partial compressibility, variation of solidification density with pressure.	30	[a]750	DeMarcus (ref. 89)
	100	Isothermal	Partial compressibility, variation of solidification density with pressure.	24	[a]380	
$\bar{\mu}=4$	150–400	Adiabatic?			[c]100–120	Peek (ref. 237)
Hydrogen (H_2), nitrogen (N_2), helium (He), oxygen (O_2).	120	Isothermal			6000	Jeffreys (ref. 75)
Hydrogen (H_2) (+ helium (He)).	150	Adiabatic			4250	Peebles (ref. 95)

[a] Distance between top of cloud layer and level at which hydrogen solidifies. Pressure at cloud layer top 10 atm.

[b] Fiducial level at $p=1$ atm (somewhat higher than cloud layer top).

[c] Depth below top of cloud layer at which density reaches 0.09 g-cm^{-3} (solidification density of H_2 at $p=0$). Value of acceleration of gravity, g, adopted$=2600$ cm-sec^{-2}.

It is not clear, however, whether or not continents or icebergs of solidified substances such as hydrogen, water-ice, ammonia-ice or simple C–H–N compounds exist. It is also possible that some heavier rock-like materials (silicates) exist in places. Atmospheric precipitations (ammonia and water) very likely occur periodically, which adds to the belief that the surface is slushy. Liquid water and methane may even be present.

17
Life

IT MAY SEEM INCONCEIVABLE that life could exist on a planet as inhospitable as Jupiter. Indeed, the Jovian habitat, with its extremely low temperatures, its poisonous and turbulent atmosphere, and its violent electrical storms, appears so hostile as to forbid the presence of any living forms. Yet, the remarkable biochemical theories on the origin of life which have appeared in the recent decade, spurred by the now classical demonstration by Oparin (ref. 238) that life originates under chemically reducing conditions, suggest that the possibility of a form of primitive life on the giant planet is not as remote as anticipated. The presence of abundant ammonia and methane with hydrogen (and probably water vapor) in the atmosphere and the frequency of electrical discharges through such an atmosphere under solar ultraviolet irradiation are the conditions required for spontaneous production of organic materials such as amino acids (refs. 239 and 240). Similar experiments have also been conducted by others. Abelson (ref. 241) synthesized amino acids from mixtures of hydrogen, methane, carbon monoxide, and ammonia. Heyns, Walter, and Meyer (ref. 242) used methane, ammonia, water, and hydrogen sulfide. More complex materials (polypeptides, etc.) have been obtained more recently. It appears possible that even a basic molecule of life such as an enzyme could be formed under such conditions. The turbulence in the primitive atmosphere would even be a favorable condition, according to Sagan (ref. 243). Temperatures from 0° to 80° C probably exist at some upper level of Jupiter's atmosphere; and if it is assumed that water vapor is present, then conditions favorable to the production of bio-organic molecules may exist. Therefore, some microbial type of life could be expected at some atmospheric level of Jupiter.

The adaptation of micro-organisms to adverse environment has been demonstrated in recent experiments in which they were placed in a simulated Jovian atmosphere rich in ammonia (50 to 95 percent) with large quantities of methane (CH_4), hydrogen (H_2), or air. A number of species survived and even multiplied. According to Siegel and Giumarro (ref. 244), who conducted the experiments, certain toxic gases are good metabolites for some micro-organisms. Some

bacteria even produce hydrogen cyanide, HCN. The results of these experiments added to the observation that life can adapt to the most adverse environments (bacteria have even been found recently inside nuclear reactors) lead to the conclusion that a Jovian microbiosphere may exist.

18
Satellites

THE 12 KNOWN SATELLITES OF JUPITER constitute a remarkable system, resembling somewhat the solar system itself, with a close inner system and a distant outer system that can also be divided into two subgroups according to their proximity to Jupiter.

INNER SYSTEM

The inner system consists of five bodies. The four large satellites of this system (called the Galilean satellites) were discovered in 1610 by Galileo within a year after he made his first telescope. These four are either identified by Roman numerals that indicate their order of distance from Jupiter or by mythological names, which were proposed by Simon Marius, who discovered them independently. The satellites are called Io or J–I, Europa (J–II), Ganymede (J–III), and Callisto (J–IV). Because the other satellites are very small, almost 3 centuries elapsed before they were discovered. Jupiter V (the tiny, innermost satellite) is difficult to observe because it is small and revolves rapidly about Jupiter close to the planetary surface. This satellite (also called Amalthea) was discovered visually by Barnard in 1892 with the aid of the Lick Observatory 36-inch refractor.

The five inner satellites revolve in nearly circular, equatorial orbits with the same direct motion as the planets (counterclockwise when seen from the North Pole of the ecliptic). They are close to their primary with the innermost satellite, Jupiter V, at approximately 2.5 radii from the center of Jupiter and the outermost, Callisto or J–IV, 26.4 radii from the center of Jupiter (fig. 18–1).

GALILEAN SATELLITES

The four Galilean satellites are very large and can easily be seen with a small telescope or good field binoculars. According to Dollfus (ref. 245), their diameters range from 3100 kilometers for Europa, the smallest, to 5600 kilometers for Ganymede, the largest (fig. 18–1, refs. 246–252). Some uncertainty still prevails, however, as to the diameter measurements of such objects which at the great distance of Jupiter subtend only 1″. The two largest, Ganymede and Callisto,

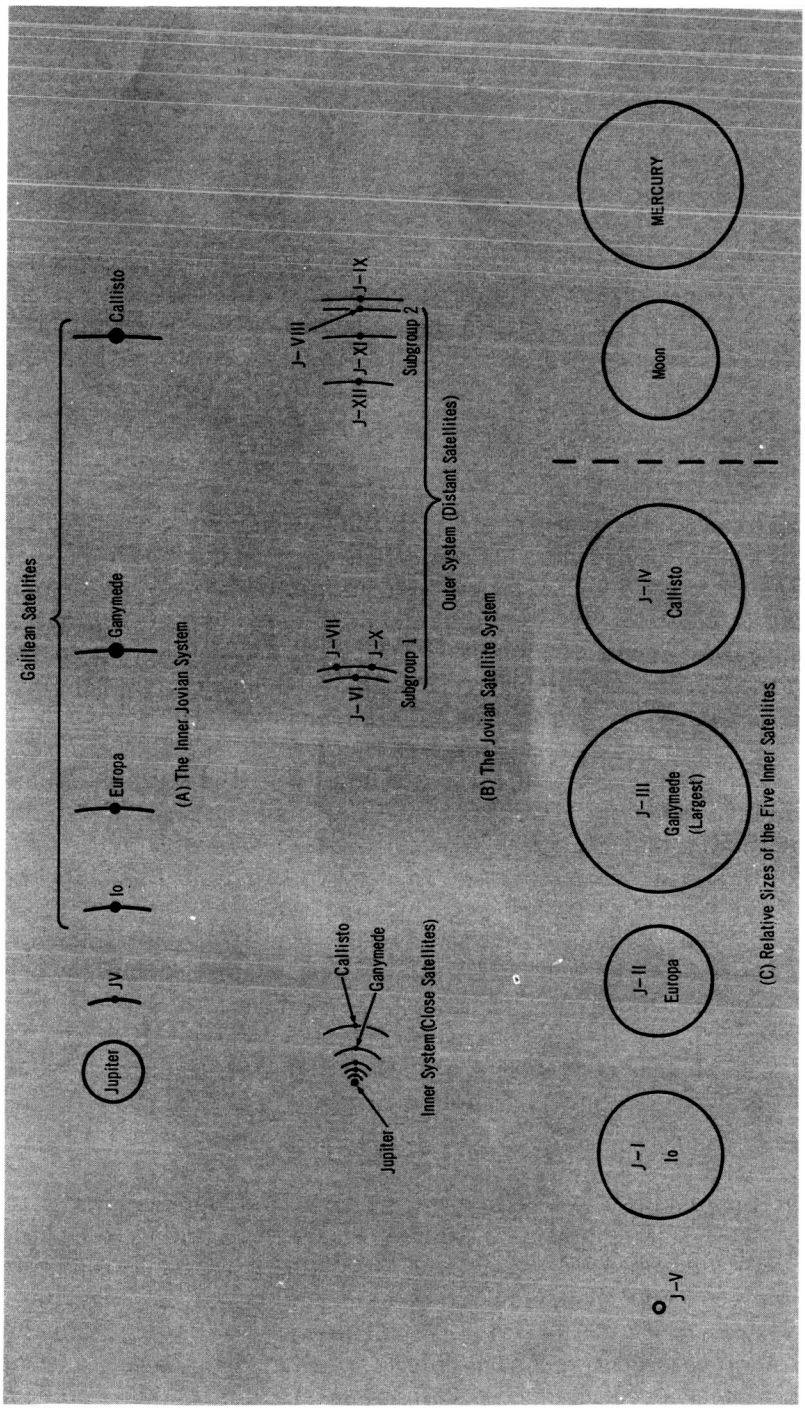

FIGURE 18-1.—The satellites of Jupiter: distances and sizes.

are approximately the size of Mercury, but much less dense. The two smallest, Io and Europa, are about the size of Earth's Moon and nearly as dense. Astronomical and physical data for the satellites are given in table 18–1.

The Galilean satellites are subject to very strong mutual perturbations, causing librations in their orbits. Laplace discovered an interesting resonance relationship between the first three satellites (J–I, J–II, and J–III). Their mean motions are roughly in the proportion 4:2:1. In terms of mean longitudes, $L_1-3L_2+2L_3=180°$. If one satellite is disturbed (for example by J–IV) the motions of the satellites adjust to satisfy the equation, which represents the periodic solution of Laplace. Consequently, all three satellites cannot be in conjunction or opposition at the same time (ref. 253).

The theory of the motions of the Galilean satellites is quite complicated. Sampson (ref. 254) and De Sitter (ref. 59) have developed detailed, complex theories to describe the movement of the inner satellites. The masses of the satellites are computed from the periodic perturbations in the longitudes and secular motions of the perijoves and nodes resulting from their mutual attractions. This calculation is particularly difficult for J–I. According to Sampson, the mass of J–I is 4.497×10^{-5} relative to Jupiter; according to De Sitter, 3.796×10^{-5}. Although Sampson's tables (ref. 255) for computing the ephemerides are difficult to use, *The American Ephemeris and Nautical Almanac* started using them in 1914 before the theory was published. Utilizing the main terms of Sampson's tables, Andoyer (ref. 256) simplified the method of predicting the positions of the satellites. His method is accurate to 0°.001 and is used in most ephemerides. The necessary data are given each year in *Connaissance des Temps* (ref. 5).

The configurations of the satellites may be determined for any hour of the day from graphs included in *The American Ephemeris and Nautical Almanac* (since 1960) which also contains exact times for the beginning and the end of all phenomena associated with Jupiter (eclipses, occultations, transits, and shadow transits).

Occultations and eclipses involving only the satellites can be seen from Earth when the common orbital plane passes through Earth, that is, when the heliocentric longitude of Jupiter is 135° or 315°. These occurrences alternate every $5^{yr}\ 7^{mo}$ and $6^{yr}\ 3^{mo}$, for example, Feb. 1950, Sept. 1955, Dec. 1961, July 1967, etc. (ref. 253). The dates for these events are predicted by methods developed by Levin (ref. 257) and are listed in the *Handbook of the British Astronomical Association.*

On rare occasions, all four Galilean satellites are invisible simultaneously as a consequence of occultation, eclipse, or transit. Example

TABLE 18–1.—*The Jovian Satellites: Astronomical and Physical Data*

Name and number of satellite	Mean opposition magnitude, V_0 (ref. 246)	Reduced visual magnitude, V_1 (O) (ref. 246)	Distance to Jupiter		Orbital motion		Period of sidereal revolution, P, days (refs. 10, 58, and 247)	Orbital eccentricity [b]
			Relative (Jupiter radius, $R=1$) a/R (ref. 10)	Absolute [a] (semimajor axis), a, kilometers	Mean daily motion (n), relative to Jupiter's motion (n'), n'/n (ref. 10)	Direction		
V (Almalthea)	+13.0	+6.3	2.539	181 260	+0.00011	Direct	0.49818	0.003 (ref. 58)
I (Io)	+4.80	−1.90	5.905	421 560	+0.00041	Direct	1.76914	0.0006±0.0004 (ref. 59)
II (Europa)	+5.17	−1.53	9.396	670 780	+0.00082	Direct	3.55118	0.0075±0.0008 (ref. 59)
III (Ganymede)	+4.54	−2.16	14.99	1 070 140	+0.00165	Direct	7.15455	0.0796±0.0013 (ref. 59)
IV (Callisto)	+5.50	−1.20	26.36	1 881 800	+0.00385	Direct	16.68902	0.4218±0.0005 (ref. 59)
VI (Hestia)	+13.7	+7.0	160.7	11 472 000	+0.0579	Direct	250.6	0.15798 (ref. 249)
VII (Hera)	+16	+9.3	164.4	11 736 000	+0.0600	Direct	260.1	0.20719 (ref. 249)
X (Demeter)	+18.6	+11.9	164	11 708 000	+0.0600	Direct	260	0.14051 (ref. 250)
XII (Andrastea)	+18.8	+12.1	290	20 703 000	−0.142	Retrograde	617	0.168702 (ref. 251)
XI (Pan)	+18.1	+11.4	313	22 345 000	−0.160	Retrograde	692	0.20678
VIII (Poseidon)	+18.8	+12.1	326	23 273 000	−0.171	Retrograde	735	0.291 to 0.660 (ref. 247)
IX (Hades)	+18.3	+11.6	332	23 701 000	−0.175	Retrograde	758	0.275±0.15 (ref. 248)

[a] Calculated from Jupiter $R_{eq}=71\,390$ kilometers.

[b] Eccentricity of orbit, e, is variable for I–IV.

Name and number of satellite	Orbital inclination, i, to Jupiter's orbit or equator, deg	Type of perturbations	Discovery	Absolute diam, D, km	Relative mass (Jupiter mass, $M=1$), m_s/M	Absolute density, ρ, g-cm^{-3}
	To equator of Jupiter					
V (Almalthea)	0.4 (ref. 58)	Oblateness of Jupiter.	1892, Barnard	160(?) (ref. 252)	----------	(?)
I (Io)	0.0317 ± 0.0014 (ref. 59)	Other satellites and oblateness of Jupiter.	1610, Galileo (and Marius)	3800 (ref. 252)	$(3.81 \pm 0.30) \times 10^{-5}$	2. 5
II (Europa)	0.4668 ± 0.0009 (ref. 59)	Other satellites	1610, Galileo (and Marius)	3100 (ref. 245)	$(2.48 \pm 0.05) \times 10^{-5}$ (ref. 59)	3. 0
III (Ganymede)	0.1788 ± 0.0010 (ref. 59)	Other satellites	1610, Galileo (and Marius)	5600 (ref. 245)	$(8.17 \pm 0.10) \times 10^{-5}$ (ref. 59)	1. 7
IV (Callisto)	0.2452 ± 0.0009 (ref. 59)	Other satellites and Sun.	1610, Galileo (and Marius)	5200 (ref. 252)	$(5.09 \pm 0.40) \times 10^{-5}$ (ref. 10)	1. 3
	To orbit of Jupiter					
VI (Hestia)	28.436 (ref. 249)	Sun	1904, Perrine	130(?) (ref. 252)	(?)	(?)
VII (Hera)	27.75 (ref. 249)		1905, Perrine	30(?) (ref. 252)	(?)	(?)
X (Demeter)	28.4 (ref. 250)		1938, Nicholson	50(?) (ref. 252)	(?)	(?)
XII (Andrastea)	146.7338 (ref. 251)		1951, Nicholson	15(?) (ref. 252)	(?)	(?)
XI (Pan)	163.377		1938, Nicholson	15(?) (ref. 252)	(?)	(?)
VIII (Poseidon)	155 to 146 (ref. 247)		1908, Melotte	40(?) (ref. 252)	(?)	(?)
IX (Hades)	157. $\pm$ 5 (ref. 248)		1914, Nicholson	40(?) (ref. 252)	(?)	(?)

dates of this occurrence are Sept. 27, 1961; June 27, 1966; Apr. 9, 1980; etc.

OPTICAL PARAMETERS.—The optical parameters of the Galilean satellites are well known, since they are large bodies and can be observed at all phase angles. Reliable photometric work was done, especially by Stebbins (ref. 258) and Stebbins and Jacobson (ref. 259), on the variations in magnitudes of these Jovian moons. Careful colorimetric measurements, from which table 18–2 is derived, were made at the MacDonald Observatory in recent years by Harris (ref. 246). It is interesting to note the pronounced orange color of Io. The albedos are listed in table 18–3.

TEMPERATURES.—Radiometric (8–14 μ) temperatures of the Galilean satellites were obtained at the 200-inch Mt. Palomar telescope by Murray et al. (ref. 130). The values are: for J–I, 135° K; for J–II 141° K; for J–III, 155° K; and for J–IV, 168° K. The investigators also compared their observed values with theoretical values calculated

TABLE 18–2.—*Colors of the Galilean Satellites*

[After ref. 246]

Mean Color Indices

Body	Mean color indices			
	U−B	B−V	V−R	R−I
Sun	+0.14	+0.63	+0.45	+0.29
Jupiter	+.48	+.83	+.50	−.03
J–I (Io)	+1.30	+1.17	+.66	+.32
J–II (Europa)	+.52	+.87	+.57	+.31
J–III (Ganymede)	+.50	+.83	+.59	+.31
J–IV (Callisto)	+.55	+.86	+.61	+.32

Difference in colors: body—Sun

Body	U	B	V	R	I
Jupiter	+0.54	+0.20	0.00	−0.05	+0.27
J–I (Io)	+1.70	+.54	.00	−.21	−.24
J–II (Europa)	+.62	+.24	.00	−.12	−.14
J–III (Ganymede)	+.56	+.20	.00	−.14	−.16
J–IV (Callisto)	+.64	+.23	.00	−.16	−.19

TABLE 18–3.—*Albedos of the Galilean Satellites*

[After ref. 246]

Body	Mean radius relative to that of Earth, R/R_E	Monochromatic geometric albedos					Visual phase integral, q_V	Visual bond albedo, A_V
		p(U)	p(B)	p(V)	p(R)	p(I)		
Jupiter	11. 20, 10. 46	0. 270	0. 370	0. 445	0. 466	0. 347	1. 65	0. 73
J–I (Io)	0. 255	. 19	. 56	. 92	1. 12	1. 15	0. 585	. 54
J–II (Europa)	. 226	. 47	. 67	. 83	0. 93	0. 95	. 585	. 49
J–III (Ganymede)	. 394	. 29	. 41	. 49	. 56	. 57	. 585	. 29
J–IV (Callisto)	. 350	. 14	. 21	. 26	. 30	. 31	. 585	. 15

on the assumption of insulating graybodies reradiating absorbed solar energy. They found a significant excess for Callisto (J–IV) especially, and a lesser one for Ganymede (J–III), apparently indicating a departure from Planckian distribution of emitted radiation.

ATMOSPHERES.—The gravitational forces associated with the large masses of these four satellites have suggested the presence of atmospheres around them; however, the spectroscopic analysis has not yet detected any trace of atmospheric absorptions. The gases suspected are nitrogen, methane, and traces of ammonia, and water vapor, which would probably form icy deposits on the surface. Binder and Cruikshank (ref. 260) have noticed a brightening of the satellite Io after eclipse by Jupiter, with a return to normal brightness some 15 minutes later. In an attempt to prove indirectly the presence of an atmosphere, they interpret this brightening as the result of a temporary deposit of ice on the ground caused by the lowering of temperature during an eclipse.

SURFACE FEATURES.—A number of observers (Lyot, Danjon, Dollfus, etc.) claim that the presumed atmospheres of the Galilean satellites are extremely thin and transparent (as in the case of Mars, only some 1200 km larger than Ganymede) and have searched for surface features on all four Galilean satellites. Dollfus (ref. 245) and others have, in fact, produced tentative maps at conjunction times and claim that this type of observation leads to verification of a locked rotation for such satellites.

JUPITER V

Tiny Jupiter V circles around giant Jupiter twice a day. Its equatorial motion, at only some 100 000 miles above the clouds, maintains a record average orbital velocity of 16.4 miles sec^{-1}. The proximity to Jupiter's bulge produces a rapid regression of the line of nodes (2°.478/day) and enables a superior determination of Jupiter's dynamical oblateness (ch. 3). Since Barnard's discovery in 1892 of Jupiter's fifth satellite, the orbit of J–V has been studied consistently. The orbital elements of Van Woerkom (ref. 58), an improvement over Robertson's (ref. 261), have been adopted by *The American Ephemeris and Nautical Almanac* since 1960 for the computation of its ephemerides of J–V.

OUTER SYSTEM

The remaining seven satellites, discovered after 1900 on photographs taken with large telescopes, constitute the outer system. They are much smaller and farther away from Jupiter than the

Galilean satellites. Their masses are unknown, insignificant quantities. Their diameters can only be estimated from their magnitudes and an assumed albedo. Their Roman numeral designations indicate the order of their discovery.

Table 18–1 lists the satellites in the order of their distances from Jupiter and gives details on their discovery. There are two subgroups in the outer system: (1) the first three satellites are approximately at 0.08 astronomical unit from Jupiter, and (2) the remaining four are approximately 0.15 astronomical unit from the center of Jupiter. The first subgroup has direct orbital motion inclined at ~28° to Jupiter's orbit and periods of revolution of ~250 days. The second subgroup has retrograde orbital motion, inclined at similar but variable angles and longer periods (620 to 760 days) around Jupiter. All seven have orbits highly inclined to Jupiter's equator with varying lines of nodes and are highly eccentric. Their motions vary in a complex manner. The orbits of the two outermost satellites, J–VIII and J–IX, are the most eccentric and are highly disturbed and not even approximately elliptical. (See fig. 18–2.) The gravitational influence of the Sun causes the significant orbital perturbations of all these outer satellites, which are located at a great distance from Jupiter. Their negligible masses lead to no significant mutual perturbations.

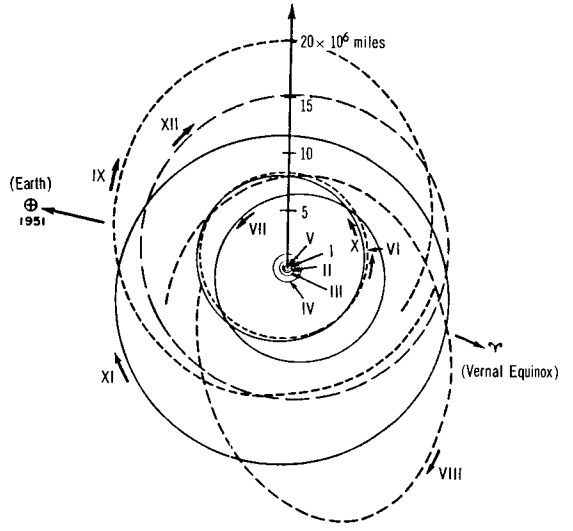

FIGURE 18–2.—The satellite system of Jupiter reduced to the ecliptic plane. (After Ehricke, 1960, according to Nicholson, 1951.)

JUPITER VIII

The most remarkable of Jupiter's faint outer satellites is Jupiter VIII. Its orbital motion is highly eccentric and variable. The marked influence of the Sun's gravitational force, 0.387 that of Jupiter's, results in greater perturbations for J–VIII than for any of the other satellites. Moreover, the motion is retrograde and the orbit is highly inclined to Jupiter's equator. The first ephemerides were in error, and soon after 1908 (discovery date) the satellite was lost. Rediscovered in 1922, it was lost a second time, and finally found again by Nicholson in 1938.

Accurate orbital positions (ephemerides) of J–VIII can only be obtained through numerical integration procedures. Experience showed that cometary methods (especially Cowell's) were the most reliable in treating the perturbations of J–VIII. The work of Grosch (ref. 247) was based on this method, and he used the 1930 to 1947 observations to provide graphs and tables of osculating elements at intervals of 80 days. Table 18–1 presents these elements and their variations. A retrograde motion was proved by Jackson (ref. 262) and Moulton (ref. 263) to be fairly stable for J–VIII.

Finally, Kovalevsky (ref. 264) has used a numerical integration of J–VIII extending over 100 years for constructing, by harmonic analysis, a general theory of the motion of this satellite, which surpasses the accuracy attained by previous efforts.

A proposed use of J–VIII is for the accurate determination of Jupiter's mass. Brouwer and Clemence (ref. 10), however, caution that it is essential to achieve high precision in the numerical calculations and to obtain reliable astrographic positions.

SEARCH FOR OTHER SATELLITES

A search was undertaken by Kuiper (ref. 265) with the 82-inch McDonald Observatory telescope for fainter and more distant Jovian satellites. A region 20′ in radius centered on Jupiter was investigated systematically, but the results were entirely negative. Also, no trace was found of the presumed ring (similar to Saturn's ring but extremely faint) around Jupiter.

References

1. Explanatory Supplement to the Astronomical Ephemeris and The American Ephemeris and Nautical Almanac. The Nautical Almanac Offices of the United Kingdom and the United States of America, H.M. Stationery Office (London), 1961, 505 pp.
2. The American Ephemeris and Nautical Almanac. Issued in annual volumes by year, Nautical Almanac Office, U.S. Naval Observatory (Washington, D.C.), Government Printing Office.
3. ECKERT, W. J.; BROUWER, D.; AND CLEMENCE, G. M.: Coordinates of the Five Outer Planets, 1653–2060. Astronomical Papers Prepared for the Use of The American Ephemeris and Nautical Almanac, vol. 12, 1951, 327 pp.
4. CLEMENCE, G. M.: Perturbations of the Five Outer Planets by the Four Inner Ones. Astronomical Papers Prepared for the Use of The American Ephemeris and Nautical Almanac, vol. 13, pt. 5, 1954, pp. 385–406.
5. Connaissance des Temps ou des Mouvements Célestes à l'Usage des Astronomes et des Navigateurs pour l'An 1960. Bureau des Longitudes, Gauthier-Villars (Paris), 1959, 669 pp.
6. GAILLOT, A.: Addition à la Théorie du Mouvement de Jupiter de M. Le Verrier. Tables Rectifiées du Mouvement de Jupiter. Ann. Obs. Paris, (Mémoires), vol. 31, 1913, pp. 1–319.
7. LEVERRIER, U.-J.: Tables du Mouvement de Jupiter, fondées sur la Comparison de la Théorie avec les Observations. Ann. Obs. Paris (Mémoires), vol. 12, ch. 22, 1876, pp. 1–178.
8. CLEMENCE, G. M.: On the Elements of Jupiter. Astrophys. J., vol. 52, no. 4, Nov. 1946, pp. 89–93.
9. HILL, G. W.: A New Theory of Jupiter and Saturn. Astronomical Papers Prepared for the Use of The American Ephemeris and Nautical Almanac, vol. 4, 1890, 577 pp.
10. BROUWER, D.; AND CLEMENCE, G. M.: Orbits and Masses of Planets and Satellites. Planets and Satellites, ch. 3. Vol. III of The Solar System, G. P. Kuiper and B. M. Middlehurst, eds., The University of Chicago Press, 1961, pp. 31–94.
11. HILL, G. W.: Tables of Jupiter Constructed in Accordance with the Methods of Hansen. Astronomical Papers Prepared for the Use of The American Ephemeris and Nautical Almanac, vol. 7, pt. 1, 1895, pp. 1–144.
12. KROTKOV, R.; AND DICKE, R. H.: Comparison Between Theory and Observation for the Outer Planets. Astron. J., vol. 64, no. 5, June 1959, pp. 157–163.
13. CLEMENCE, G. M.: Motion of Jupiter and Mass of Saturn. Astron. J., vol. 65, no. 1, Feb. 1960, pp. 21–22.
14. HERTZ, H. G.: The Mass of Saturn and the Motion of Jupiter, 1884–1948.

248-761 O-67—10

Astronomical Papers Prepared for the Use of The American Ephemeris and Nautical Almanac, vol. 15, pt. 2, 1953, pp. 167–215.

15. HEATH, M. B. B.: Oppositions of Jupiter, 1956 to 2000. J. Brit. Astron. Assoc., vol. 66, no. 5, Apr. 1956, pp. 166–167.
16. Planetary Coordinates for the Years 1940–1960 Referred to the Equinox of 1950. H.M. Nautical Almanac Office, H.M. Stationery Office (London), 1939, 150 pp.
17. Planetary Coordinates for the Years 1960–1980 Referred to the Equinox of 1950. H.M. Nautical Almanac Office, H.M. Stationery Office (London), 1958, 180 pp.
18. ENCKE, J. F.: Über die Berechnung der speziellen Störungen (Fortsetzung) — Störungen der Vesta durch Jupiter. Berlin. Astron. Jahrb. 1838, 1836, pp. 264–293.
19. AIRY, G. B.: Continuation of Researches into the Value of Jupiter's Mass. Mem. Roy. Astron. Soc., vol. 10, 1838, pp. 43–47.
20. BESSEL, M.: Recherches de M. Bessel sur les Satellites et sur la Masse de Jupiter. Compt. Rend. Acad. Sci., vol. 13, 1841, pp. 58–59.
21. JACOB, W. S.: Measures of Jupiter and Its Satellites, Taken with the Madras Equatorial. Mem. Roy. Astron. Soc., vol. 28, 1860, pp. 109–114.
22. HANSEN, P. A.: Tafeln der Egeria mit Zugrundelegung der in den Abhandlungen der K. S. Gesellschaft der Wissenschaften in Leipzig veröffentlichten Störungen dieses Planeten. Vierteljahrsschr. Astron. Ges. (Leipzig), vol. 3, 1868, pp. 88–93.
23. MÖLLER, A.: Bericht über die Resultate einer neuen Berechnung der Elemente des Faye'schen Cometen. Vierteljahrsschr. Astron. Ges. (Leipzig), vol. 7, 1872, pp. 85–97.
24. KRÜGER, A.: Über die Masse des Jupiter, abgeleitet aus der Bewegung der Themis. Astron. Nachr., vol. 81, no. 1941, 1873, cols. 331–336.
25. SCHUR, W.: Bestimmung der Masse des Jupiter aus Heliometer Messungen der Abstände seiner Satelliten. Vierteljahrsschr. Astron. Ges. (Leipzig), vol. 16, no. 4, 1881, pp. 292–296.
26. VON HAERDTL, E.: Über die Bahn des periodischen Kometen Winnecke in den Jahren 1858–1886. Astron. Nachr., vol. 120, no. 2873, 1889, cols. 257–272.
27. VON HAERDTL, E.: Die Bahn des periodischen Kometen Winnecke in den Jahren 1858–1886 nebst einer neuen Bestimmung der Jupitermasse. Denkschr. Kaiserl. Akad. Wiss. Wien, vol. 56, 1889.
28. HILL, G. W.: Tables of Saturn, Constructed in Accordance With the Methods of Hansen. Astronomical Papers Prepared for the Use of The American Ephemeris and Nautical Almanac, vol. 7, pt. 2, 1895, pp. 145–285.
29. NEWCOMB, S.: On the Mass of Jupiter and the Orbit of Polyhymnia. Astronomical Papers Prepared for The American Ephemeris and Nautical Almanac, vol. 5, pt. 5, 1895, pp. 379–449.
30. LEVEAU, G.: Tables du Mouvement de Vesta fondées sur la Comparison de la Théorie avec les Observations. Ann. Obs. Paris, vol. 22, 1896, pp. A.1–A.317 (see p. A57).
31. LEVEAU, G.: Détermination des Eléments Solaires et des Masses de Mars et Jupiter par les Observation Méridiennes de Vesta. Compt. Rend. Acad. Sci., vol. 145, 1907, pp. 903–906.
32. DE SITTER, W.; AND BROUWER, D.: On the System of Astronomical Constants. Bull. Astron. Inst. Neth., vol. 8, no. 307, July 1908, pp. 213–231.

33. MAKEMSON, M. W.; BAKER, R. M. L., JR.; AND WESTROM, G. B.: Analysis and Standardization of Astrodynamic Constants. J. Astron. Sci., vol. 8, no. 1, spring, 1961, pp. 1–13.
34. CLEMENCE, G. M.: Quoted anonymously in: Astronomical Notes from Hamburg—2. Sky and Telescope, vol. 29, no. 1, Jan. 1965, pp. 19–22.
35. NEWCOMB, S.: The Elements of the Four Inner Planets and the Fundamental Constants of Astronomy. Government Printing Office (Washington, D.C.), 1895, 202 pp. (Suppl. The American Ephemeris and Nautical Almanac for 1897.)
36. DE SITTER, W.: Determination of the Mass of Jupiter and Elements of the Orbits of Its Satellites from Observations Made with the Cape Heliometer—by D. Gill and W. E. Finlay. Ann. Cape Obs., vol. 12, pt. 1, 1915, pp. 1–173.
37. HILL, G. W.: On the Derivation of the Mass of Jupiter from the Motion of Certain Asteroids. Collected Mathematical Works, vol. I, 1873, pp. 105–108.
38. RABE, E.: (Abstract) The Orbital Motion of the Minor Planet (1362) Griqua and the Mass of Jupiter. Astron. J., vol. 64, no. 2, Mar. 1959, pp. 53–54.
39. PORTER, J. G.: Comets and Meteor Streams. Chapman and Hall (London), 1952, 123 pp.
40. STRÖMGREN, E.: Über den Ursprung der Kometen. Publikationer og mindre Meddelelser frø Københavns Observatorium, no. 19, 1914, 62 pp.
41. RUSSELL, H. N.: On the Origin of Periodic Comets. Astron. J., vol. 33, no. 7, Sept. 15, 1920, pp. 49–61.
42. SEE, T. J. J.: Researches on the Figure and Dimensions of Jupiter and on the Dimensions of His Satellites. Astron. Nachr., vol. 153, no. 3670, 1900, cols. 401–410.
43. SCHUR, W.: Untersuchungen über die Dimensionen des Planeten Jupiter und über die Gestalt der Scheibe in der Nahe der Quadraturen mit der Sonne. Astron. Nachr., vol. 141, no. 3374, 1896, cols. 225–232.
44. HARTWIG, E.: Über die Durchmesser der Planeten Merkur, Venus, Mars, Jupiter, und Saturn. Ber. XXI der Naturforsch. Ges. Bamberg, 1911, 21 pp.
45. KAISER, F.: (Excerpt) Astron. Nachr., vol. 45, no. 1090, 1857, cols. 209–212.
46. KAISER, F.: Messungen von Planetendurchmessern mit Airys Doppelbildmicrometer. Ann. Sternwarte Lieden, vol. 3, 1872, pp. 209–274.
47. WIRTZ, C.: Beobachtungen der Grossen Planeten. Ann. Kaiserl. Universitäts-Sternwarte Strassburg, vol. 4, pt. 2, 1912, pp. 243–286.
48. RABE, W.: Untersuchungen über die Durchmesser der grossen Planeten. Astron. Nachr., vol. 234, no. 5600–01, 1926, cols. 153–200.
49. STRUVE, W.: Micrometer-Messungen des Jupiters und seiner Trabanten mit dem grossen Refractor von Fraunhofer angestellt. Astron. Nachr., vol. 5, no. 97, 1827, cols. 13–16. Corrections given by W. Struve in: Micrometerbeobachtungen des Saturns mit der grossen Refractor von Fraunhofer in Dorpat angestellt. Astron. Nachr., vol. 6, no. 139, 1828, cols. 389–392.
50. SECCHI, A.: (Excerpt) Astron. Nachr., vol. 43, no. 1017, 1856, cols. 135–142.
51. SCHMIDT, J.: Beobachtungen von Herrn J. F. Julius Schmidt, Direktor der K. Sternwarte zu Athen. Astron. Nachr., vol. 65, no. 1543, 1865, cols. 97–104.
52. BARNARD, E. E.: Micrometrical Observations of the Fifth Satellite of Jupiter during the Opposition of 1893, with Measures of Diameters of Jupiter,

1892–4, with the 36-inch Equatorial of the Lick Observatory. Astron. J., vol. 14, no. 13, Aug. 25, 1894, pp. 97–104.

53. Dyson, F. W.; and Lewis, T.: Diameters of Jupiter Measured with the Filar and Double-Image Micrometers at the Royal Observatory, Greenwich. Monthly Notices Roy. Astron. Soc., vol. 56, no. 8, 1896, pp. 429–431.
54. Lohse, O.: Untersuchungen über die physische Beschaffenheit des Planeten Jupiter. Publ. Astrophysik. Obs. zu Potsdam, vol. 21, no. 62, 1911, pp. 1–182.
55. Sampson, R. A.: A Discussion of the Eclipses of Jupiter's Satellites, 1878–1903. Ann. Astron. Obs. Harvard College, vol. 52, pt. II, 1909, pp. 151–343.
56. Adams, W. S.: The Polar Compression of Jupiter. Astron. J., vol. 20, no. 17, Dec. 5, 1899, pp. 133.
57. Cohn, F.: Bestimmung der Bahnelemente des V Jupitersmondes. Astron. Nachr., vol. 142, nos. 3403–4, 1897, cols. 289–334.
58. Van Woerkom, A. J. J.: The Motion of Jupiter's Fifth Satellite, 1892–1949. Astronomical Papers Prepared for the Use of The American Ephemeris and Nautical Almanac, vol. 13, pt. 1, 1950, pp. 1–77.
59. De Sitter, W.: Jupiter's Galilean Satellites. Monthly Notices Roy. Astron. Soc., vol. 91, no. 7, May 1931, pp. 706–738.
60. Peek, B. J.: The Planet Jupiter. Faber and Faber (London), 1958, 283 pp.
61. Marth, A.: Ephemeris for Physical Observations of Jupiter, 1896–97. Monthly Notices Roy. Astron. Soc., vol. 56, no. 10, 1896, pp. 516–534.
62. Shain, C. A.: Location on Jupiter of a Source of Radio Noise. Nature, vol. 176, no. 4487, Oct. 29, 1955, pp. 836–837.
63. Morrison, B. L.: Ephemeris of the Radio Longitude of the Central Meridian of Jupiter, System III (1957.0). U.S. Naval Observatory Circular No. 92, May 1, 1962, and Circular No. 94, Apr. 19, 1964.
64. Shain, C. A.: 18.3 Mc/sec Radiation from Jupiter. Australian J. Phys., vol. 9, Mar. 1956, pp. 61–73.
65. Carr, T. D.; Smith, A. G.; Pepple, R.; and Barrow, C. H.: 18-Megacycle Observations of Jupiter in 1957. Astrophys. J., vol. 127, no. 2, Mar. 1958, pp. 274–283.
66. Shain, C. A.: Galactic Radiation at 18.3 Mc/s. Australian J. Sci. Res., series A, vol. 4, no. 3, 1951, pp. 258–267.
67. Carr, T. D.; Smith, A. G.; Bollhagen, H.; Six, N. F., Jr.; and Chatterton, N. E.: Recent Decameter Wavelength Observations of Jupiter, Saturn, and Venus. Astrophys. J., vol. 134, no. 1, July 1961, pp. 105–125.
68. Douglas, J. N.: (Abstract) A Uniform Statistical Analysis of Jovian Decameter Radiation, 1950–1960. Astron. J., vol. 65, no. 9, Nov. 1960, pp. 487–488.
69. Smith, A. G.; Lebo, G. R.; Six, N. F., Jr.; Carr, T. D.; Bollhagen, H.; May, J.; and Levy, J.: Decameter Wavelength Observations of Jupiter. Astrophys. J., vol. 144, no. 2, Feb. 15, 1965, pp. 457–477.
70. Six, N. F., Jr.: Characteristics and Origin of the Nonthermal Radio Emission from Jupiter. Scientific Research Laboratories, Brown Engineering Company, Huntsville, Alabama; Tech. Note R–60, July 1963, 62 pp.
71. Douglas, N. J.; and Smith, H. J.: Change in Rotation Period of Jupiter's Decameter Radio Sources. Nature, vol. 199, no. 4898, 1963, pp. 1080–1081.
72. Munk, W. H.; and MacDonald, G. J. F.: The Rotation of the Earth. A Geophysical Discussion. Cambridge University Press, 1960, 323 pp.

73. De Damoiseau, T.: Tables Ecliptiques des Satellites de Jupiter, d'après la Théorie de leurs Attractions Mutuelles et les Constantes déduites des Observations. Bureau des Longitudes, Bachelier (Paris), 1836, 232 pp.
74. Souillart, M.: Théorie Analytique des Mouvements des Satellites de Jupiter. Mem. Acad. Sci. (Savants Etrangers), vol. 30, no. 1, 1899, pp. 1–193.
75. Jeffreys, H.: On the Internal Constitution of Jupiter and Saturn. Monthly Notices Roy. Astron. Soc., vol. 84, no. 7, May 1924, pp. 534–538.
76. Wildt, R.: Planetary Interiors. Planets and Satellites, ch. 5. Vol. III of The Solar System, G. P. Kuiper and B. M. Middlehurst, eds. University of Chicago Press, 1961, pp. 159, 212.
77. DeMarcus, W. C.: Planetary Interiors. In: Astrophysics III, The Solar System, vol. 52 of Handbuch der Physik, (Encyclopedia of Physics) S. Flügge ed., Springer-Verlag (Berlin), 1959, pp. 419–448.
78. Jeffreys, H.: The Constitution of the Four Outer Planets. Monthly Notices Roy. Astron. Soc., vol. 83, no. 6, Apr. 1923, pp. 350–354.
79. Wildt, R.: Über den inneren Aufbau der grossen Planeten. Nachr. Ges. Akad. Wiss. Göttingen, Math.-Physik. Kl. (N.F.), vol. 1, 1934, pp. 67–78 (Fachgruppe II).
80. Wildt, R.: The Constitutions of the Planets. Monthly Notices Roy. Astron. Soc., vol. 107, 1947, pp. 84–102.
81. Kothari, D. S.: Theory of Pressure-Ionization and Its Applications. Proc. Roy. Soc., vol. 165A, 1938, pp. 486–500.
82. Alfvén, H.: On the Cosmogony of the Solar System I. Ann. Stockholm Obs., vol. 14, no. 2, 1942, pp. 1–33.
83. Alfvén, H.: On the Cosmogony of the Solar System II. Ann. Stockholm Obs., vol. 14, no. 5, 1943, pp. 1–32.
84. Alfvén, H.: On the Origin of the Solar System. Clarendon Press (Oxford), 1954, 194 pp.
85. Öpik, E. J.: Jupiter: Chemical Composition, Structure, and Origin of a Giant Planet. Icarus, vol. 1, no. 3, Oct. 1962, pp. 200–257.
86. Wigner, E.; and Huntington, H. B.: Possibility of a Metallic Modification of Hydrogen. J. Chem. Phys., vol. 3, 1935, pp. 764–770.
87. Kronig, R.; deBoer, J.; and Korringa, J.: On the Internal Constitution of the Earth. Physica, vol. 12, 1946, pp. 245–256.
88. Stewart, J. W.: Compression of Solidified Gases to 20,000 kg/cm^2 at Low Temperature. J. Phys. Chem. Solids, vol. 1, no. 3, Nov. 1956, pp. 146–158.
89. DeMarcus, W. C.: The Constitution of Jupiter and Saturn. Astron. J., vol. 63, no. 1, Jan. 1958, pp. 2–28.
90. Ramsey, W. H.: On the Constitution of the Major Planets. Monthly Notices Roy. Astron. Soc., vol. 111, no. 5, 1951, pp. 427–447.
91. DeMarcus, W. C.: Theoretical Pressure-Density Relations with Applications to the Constitution of the Planets. Ph.D. Thesis, Yale Univ., 1951.
92. Abrikosov, A. A.: The Equation of State of Hydrogen at High Pressures. Astron. Zh., vol. 31, no. 2, Mar.–Apr. 1954, pp. 112–123 (in Russian).
93. Miles, B.; and Ramsey, W. H.: On the Internal Structures of Jupiter and Saturn. Monthly Notices Roy. Astron. Soc., vol. 112, no. 2, 1952, pp. 234–243.
94. Fessenkov, V. G.; and Massevich, A. G.: On Questions Concerning the Structure and Chemical Composition of the Large Planets. Astron. Zh., vol. 28, no. 5, Sept.–Oct. 1951, pp. 317–337 (in Russian).
95. Peebles, P. J. E.: The Structure and Composition of Jupiter and Saturn. Astrophys. J., vol. 140, no. 1, July 1964, pp. 328–347.

96. FIELD, G. B.: The Source of Radiation from Jupiter at Decimeter Wavelengths. 3. Time Dependence of Cyclotron Radiation. J. Geophys. Res., vol. 66, no. 5, May 1961, pp. 1395–1405.
97. CHANG, D. B.; AND DAVIS, L., JR.: Synchrotron Radiation as the Source of Jupiter's Polarized Decimeter Radiation. Astrophys. J., vol. 136, no. 2, Sept. 1962, pp. 567–581.
98. WARWICK, J. W.: Dynamic Spectra of Jupiter's Decametric Emission, 1961. Astrophys. J., vol. 137, no. 1, Jan. 1963, pp. 41–60.
99. BERGE, G. L.; AND MORRIS, D.: Decimeter Measurements Relating to the Possible Displacement of Jupiter's Magnetic Dipole. Astrophys. J., vol. 140, no. 3, Oct. 1964, pp. 1330–1332.
100. MORRIS, D.; AND BERGE, G. L.: Measurements of the Polarization and Angular Extent of the Decimeter Radiation from Jupiter. Astrophys. J., vol. 136, no. 1, July 1962, pp. 276–282.
101. BASH, F. H.; DRAKE, F. D.; GUNDERMANN, E.; AND HEILES, C. E.: 10-cm Observations of Jupiter, 1961–1963. Astrophys. J., vol. 139, no. 3, Apr. 1964, pp. 975–985.
102. AXFORD, W. I.; DESSLER, A. J.; AND GOTTLIEB, B.: Termination of Solar Wind and Solar Magnetic Field. Astrophys. J., vol. 137, no. 4, May 1963, pp. 1268–1278.
103. MEAD, G. D.; AND BEARD, D. B.: Shape of the Geomagnetic Field Solar Wind Boundary. J. Geophys. Res., vol. 69, no. 7, Apr. 1964, pp. 1169–1180.
104. CARR, T. D.; BROWN, G. W.; SMITH, A. G.; HIGGINS, C. S.; BOLLHAGEN, H.; MAY, J.; AND LEVY, J.: Spectral Distribution of the Decametric Radiation from Jupiter in 1961. Astrophys. J., vol. 140, no. 2, Aug. 1964, pp. 778–795.
105. RADHAKRISHNAN, V.; AND ROBERTS, J. A.: Polarization and Angular Extent of the 960-Mc/sec Radiation from Jupiter. Phys. Rev. Letters, vol. 4, no. 10, May 15, 1960, pp. 493–494.
106. TAYLOR, D. J.: Spectrophotometry of Jupiter's 3400-10,000 Å Spectrum and a Bolometric Albedo for Jupiter. Icarus, vol. 4, no. 4, Sept. 1965, pp. 362–373.
107. MENZEL, D. H.; COBLENTZ, W. W.; AND LAMPLAND, C. O.: Planetary Temperatures Derived from Water-Cell Transmissions. Astrophys. J., vol. 63, no. 3, Apr. 1926, pp. 177–187.
108. MURRAY, B. C.; AND WILDEY, R. L.: Stellar and Planetary Observations at 10 Microns. Astrophys. J., vol. 137, no. 2, Feb. 1963, pp. 692–693.
109. ZABRISKIE, F. R.: Hydrogen Content of Jupiter's Atmosphere. Astron. J., vol. 67, no. 3, Apr. 1962, pp. 168–170.
110. SPINRAD, H.: Spectroscopic Research on the Major Planets. Appl. Optics, vol. 3, no. 2, Feb. 1964, pp. 181–186.
111. OWEN, T.: Comparisons of Laboratory and Planetary Spectra. II. The Spectrum of Jupiter from 9700 to 11,200 Å. Astrophys. J., vol. 141, no. 2, Feb. 15, 1965, pp. 444–456.
112. SINTON, W. M.; AND STRONG, J.: Radiometric Observations of Venus. Astrophys. J., vol. 131, no. 2, Mar. 1960, pp. 470–490.
113. SINTON, W. M.: Physical Researches on the Brighter Planets. Final Report. Air Force Cambridge Res. Lab., Rept. AFCRL–64–926, Sept. 30, 1964, 15 pp.
114. THORNTON, D. D.; AND WELCH, W. J.: 8.35-mm Radio Emission from Jupiter. Icarus, vol. 2, no. 3, Oct. 1963, pp. 228–232.

115. GIORDMAINE, J. A.; ALSOP, L. E.; TOWNES, C. H.; AND MAYER, C. H.: (Abstract) Observations of Jupiter and Mars at 3-cm Wave Length. Astron. J., vol. 64, no. 8, Oct. 1959, pp. 332–333.
116. MAYER, C. H.; MCCULLOUGH, T. P.; AND SLOANAKER, R. M.: Observations of Mars and Jupiter at a Wave Length of 3.15 cm. Astrophys. J., vol. 127, no. 1, Jan. 1958, pp. 11–16.
117. BIBINOVA, V. P.; KUZMIN, A. D.; SALOMONOVICH, A. E.; AND SHAVLOVSKY I. V.: Observations of the Radio Emission of Venus and Jupiter at 3.3 cm. Astron. Zh., vol. 39, no. 6, Nov.–Dec. 1962, pp. 1083–1088. Translation in Soviet Astronomy-AJ, vol. 6, no. 6, May–June 1963, pp. 840–844.
118. DRAKE, F. D.; AND EWEN, H. I.: Broad-band Microwave Source Comparison Radiometer for Advanced Research in Radio Astronomy. Proc. Inst. Radio Engr., vol. 46, 1958, pp. 53–60.
119. SLOANAKER, R. M.: (Abstract) Apparent Temperature of Jupiter at a Wave Length of 10 cm. Astron. J., vol. 64, no. 8, Oct. 1959, p. 346.
120. MCCLAIN, E. F.: (Abstract) A Test for Non-Thermal Radiation from Jupiter at a Wave Length of 21 cm. Astron. J., vol. 64, no. 8, Oct. 1959, pp. 339–340.
121. DRAKE, F. D.; AND HVATUM, S.: (Abstract) Non-thermal Microwave Radiation from Jupiter. Astron. J., vol. 64, no. 8, Oct. 1959, pp. 329–330.
122. ROBERTS, J. A.; AND STANLEY, G. J.: Radio Emission from Jupiter at a Wavelength of 31 Centimeters. Publ. Astron. Soc. Pacific, vol. 71, no. 423, Dec. 1959, pp. 485–496.
123. HARDEBECK, H. E.: Radiometric Observations of Jupiter at 430 Mc/s. Astrophys. J., vol. 141, no. 2, Feb. 15, 1965, p. 837.
124. KUIPER, G. P.: Planetary Atmospheres and Their Origin. The Atmospheres of the Earth and Planets, ch. 12, G. P. Kuiper, ed., University of Chicago Press, 1952, 434 pp., pp. 306–405.
125. TRAFTON, L. M.: The Thermal Opacity in the Major Planets. Astrophys. J., vol. 140, no. 3, Oct. 1964, pp. 1340–1341.
126. TRAFTON, L. M.: A Study of the Energy Balance in the Atmospheres of the Major Planets. Ph.D. Thesis, California Institute of Technology, Mar. 19, 1965, 248 pp.
127. WILDEY, R. L.: Hot Shadows on Jupiter. Science, vol. 147, no. 3661, Feb. 26, 1965, pp. 1035–1036.
128. WILDEY, R. L.: On the Interpretation of Thermal Emission Maps of Jupiter, J. Geophys. Res., vol. 70, no. 15, Aug. 1, 1965, pp. 3796–3797.
129. WILDEY, R. L.; MURRAY, B. C.; AND WESTPHAL, J. A.: Thermal Infrared Emission of the Jovian Disk. J. Geophys. Res., vol. 70, no. 15, Aug. 1, 1965, pp. 3711–3719.
130. MURRAY, B. C.; WILDEY, R. L.; AND WESTPHAL, J. A.: Observations of Jupiter and the Galilean Satellites at 10 Microns. Astrophys. J., vol. 137, no. 3, Apr. 1964, pp. 986–993.
131. ROBERTS, J. A.; AND KOMESAROFF, M. M.: Observations of Jupiter's Radio Spectrum and Polarization in the Range 6 cm to 100 cm. Icarus, vol. 4, no. 2, May 1965, pp. 127–156.
132. BURKE, B. F.; AND FRANKLIN, K. L.: Observations of a Variable Radio Source Associated with the Planet Jupiter. J. Geophys. Res., vol. 60, no. 2, June 1955, pp. 213–217.
133. ELLIS, G. R. A.: Radiation from Jupiter at 4.8 Mc/s. Nature, vol. 194, no. 4829, May 1962, pp. 667–668.

134. KRAUS, J. D.: Planetary and Solar Emission at 11 Meters Wavelength. Proc. IRE, vol. 46, Jan. 1958, pp. 266–274.
135. GARDNER, F. F.; AND SHAIN, C. A.: Further Observations of Radio Emission from the Planet Jupiter. Australian J. Phys., vol. 11, Mar. 1958, p. 55.
136. DOUGLAS, J. N.; AND SMITH, H. J.: Presence and Correlation of Fine-Structure in Jovian Decametric Radiation. Nature, vol. 192, Nov. 25, 1961, p. 741.
137. DOUGLAS, J. N.; AND SMITH, H. J.: Decametric Radiation from Jupiter. I. Synoptic Observations 1957–1961. Astron. J., vol. 68, Apr. 1963, pp. 163–180.
138. SMITH, A. G.: Radio Spectrum of Jupiter. Science, vol. 134, no. 3479, Sept. 2, 1961, pp. 587–595.
139. DOUGLAS, J. N.: Decametric Radiation from Jupiter. IEEE Trans. on Military Electronics, vol. MIL–8, nos. 3 and 4, July–Oct. 1964, pp. 173–187.
140. GALLET, R. M.; AND BOWLES, K. L.: Some properties of the Radio Emissions of Jupiter. Astron. J., vol. 61, May 1956, p. 194.
141. BURKE, B. F.: Radio Observations of Jupiter. I. Planets and Satellites, ch. 13. Vol. III of The Solar System, G. P. Kuiper and B. M. Middlehurst, eds. University of Chicago Press, 1961, pp. 473–499.
142. FRANKLIN, K. L.; AND BURKE, B. F.: Radio Observations of the Planet Jupiter. J. Geophys. Res., vol. 63, no. 4, Dec. 1958, pp. 807–824.
143. STONE, R. G.; ALEXANDER, J. K.; AND ERICKSON, W. C.: Low-Level Decameter Emissions from Jupiter. Astrophys. J., vol. 140, no. 1, July 1964, pp. 374–377.
144. SLEE, O. B.; AND HIGGINS, C. S.: Long Baseline Interferometry of Jovian Decametric Radio Bursts. Nature, vol. 197, no. 4867, Feb. 23, 1963, pp. 781–783.
145. SMITH, A. G.; AND CARR, T. D.: Radio-Frequency Observations of the Planets in 1957–58. Astrophys. J., vol. 130, no. 2, Sept. 1959, pp. 641–647.
146. DOWDEN, R. L.: Polarization Measurements of Jupiter Radio Outbursts at 10.1 Mc/sec. Australian J. Phys., vol. 16, Sept. 1963, pp. 398–410.
147. SHERRILL, W. M.; AND CASTLES, M. P.: Survey of the Polarization of Jovian Radiation at Decameter Wavelengths. Astrophys. J., vol. 138, no. 2, Sept. 1963, pp. 587–598.
148. BARROW, C. H.: Polarization Observation of Jupiter at Decameter Wavelength. Icarus, vol. 3, no. 1, May 1964, pp. 66–77.
149. BIGG, E. K.: Influence of the Satellite Io on Jupiter's Decametric Emission. Nature, vol. 203, no. 4949, Sept. 5, 1964, pp. 1008–1010.
150. DULK, G. A.: Io-Related Radio Emission from Jupiter. Science, vol. 148, no. 3677, June 18, 1965, pp. 1585–1589.
151. LEBO, G. R.; SMITH, A. G.; AND CARR, T. D.: Jupiter's Decametric Emission Correlated with the Longitudes of the First Three Galilean Satellites. Science, vol. 148, no. 3678, June 25, 1965, pp. 1724–1725.
152. ZHELEZNIAKOV, V. V.: On the Theory of the Sporadic Radio Emission from Jupiter. Astron. Zh., vol. 35, no. 2, Mar.–Apr. 1958, pp. 230–240; or Translation in: Soviet Astronomy AJ, vol. 2, no. 2 (Mar.–Apr. 1958) publ. May 1959, pp. 206–215.
153. GALLET, R. M.: Radio Observations of Jupiter. II. Planets and Satellites, ch. 14. Vol. III of The Solar System, G. P. Kuiper and B. M. Middlehurst, eds. University of Chicago Press, 1961, pp. 500–533.
154. STROM, S. E.; AND STROM, K. M.: A Possible Explanation for Jovian Decameter Bursts. Astrophys. J., vol. 136, no. 1, July 1962, pp. 307–310.

155. SAGAN, C.; AND MILLER, S. L.: (Abstract) Molecular Synthesis in Simulated Reducing Planetary Atmospheres. Astron. J., vol. 65, no. 9, Nov. 1960, p. 499.
156. HIRSHFIELD, J. L.; AND BEKEFI, G.: Decameter Radiation from Jupiter. Nature, vol. 198, no. 4875, Apr. 6, 1963, pp. 20–22.
157. ELLIS, G. R. A.; AND MCCULLOUGH, P. M.: Decametric Radio Emission of Jupiter. Nature, vol. 198, no. 4877, Apr. 20, 1963, p. 275.
158. CHANG, D. B.: Amplified Whistlers as the Source of Jupiter's Sporadic Decameter Radiation. Astrophys. J., vol. 138, no. 4, Nov. 1963, pp. 1231–1241.
159. ROBERTS, J. A.: Radio Emission from the Planets. Planetary and Space Science, vol. 11, no. 3, Mar. 1963, pp. 221–259.
160. MORRIS, D.; AND BARTLETT, J. F.: Polarization of the 2840 Mc/s Radiation from Jupiter. (Physics of Planets) Mem. Soc. Roy. Sci. Liege, series V, vol. 7, 1963, pp. 564–568.
161. ROSE, W. K.; BOLOGNA, J. M.; AND SLOANAKER, R. M.: (Abstract) Linear Polarization of Jupiter, Saturn, and Weak Radio Sources Using a 9.4-cm Maser. Astron. J., vol. 68, no. 2, Mar. 1963, p. 78.
162. GARY, B.: An Investigation of Jupiter's 1,400 Mc/sec Radiation. Astron. J., vol. 68, no. 8, Oct. 1963, pp. 568–572.
163. MCCLAIN, E. F.: (Abstract) A Test for Non-thermal Radiation from Jupiter at a Wave Length of 21 cm. Astron. J., vol. 64, no. 8, Oct. 1959, pp. 339–340.
164. SLOANAKER, R. M.; AND BOLAND, J. W.: Observations of Jupiter at a Wavelength of 10 cm. Astrophys. J., vol. 133, no. 2, Mar. 1961, pp. 649–656.
165. MILLER, A. C.; AND GARY, B. L.: Measurements of the Decimeter Radiation from Jupiter. Astron. J., vol. 67, no. 10, Dec. 1962, pp. 727–731.
166. KERR, F. J.: 210-Foot Radio Telescope's First Results. Sky and Telescope, vol. 24, no. 5, Nov. 1962, pp. 254–260.
167. FIELD, G. B.: The Source of Radiation from Jupiter at Decimeter Wavelengths. J. Geophys. Res., vol. 64, no. 9, Sept. 1959, pp. 1169–1177.
168. FIELD, G. B.: The Source of Radiation from Jupiter at Decimeter Wavelengths. 2. Cyclotron Radiation by Trapped Electrons. J. Geophys. Res., vol. 65, no. 6, June 1960, pp. 1661–1671.
169. SHARONOV, V. V.: Physical Interpretation of Color Phenomena of the Disk of Jupiter. Doklady Akad. Nauk SSSR vol. 39, no. 5, 1943, pp. 173–175.
170. MÜLLER, G.: Helligkeitsmessungen der bei den Planetenbeobachtungen benützen Vergleichsterne. Publ. Astrophys. Obs. Potsdam, vol. 8, no. 4, 1893, pp. 197–335.
171. BECKER, W.: Über Helligkeitsschwankungen der Planeten Mars, Jupiter, Saturn, Uranus, Neptun und damit zusammenhängende Erscheinungen. Sitzber. Preuss. Akad. Wiss., vol. 28, 1933, pp. 839–859.
172. HARRIS, D. L.: Photometry and Colorimetry of Planets and Satellites. Planets and Satellites, ch. 8. Vol. III of The Solar System, G. P. Kuiper and B. M. Middlehurst, eds. University of Chicago Press, 1961, pp. 272–342.
173. ZOLLNER, J. C. F.: Photometrische Untersuchungen. W. Engelmann (Leipzig), 1865.
174. KING, E. S.: Photovisual Magnitudes of Stars and Planets. Ann. Harvard Coll. Obs., vol. 81, no. 4, 1919, pp. 201–215.
175. KING, E. S.: Revised Magnitudes and Color Indices of the Planets. Ann. Harvard Coll. Obs., vol. 85, no. 4, 1923, pp. 63–71.

176. RUBASCHEV, B. M.: Problems of Solar Activity. NASA TT F-244, translation of Probl. Soln. Aktivn., Nauka Publishing House (Moscow), 1964, 397 pp.
177. BOGGESS, A., III; AND DUNKELMAN, L.: Ultraviolet Reflectivities of Mars and Jupiter. Astrophys. J., vol. 129, no. 1, Jan. 1959, pp. 236–237.
178. STECHER, T. P.: An Observation of Jupiter in the Ultraviolet. Ann. Astrophys., vol. 28, no. 4, 1965, pp. 788–790.
179. PLAETSCHKE, J.: Photographische Photometrie der Jupiterscheibe. Z. Astrophys., vol. 19, no. 2, 1939, pp. 69–115.
180. DOLLFUS, A.: Polarization Studies of Planets. Planets and Satellites, ch. 9. Vol. III of The Solar System, G. P. Kuiper and B. M. Middlehurst, eds. University of Chicago Press, 1961, 601 pp., pp. 343–399.
181. BARABASHOV, N.; AND SEMEJKIN, B.: Photographische Photometrie des Planeten Jupiter und Untersuchungen der Jupiter-und Saturnatmosphären. Z. Astrophys., vol. 8, no. 3, 1934, pp. 179–189.
182. WILDT, R.: On the Chemical Nature of the Colouration in Jupiter's Cloud Forms. Monthly Notices Roy. Astron. Soc., vol. 99, no. 8, June 1939, pp. 616–623.
183. UREY, H. C.: The Atmospheres of the Planets. In Astrophysics III: The Solar System. Vol. 52 of Handbuch der Physik (Encyclopedia of Physics), S. Flügge, ed. Springer-Verlag (Berlin), 1959, pp. 363–418.
184. RICE, F. O.: The Chemistry of Jupiter. Sci. Am., vol. 194, no. 6, 1956, pp. 119–128.
185. RICE, F. O.: Colors on Jupiter. J. Chem. Phys., vol. 24, no. 6, June 1956, p. 1259.
186. RICE, F. O.; AND COSGRAVE, D. P.: Some Experiments on Rice's Blue Material: Colors on Jupiter. Nature, vol. 188, 1960, p. 1023.
187. PAPAZIAN, H. A.: The Colors of Jupiter. Publ. Astron. Soc. Pacific, vol. 71, no. 420, June 1959, pp. 237–239.
188. WILLIAMS, A. S.: On the Observed Changes in the Colour of Jupiter's Equatorial Zone. Monthly Notices Roy. Astron. Soc., vol. 80, no. 5, Mar. 1920, pp. 467–475.
189. HESS, S. L.: Variations in Atmospheric Absorption Over the Disks of Jupiter and Saturn. Astrophys. J., vol. 118, no. 1, July 1953, pp. 151–160.
190. SQUIRES, P.: The Equatorial Clouds of Jupiter. Astrophys. J., vol. 126, no. 1, July 1957, pp. 185–194.
191. BAYLEY, D. P.: The Colours of Jupiter's Polar Regions. J. Brit. Astron. Assoc., vol. 55, no. 5, July 1945, pp. 116–120.
192. HARGREAVES, F. J.: The Circulating Current in the South Tropical Zone of Jupiter. J. Brit. Astron. Assoc., vol. 49, no. 9, July 1939, pp. 334–336.
193. SLIPHER, V. M.: A Photographic Study of the Spectrum of Jupiter. Bull. Lowell Obs., vol. 1, Bull. no. 16, 1905, pp. 111–115.
194. SLIPHER, V. M.: The Spectra of the Major Planets. Bull. Lowell Obs., vol. 1, Bull. no. 42, 1909, pp. 231–238.
195. SLIPHER, V. M.: Spectrographic Studies of the Planets. Monthly Notices Roy. Astron. Soc., vol. 93, no. 9, Oct. 1933, pp. 657–689.
196. WILDT, R.: Absorptionsspektren and Atmospharen der grossen Planeten. Nachr. Ges. Akad. Wiss. Göttingen, vol. 1, 1932, pp. 87–96.
197. DUNHAM, T.: The Atmospheres of Jupiter and Saturn. Publ. Astron. Soc. Pacific, vol. 46, no. 272, Aug. 1934, pp. 231–233.
198. HERZBERG, G.: The Atmospheres of the Planets. J. Roy. Astron. Soc. Canada, vol. 45, 1951, pp. 100–123.

199. KIESS, C. C.; CORLISS, C. H.; AND KIESS, H. K.: High-Dispersion Spectra of Jupiter. Astrophys. J., vol. 132, no. 1, July 1960, pp. 221–231.
200. SPINRAD, H.; AND TRAFTON, L.: High Dispersion Spectra of the Outer Planets. I. Jupiter in the Visual and Red. Icarus, vol. 2, no. 1, June 1963, pp. 19–28.
201. OWEN, T. C.: Comparisons of Laboratory and Planetary Spectra. I. The Spectrum of Jupiter from 9,000 Å to 10,100 Å. Publ. Astron. Soc. Pacific, vol. 75, no. 445, Aug. 1963, pp. 314–322.
202. WILDT, R.: Photochemistry of Planetary Atmospheres. Astrophys. J., vol. 86, no. 3, Oct. 1937, pp. 321–336.
203. CADLE, R.: The Photochemistry of the Upper Atmosphere of Jupiter. J. Am. Sci., vol. 19, no. 4, July 1962, pp. 281–285.
204. RUSSELL, H. N.: The Solar System and Its Origin. Macmillan Co., 1935.
205. HERZBERG, G.: On the Possibility of Detecting Molecular Hydrogen and Nitrogen in Planetary and Stellar Atmospheres by Their Rotation-Vibration Spectra. Astrophys. J., vol. 87, no. 4, May 1938, pp. 428–437.
206. JAMES, H. M.; AND COOLIDGE, A. S.: Quadrupole Rotation-Vibration Spectrum of H_2. Astrophys. J., vol. 87, no. 4, May 1938, pp. 438–459.
207. KOLOS, W.; AND ROOTHAAN, C. C. J.: Accurate Electronic Wave Functions for the H_2 Molecule. Rev. Mod. Phys., vol. 32, no. 2, Apr. 1960, pp. 219–232.
208. FOLTZ, J. V.; AND RANK, D. H.: Intensity of the 4–0 Quadrupole Band of Molecular Hydrogen. Astrophys. J., vol. 138, no. 4, Nov. 1963, pp. 1319–1321.
209. FIELD, G. B.: Hydrogen Molecules and Astronomy: A Review. W. B. Sommerville et al., ed. Princeton University Observatory, 1962, p. 32.
210. SAGAN, C.: (Abstract) The Production of Organic Molecules in Planetary Atmospheres. Astron. J., vol. 65, no. 9, Nov. 1960, p. 499.
211. BARDWELL, J.; AND HERZBERG, G.: Laboratory Experiments on the Detectability of Silane (SiH_4) and Methyl Deuteride (CH_3D) in the Atmospheres of the Outer Planets. Astrophys. J., vol. 117, no. 3, May 1953, pp. 462–465.
212. EUCKEN, J.: Physikalisch-chemische Betrachtungen über die früheste Entwicklungsgeschichte der Erde. Nachr. Akad. Wiss. Göttingen, Mathphysik. Kl., 1944, no. 1, pp. 1–25.
213. BAUM, W. A.; AND CODE, A. D.: Photometric Observations of the Occultation of σ-Arietis by Jupiter. Astron. J., vol. 58, no. 4, May 1953, pp. 108–112.
214. PEEBLES, P. J. E.: The Big Planets. Intern. J. Sci. Tech., no. 35, Nov. 1964, pp. 32–38 and p. 79.
215. ALLER, L. H.: The Abundance of the Elements. Interscience Publishers (New York), 1961, 283 pp.
216. GROSS, S. H.; AND RASOOL, S. I.: The Upper Atmosphere of Jupiter. Icarus, vol. 3, no. 4, Nov. 1964, pp. 311–322.
217. GALLET, R.: (quoted by Peebles, 1964) a paper presented at NASA Institute for Space Studies. New York, Oct. 1962. To be published in Proc. Conf. Planet Jupiter, H. J. Smith, ed.
218. SCHOENBERG, E.: Zur Dynamik der Jupiteratmosphäre. Astron. Nachr., vol. 273, 1943, pp. 113–123.
219. HADLEY, G.: Concerning the Cause of the General Trade Winds. Phil. Trans. Roy. Soc. London (London), vol. 39, no. 437, 1735, pp. 58–62. Reprinted in Abbe, C.: The Mechanics of the Earth's Atmosphere.

Third Collection, Smithsonian Miscellaneous Collections, vol. 51, no. 4, The Smithsonian Institution (Washington, D.C.), 1910, pp. 5–7.

220. HESS, S. L.: The General Atmospheric Circulation of Jupiter. The Study of Planetary Atmospheres. Final Report, Lowell Obs., 1952, pp. 47–54.
221. ROSSBY, C. G.: On the Distribution of Angular Velocity in Gaseous Envelopes Under the Influence of Large-Scale Horizontal Mixing Processes. Bull. Am. Meteorol. Soc., vol. 28, no. 2, Feb. 1947, pp. 53–68.
222. STARR, V. P.: What Constitutes Our New Outlook on the General Circulation? J. Meteorol. Soc. Japan, series II, vol. 36, no. 5, 1958, pp. 167–173.
223. OWEN, T. C.; AND STALEY, D. O.: A Possible Jovian Analogy to the Terrestrial Equatorial Stratospheric Wind Reversal. J. Atm. Sci., vol. 20, no. 4, 1963, pp. 347–350.
224. MINTZ, Y.: The General Circulation of Planetary Atmospheres. Appendix 8 to The Atmospheres of Mars and Venus, Publication 944, National Academy of Sciences—National Research Council, 1961, pp. 114–146.
225. FOCAS, J. H.; AND BANOS, C. J.: Photometric Study of the Atmospheric Activity on the Planet Jupiter and Peculiar Activity in its Equatorial Area. Ann. Astrophys., vol. 27, no. 1, Jan.–Feb. 1964, pp. 36–45.
226. HESS, S. L.; AND PANOFSKY, H. A.: The Atmospheres of the Other Planets. Compendium of Meteorol., Am. Meteorol. Soc. (Boston), 1951, pp. 391–398.
227. SHAPIRO, R.: A Quantitative Study of Bright and Dark Spots on Jupiter's Surface. The Study of Planetary Atmospheres. Final Report, Lowell Obs., 1952a, pp. 97–113.
228. SHAPIRO, R.: The Distribution and Velocities of Bright and Dark Spots on Jupiter's Surface in 1928. The Study of Planetary Atmospheres. Final Report, Lowell Obs., 1952b, pp. 116–126.
229. MINTZ, Y.: On the Formation of Disturbances in the Atmosphere of Jupiter in Response to Changes in the State of the Sun. The Study of Planetary Atmospheres. Final Report, Lowell Obs., 1952, pp. 200–207.
230. PALMER, C. E.: On High-Level Cyclones Originating in the Tropics. Trans. Am. Geophys. Union, vol. 32, no. 5, Oct. 1951, pp. 683–696.
231. PALMER, C. E.: The Impulsive Generation of Certain Changes in the Tropospheric Circulation. J. Meteorol., vol. 10, no. 1, Feb. 1953, pp. 1–9.
232. SAGAN, C.: On the Nature of the Jovian Red Spot. (Physics of Planets) Mem. Soc. Roy. Sci. Liege, series V, vol. 7, 1963, pp. 506–515.
233. HIDE, R.: On the Hydrodynamics of Jupiter's Atmosphere. (Physics of Planets) Mem. Soc. Roy. Sci. Liege, series V, vol. 7, 1963, pp. 481–505.
234. PROUDMAN, J.: On the Motions of Solids in a Liquid Possessing Vorticity. Proc. Roy. Soc. London, series A, vol. 92, 1916, pp. 408–424.
235. TAYLOR, G. I.: Experiments on the Motion of Solid Bodies in Rotating Fluids. Proc. Roy. Soc. London, series A, vol. 104, 1923, pp. 213–218.
236. GRACE, S. F.: Free Motion of a Sphere in a Rotating Liquid at Right Angles to the Axis of Rotation. Proc. Roy. Soc. London, series A, vol. 104, 1923, pp. 278–301.
237. PEEK, B. M.: The Physical State of Jupiter's Atmosphere. Monthly Notices Roy. Astron. Soc., vol. 97, no. 8, June 1937, pp. 574–582.
238. OPARIN, A. I.: The Origin of Life. The Macmillan Co., First ed., 1938, Academic Press, Third ed., 1957.
239. MILLER, S. L.: Production of Amino Acids Under Possible Primitive Earth Conditions. Science, vol. 117, 1953, pp. 528–529.
240. MILLER, S. L.: Production of Organic Compounds Under Possible Primitive Earth Conditions. J. Am. Chem. Soc., vol. 77, 1955, pp. 2351–2360.

241. ABELSON, P. H.: Paleobiochemistry. Inorganic Synthesis of Amino Acids. Carnegie Institute of Washington Year Book, vol. 55, 1956, pp. 171.
242. HEYNS, K.; WALTER, W.; AND MEYER, E.: Modelluntersuchungen zur Bildung Organischer Verbindungen in Atmosphären einfacher Gase durch Elektrische Entladungen. Naturw., vol. 44, 1957, pp. 385–389.
243. SAGAN, C.: Exobiology. A Critical Review in Life Sciences and Space Research II. M. Florkin and A. Dollfus, eds. North-Holland Publ. Co. (Amsterdam), 1964, pp. 35–53.
244. SIEGEL, S. M.; AND GIUMARRO, C.: Survival and Growth of Terrestrial Micro-organisms in Ammonia-rich Atmospheres. Icarus, vol. 4, 1965, pp. 37–40.
245. DOLLFUS, A.: Visual and Photographic Studies of Planets at the Pic du Midi. Planets and Satellites, ch. 15. Vol. III of The Solar System, G. P. Kuiper and B. M. Middlehurst, eds. University of Chicago Press, 1961, pp. 534–571.
246. HARRIS, D. L.: Photometry and Colorimetry of Planets and Satellites. Planets and Satellites, ch. 8. Vol. III of The Solar System, G. P. Kuiper and B. M. Middlehurst, eds. University of Chicago Press, 1961, pp. 272–342.
247. GROSCH, H. R. J.: The Orbit of the Eighth Satellite of Jupiter. Astron. J., vol. 53, no. 6, May 1948, pp. 180–187.
248. NICHOLSON, S. B.: Orbit of the Ninth Satellite of Jupiter. Astrophys. J., vol. 100, no. 1, July 1944, pp. 57–62.
249. BOBONE, J.: Tablas del VI (Sexto) Satellite de Jupiter. Astron. Nachr., vol. 262, nos. 6279–80, 1937, cols. 321–346.
250. WILSON, R. H., JR.: Revised Orbit and Ephemeris for Jupiter X. Publ. Astron. Soc. Pacific, vol. 51, no. 302, Aug. 1939, pp. 241–242.
251. HERRICK, S.: Jupiter IX and Jupiter XII. Publ. Astron. Soc. Pacific, vol. 64, no. 380, Oct. 1952, pp. 237–241.
252. KOVALEVSKY, J.: Les Satellites de Jupiter. Astron. Bull. Soc. Astron. France, vol. 74, June 1960, pp. 259–264.
253. PORTER, J. G.: The Satellites of the Planets. J. Brit. Astron. Assoc., vol. 70, no. 1, Jan. 1960, pp. 33–59.
254. SAMPSON, R. A.: Theory of the Four Great Satellites of Jupiter. Mem. Roy. Astron. Soc., vol. 63, 1921, 270 pp.
255. SAMPSON, R. A.: Tables of the Four Great Satellites of Jupiter. (Calculated by F. C. H. Carpenter and W. F. Doak.) Published by the University of Durham (London), 1910, 299 pp.
256. ANDOYER, H.: Sur le Calcul des Éphémerides des Quatre Anciens Satellites de Jupiter. Bull. Astron., vol. 32, 1915, pp. 177–224.
257. LEVIN, A. E.: Mutual Eclipses and Occultations of Jupiter's Satellites. Mem. Brit. Astron. Assoc., vol. 30, no. 3, Dec. 1934, pp. 85–119.
258. STEBBINS, J.: The Light-Variations of the Satellites of Jupiter and Their Applications to Measures of the Solar Constant. Lick Obs. Bull., vol. 13, Bull. no. 385, 1927, pp. 1–18.
259. STEBBINS, J.; AND JACOBSON, T. S.: Further Photometric Measures of Jupiter's Satellites and Uranus, with Tests of the Solar Constant. Lick Obs. Bull., vol. 13, Bull. no. 401, 1928, pp. 180–195.
260. BINDER, A. B.; AND CRUIKSHANK, D. P.: Evidence for an Atmosphere on Io. Icarus, vol. 3, no. 4, Nov. 1964, pp. 299–305.
261. ROBERTSON, J.: Orbit of the Fifth Satellite of Jupiter. Astron. J., vol. 35, no. 24, Aug. 1924, pp. 190–193.
262. JACKSON, J.: Retrograde Satellite Orbits. Monthly Notices Roy. Astron. Soc., vol. 74, no. 2, Dec. 1913, pp. 82–92.

263. MOULTON, F. R.: On the Stability of Direct and Retrograde Satellite Orbits. Monthly Notices Roy. Astron. Soc., vol. 75, no. 2, Dec. 1914, pp. 40–57.

264. KOVALEVSKY, J.: Methode Numérique de Calcul des Perturbations Générales. Application au VIII^{e} Satellite de Jupiter. Bull. Astron., series 2, vol. 23, no. 1, 1959, pp. 1–89.

265. KUIPER, G. P.: Limits of Completeness. Planets and Satellites, ch. 18. Vol. III of The Solar System, G. P. Kuiper and B. M. Middlehurst, eds. University of Chicago Press, 1961, pp. 575–591.

Glossary

Adiabatic process—A thermodynamic change of state of a system in which there is no transfer of heat or mass across the system's boundaries.

Albedo—The ratio of electromagnetic radiation reflected by a body to that incident upon it.

Anticyclone—An area of relatively high pressure from which the wind blows spirally outward in a clockwise direction in the northern hemisphere and counterclockwise in the southern hemisphere.

Aphelion—The point on a heliocentric elliptical orbit farthest from the Sun.

Apparition (of a planet)—The indefinite period to time centered at opposition (or inferior conjunction) during which a planet is favorably located for observation.

Ascending node (of an orbit)—That point on an orbit at which a body (planet or satellite) crosses from south to north the reference plane (e.g., the ecliptic for the planets) on the celestial sphere. The opposite point, separated by 180° of longitude, is the descending node.

Astronomical unit (A.U.)—A fundamental unit of length used in astronomy. Originally, the astronomical unit was defined as the mean distance of Earth from the Sun. In celestial mechanics, it is defined as the radius of an idealized circular and unperturbed orbit of Earth around the Sun. The recent radar determination of Mühleman (1964) is 1 astronomical unit=149 598 900±600 kilometers.

Bond albedo (or Russell-Bond albedo)—The ratio of the total flux, reflected in all directions by a sphere (planet), to the total flux incident in parallel rays from a distant source (Sun) and expressed as the product, $A=p\cdot q$, of a full-phase albedo factor p (geometrical albedo) and a phase-varying factor q (phase integral).

Brilliancy (of a disk)—A geometrical measure of disk brightness, independent of albedo, that is determined only by phase k, the apparent semidiameter s, and solar distance r according to the defining formula: $L=k\frac{s^2}{r^2}$.

Conjunction—The configuration of the Sun, a planet, and Earth when the heliocentric longitudes of the latter two are equal. The three bodies then lie most nearly in a straight line. When the planet is between the Sun and Earth, the planet is said to be in inferior conjunction; when the Sun is between Earth and the planet, the planet is said to be in superior conjunction.

Coriolis force—The deflecting force caused by a planet's rotation that acts on a moving particle on the planet, normal to the particle's relative velocity. The deflection is to the right in the northern hemisphere and to the left in the southern.

Cyclone—An area of relatively low atmospheric pressure from which the wind blows spirally inward: counterclockwise in the northern hemisphere, clockwise in the southern.

Cyclotron radiation—Radiation emitted from the Van Allen belts of a planet; the emission results from the acceleration of trapped electrons to nonrelativistic energies. The electrons spiral along magnetic lines of force and accelerate in a manner similar to that of a cyclotron.

Day (ephemeris)—Average value of the mean solar day taken over the last three centuries.

Day (sidereal)—Time interval between two successive transits of the vernal equinox over the same meridian.

Day (solar)—Time interval between two consecutive transits of the Sun over a meridian. Since this time interval varies with Earth's orbital motion, a mean solar day was chosen, based on a mean annual motion of Earth (assuming an equivalent circular orbit) or a fictitious mean Sun.

Declination (of a celestial point)—The angle between a point and the celestial equator, measured along the hour circle through the point and counted as north (+) or south (−) of the equator.

Disk—The flattened appearance of a celestial body as it is observed, or the projection on the celestial sphere of that portion of the observed body which is visible.

Dry adiabatic lapse-rate—The rate of decrease of temperature with height of a parcel of dry air lifted adiabatically through an atmosphere in hydrostatic equilibrium.

Ecliptic—The annual, apparent path of the Sun's center on the celestial sphere, as seen from Earth, or the intersection of Earth's orbital plane with the celestial sphere.

Elongation (of a planet)—The angle between the Sun and a planet and Earth with the vertex at the center of Earth. Elongation is measured east or west of the Sun.

Ephemeris (fundamental)—An astronomical table predicting the positions of celestial bodies at regular intervals of time (also called almanac).

Ephemeris time—Uniform or Newtonian time based on the mean rotation of Earth during the year 1900.

Epoch—An arbitrary instance of time at which positions are measured or calculated.

Geometrical albedo—The ratio of the actual brightness of a reflecting body (planet or satellite) at full solar phase to that of a self-luminous body of the same size and position and radiating a flux of light equal to that incident on the first body.

Graybody—A hypothetical body that absorbs, independently of wavelength, some constant fraction between zero and one of all electromagnetic radiation incident upon that body.

Gregorian date—A date on the official calendar in use throughout the Christian world. The Gregorian calendar was instituted in 1582 by Pope Gregory XIII to correct errors accumulating in the Julian calendar.

Heliocentric—Sun centered; term derived from helios, the Greek word for sun.

Julian date—The number of mean solar days that have elapsed since the adopted epoch of Greenwich mean noon on January 1, 4713 B.C.

Kepler's laws—Three laws of undisturbed planetary motion formulated by Kepler:

1st law: The orbits of the planets are ellipses with the Sun at one focus.

2nd law: The radius vector Sun-to-planet sweeps equal areas in equal times.

3rd law: The squares of the planets' periods of revolution are proportional to the cubes of their mean solar distances (semimajor axes of ellipses).

Laplacian plane (or proper plane)—A plane that is fixed relative to the planet's equator, and upon which the precessing orbital plane of a satellite maintains a

nearly constant inclination. The plane's position is determined by the balance of the orthogonal components of the disturbing forces (e.g., from the planet's oblateness or the Sun's attraction).

Libration—Periodic oscillation about a mean position as, for example, caused by perturbations.

Limb—Edge of the illuminated part of a disk.

Line of apsides—A straight line infinitely extending the major axis of an elliptical orbit. This line passes through those points closest (periapsis) and farthest (apoapsis) from the dynamical center.

Line of nodes—A straight line that joins the intersection points (nodes) of the two great celestial circles that determine the orbital plane and the reference plane used to describe the motion of a planet or satellite.

Magnitude (stellar)—An inverse logarithmic measure of the brightness of a celestial body such that an increase of five magnitudes represents a hundred-fold decrease in the body's brightness.

Mie scattering—That scattering of radiation which is produced by spherical particles of any size (for comparison see "Rayleigh scattering").

Mixing ratio—The ratio of the mass of the gas considered to that of the remaining gases in a given atmospheric mass.

North celestial pole—The northern point of intersection of Earth's rotation axis with the celestial sphere.

Occultation—The obscuring of an observed body by a larger body passing in front of it.

Opposition—The configuration of Sun, Earth, and planet when the heliocentric longitudes of the latter two are equal. The three bodies, with Earth in the middle, are then most nearly in a straight line.

Osculating orbit—The instantaneous elliptical orbit that a planet or satellite would follow at the date considered (epoch of osculation) if all disturbing forces were removed.

Pericenter (or, perifocus)—That point on an orbit which is closest to the attracting center.

Perihelion—That point on a heliocentric elliptical orbit which is closest to the Sun.

Perijove—That point on a zenocentric orbit which is closest to Jupiter.

Phase—The fraction illuminated of the disk area.

Phase angle—The angle between the Sun and Earth, as observed from a planet whose center is the vertex.

Phase curve or law—The plot or mathematical law of the phase function $\phi(\alpha)$ of a planet versus phase angle α.

Phase function—The ratio of the brightness of a planet at any phase angle α to that at full phase ($\alpha=0$), assuming the planet at unit distances from the Sun and Earth.

Phase integral—The phase varying factor that modifies the geometrical albedo (or, full-phase factor) that enters into the definition of the Bond albedo of a planet. It is expressed as the integral:

$$q=\int_0^{2\pi}\phi(\alpha)\sin\alpha\,d\alpha$$

of the phase function $\phi(\alpha)$.

Polarization, amount or degree of—The proportion of polarized light to total light; it is defined by:

$$P=\frac{I_1-I_2}{I_1+I_2}$$

where I_1 is the component of intensity perpendicular to the plane of vision (defined by directions of illumination and observation) and I_2 is the intensity

component contained in this plane.

Polarization curve—The plot of degree of polarization versus phase angle of a planet.

Precession—The very slow (long-period) motion (26 000 years for Earth) of a planet's rotation axis about the north pole of the ecliptic, caused by the action of the Sun and any large satellite upon the planet's equatorial bulge; resembles the motion of a spinning top.

Rayleigh scattering—That scattering or radiation which is produced by spherical particles of radii smaller than about one-tenth the wavelength of the radiation (Rayleigh limit). Also called "molecular scattering."

Retrograde sense—The opposite of direct sense of rotation; that is, clockwise.

Right ascension—The angular arc measured along the celestial equator from the vernal equinox eastward (i.e., counterclockwise) to the intersection with the hour circle of the point (semigreat circle passing through the north celestial pole and the point).

Rotational lines—Spectral lines caused by rotational energy changes in a molecule.

Scale height (of an atmosphere)—The distance in which an isothermal atmosphere decreases in density from 1 to $1/e$.

Shadow transit of a satellite—The passage of a satellite's shadow, umbra, across the primary's illuminated disk.

Synchronous rotation—Rotation of a planet or satellite such that the rotation period is equal to the period of revolution around the Sun or primary; thus, the same side of the rotating body always faces the attracting body (for example, the Moon).

Synchrotron radiation—That radiation emitted from a planet's Van Allen belts wherein trapped electrons are accelerated to relativistic energies (i.e., with velocities approaching that of light) as in a synchrotron.

Synodic period of revolution (of two planets or satellites)—The time interval between consecutive oppositions or conjunctions of two bodies revolving around the same center.

Terminator—The line separating the illuminated from the nonilluminated portions of a planet or satellite; one observes a morning or evening terminator on the disk.

Twilight arc—The planetocentric angular arc that measures the displacement, resulting from atmospheric scattering of light on the planet, of the actual terminator from the theoretical terminator.

Vernal equinox—The point at which the Sun in its annual apparent path around Earth appears to cross the celestial equator from south to north at a certain time of the year (presently on Mar. 21), or the ascending node of the ecliptic on the equator.

Year, Julian—The mean length of the year on the Julian calendar; it is equal to 365.25 mean solar days, or $365^{d}6^{h}$ exactly.

Year, sidereal—The time interval between two successive returns of the Sun to a fixed celestial point (fixed star); it is the true period of revolution of Earth and is equal to 365.25636 mean solar days, or $365^{d}6^{h}9^{m}10^{s}$.

Year, tropical—The time interval between two successive returns of the Sun to the vernal equinox. Because of precession, it is shorter than the sidereal or true year. It is equal to 365.24220 mean solar days, or $365^{d}5^{h}48^{m}46^{s}$.

Zenocentric—Jupiter centered; the prefix "zeno" is derived from the Greek name for the chief of the gods, Zeus; the Latin equivalent is Jupiter.

Zenocentric latitude—That latitude at the center of Jupiter similar to geocentric or areocentric.

Zenographical latitude—Latitude on Jupiter, similar to geographical or areographical.

U.S. GOVERNMENT PRINTING OFFICE : 1967 O—248-761